รายงานวิจัยฉบับสมบูรณ์

ภาวะเมทิลเลชั่นระดับสูงของไลน์-1 ในเนื้อเยื่อปกติรอบเซลล์มะเร็ง

LINE-1 Hypermethylation in Tumor Supporting Tissue

โดย ดร. นครินทร์ กิตกำธร และคณะ

กรกฎาคม 2558

สัญญาเลขที่
RSA5580013

รายงานวิจัยฉบับสมบูรณ์

ภาวะเมทิลเลชั่นระดับสูงของไลน์-1 ในเนื้อเยื่อปกติรอบเซลล์มะเร็ง
LINE-1 Hypermethylation in Tumor Supporting Tissue

ผู้วิจัย	สังกัด
1 รศ.ดร. นครินทร์ กิตกำธร	คณะทันตแพทยศาสตร์ มหาวิทยาลัยมหิดล
2 นายเจริญชัย พุฒิปัญญาเลิศ	บัณฑิตวิทยาลัย จุฬาลงกรณ์มหาวิทยาลัย
3 ศาสตราจารย์ นพ. อภิวัฒน์ มุทิรางกูร	คณะแพทยศาสตร์ จุฬาลงกรณ์มหาวิทยาลัย

สนับสนุนโดยสำนักงานคณะกรรมการการอุดมศึกษา และสำนักงานกองทุนสนับสนุนการวิจัย
(ความเห็นในรายงานนี้เป็นของผู้วิจัย สกอ. และ สกว. ไม่จำเป็นต้องเห็นด้วยเสมอไป)

กิตติกรรมประกาศ

ผลงานวิจัยของคณะผู้วิจัยนี้ได้รับการสนับสนุนจาก ทุนเพิ่มขีดความสามารถด้านการวิจัยของอาจารย์รุ่นกลางในสถาบันอุดมศึกษา รหัสทุน RSA 5580013 โดยความร่วมมือของสำนักงานกองทุนส่งเสริมการวิจัย, สำนักงานคณะกรรมการอุดมศึกษา และมหาวิทยาลัยมหิดล

ขอขอบคุณ รองศาสตราจารย์ นายแพทย์ สมบูรณ์ คีลาวัฒน์ และ ดร. สุปราณี บูรณะประดิษฐ์กุล สำหรับความช่วยเหลือในส่วนของการเก็บตัวอย่าง

ขอขอบคุณเจ้าหน้าที่ของภาควิชาพยาธิวิทยา, ภาควิชาจุลชีววิทยา และภาควิชากายวิภาคศาสตร์ คณะแพทยศาสตร์ จุฬาลงกรณ์มหาวิทยาลัย และภาควิชาชีววิทยาช่องปาก มหาวิทยาลัยมหิดล ในการช่วยเหลืออำนวยความสะดวกสถานที่และอุปกรณ์การทำวิจัย

Project Code : RSA5580013

Project Title : LINE-1 Hypermethylation in Tumor Supporting Tissue

Investigator : Dr. Nakarin Kitkumthorn; Faculty of Dentistry, Mahidol University

E-mail Address : Nakarinkit@gmail.com

Project Period : 16th July 2012- 15th July 2015

Abstract:

The objective of this study is to evaluate the LINE-1 methylation status in breast cancer supporting tissue and also assess the potential of LINE 1 hypermethylated genes as a molecular marker for micrometastatic cancer screening. In the beginning, formalin-fixed paraffin-embedded lymph nodes were collected from 70 breast cancer patients and divided into 3 groups 1) lymph nodes of non-metastatic breast cancer (n=12), 2) lymph nodes negative of metastatic breast cancer (n=26), 3) matched lymph nodes positive of metastatic breast cancer (n=26). LINE-1 methylation was measured by qCOBRA-LINE-1 (quantitative COmbine Bisulfited Restriction Analysis-LINE-1) technique. The results showed the percentage of LINE-1 methylation among 3 groups were stepwise increase from group 1, 2, and 3, respectively. Additionally, laser-captured microdissection samples from lymph nodes group 3 (n=6), we found higher level of LINE-1 methylation in adjacent breast cancer stromal cell than matched breast cancer cells significantly. Next, we cocultured MCF-7, HeLa and WSU-HN 17 cell lines with peripheral blood mononuclear cells (PBMCs) in the Transwell® microplate. The percentage of LINE-1 methylation was gained in PBMCs after incubated with MCF-7 only. After that, by using CU-DREAM Ex (Connection Up- or Drown-Regulation Expression Analysis of Microarrays Extension, website; http://pioneer.netserv.chula.ac.th/~achatcha/cu-dream) program, we evaluated candidate genes and gene containing LINE-1 data from GSE10797, GSE9014, GSE5364 and GSE10810. Afterthat, seven hundred and nine upregulated genes were selected and classified into 3 groups followed their functions; immunological process, inflammation and angiogenesis. Finally, five selected candidate genes were test their expressions by immunohistochemistry technique. Interestingly, MUC-1 was observed to be a promising marker in micrometastasis tumor detection in histologically negative lymph node of breast cancer patient.

Keywords: Breast cancer, LINE-1 hypermethylation, Lymph node, Tumor supporting tissue

รหัสโครงการ: RSA5580013

ชื่อโครงการ: ภาวะเมทิลเลชั่นระดับสูงของไลน์-1 ในเนื้อเยื่อปกติรอบเซลล์มะเร็ง

ชื่อนักวิจัย และสถาบัน: ดร. นครินทร์ กิตกำธร คณะทันตแพทยศาสตร์ มหาวิทยาลัยมหิดล

E-mail Address : Nakarinkit@gmail.com

ระยะเวลาโครงการ: 16 กรกฎาคม พ.ศ. 2555 ถึง 15 กรกฎาคม พ.ศ. 2558

บทคัดย่อ:

การศึกษาครั้งนี้จึงมีวัตถุประสงค์เพื่อตรวจวัดระดับเมทิลเลชั่นของไลน์-1 ในเซลล์ปกติรอบๆ เซลล์มะเร็งและประเมินการใช้ยีนที่มีไลน์-1 เมทิลเลชั่นระดับสูงในการตรวจหาเซลล์มะเร็งซ่อนเร้น โดยเริ่มจากนำต่อมน้ำเหลืองผู้ป่วยในบล็อกพาราฟิน 3 กลุ่ม ได้แก่ กลุ่มที่ 1 ต่อมน้ำเหลืองในผู้ป่วยที่ไม่มีการแพร่กระจายของมะเร็ง จำนวน 12 ราย, กลุ่มที่ 2 และ 3 เป็นต่อมน้ำเหลืองของผู้ป่วยที่มีมะเร็งแพร่กระจาย โดยกลุ่ม 2 ไม่พบเซลล์มะเร็ง และกลุ่ม 3 เป็นคนไข้คนเดียวกันที่พบเซลล์มะเร็ง จำนวนกลุ่มละ 26 ราย นำมาตรวจระดับไลน์-1 เมทิลเลชั่นโดยใช้วิธีการ qCOBRA-LINE-1 (quantitative COmbine Bisulfited Restriction Analysis-LINE-1) ผลการทดลองที่ได้แสดงให้เห็นว่า ไลน์-1 เมทิลเลชั่นมีค่าสูงขึ้นจากกลุ่ม1 กลุ่ม 2 และ กลุ่ม 3 ตามลำดับ ซึ่งผลที่ได้จำเพาะในมะเร็งเต้านมเท่านั้น นอกจากนี้ยังทำทดลองเพิ่มโดยใช้วิธี laser-captured microdissection จำนวน 6 ราย พบว่าระดับไลน์-1 เมทิลเลชั่นสูงในเซลล์ปกติรอบๆเซลล์มะเร็งสูงกว่าเซลล์มะเร็งอย่างมีนัยสำคัญ การทดลองต่อมาเป็นการยืนยันผลโดยการทำ coculture ระหว่างเซลล์ไลน์ MCF-7, HeLa และWSU-HN 17 กับ blood mononuclear cells (PBMCs) ใน Transwell® microplate พบว่าระดับไลน์-1 เมทิลเลชั่นมีค่าสูงขึ้นเฉพาะ ในกรณี MCF-7 และลดลงในกรณี HeLa และ HN 17 จากการศึกษาด้วยโปรแกรม CU-DREAM Ex (Connection Up- or Drown- Regulation Expression Analysis of Microarrays Extension) โดยใช้ข้อมูลของ GSE10797, GSE9014, GSE5364 และ GSE10810 สามารถหายีนที่มีไลน์-1 และมีระดับการแสดงออกสูงขึ้นได้จำนวน 709 ยีน ในจำนวนนี้คัดเลือกยีนที่มีค่าสูงจำนวน 5 ยีน มาทำเทคนิก immunohistochemistry ต่อ จากผลการทดลองพบว่า MUC-1 สามารถนำมาพัฒนาตรวจหาเซลล์มะเร็งซ่อนเร้นในต่อมน้ำเหลืองที่ไม่มีเซลล์มะเร็งจากการดูด้วยลักษณะทางจุลพยาธิวิทยาได้

คำสำคัญ : มะเร็งเต้านม, ภาวะเมทิลเลชั่นระดับสูงของไลน์ 1, เนื้อเยื่อรอบเซลล์มะเร็ง

Table of contents

1. Introduction

Cancer is the second most common cause of death worldwide after heart diseases (1). One third of cancers may be cured, or treated better if cases are diagnosed and treated early. DNA methylation is the addition of a methyl group to the fifth carbon atom in the cytosine pyridine ring, resulting in formation of 5-methyl cytosine (2). The biological role of DNA methylation was controlling gene expression and maintaining genomic integrity (3). Two main altering transcription control procedures were observed in cellular transformation; promoter hypermethylation of tumor suppressor gene and genome-wide hypomethylation (4). Loss of DNA methylation has been regarded as a common epigenetic event in cancer cells. LINE-1 is one of interspersed repetitive sequence (IRS) and constitutes 17% of human genome (5, 6). Therefore, LINE-1 hypomethylation is responsible for genome-wide hypomethylation.

Cancer cells are frequently characterized by hypomethylation of the LINE-1 (7). Our previous researches are trying to characterize the LINE-1 methylation status in peripheral blood mononuclear cell (PBMC) of cancer patients (8). Interestingly, we observed LINE-1 hypermethylation only in the PBMC of breast cancer patient but not presented in colon cancer and nasopharyngeal cancer (Figure 1). Thus, this result makes us hypothesize us to expand the study of breast cancer cell influenced LINE-1 hypermethylation in other surrounding tissues.

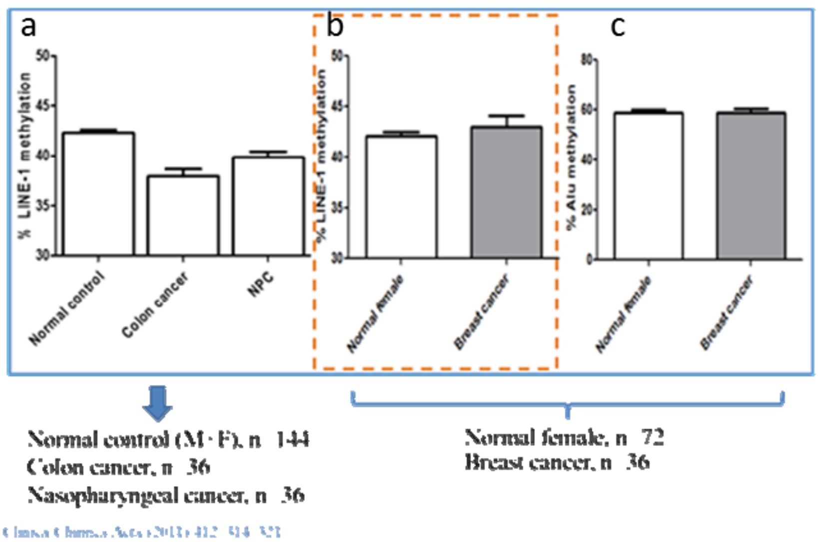

Figure 1. IRS methylation in PBMC of cancer patients, a) LINE-1 hypomethylation in PBMC of colon cancer and nasopharyngeal cancer patients. b) LINE-1 hypermethylation in PBMC of breast cancer patients. c) Alu methylation in breast cancer patients

In addition, using CU-DREAM Ex (Connection Up- or Drown- Regulation Expression Analysis of Microarrays Extension) program(10) , we observed that genes, containing LINE-1 were upregulated significantly in normal surrounding cells of breast cancer. Moreover, LINE-1 was demonstrated to play a role in gene regulation. LINE-1 hypermethylation in genes, containing intragenic LINE-1 can upregulate gene expression (9). Therefore, we proposed that the LINE-1 hypermethylation in normal surrounding cells are associated with upregulation of genes that containing LINE-1. This proposed study will try to evaluate the LINE-1 methylaiton status in normal tissue surrounding breast cancer cells. This project will also assess the potential of LINE 1 hypermethylation and other candidate genes as a molecular marker for micrometastatic cancer screening in metastatic lymph node. Furthermore, this effort will provide the biological data of host immune response in cancer microenvironment as a strategy of targeted immunotherapy and prevention

2. Objectives

2.1. To analyze methylation level of LINE-1 in tumor supporting tissue

2.2. To analyze methylation level of LINE-1 in metastatic lymph nodes

2.3 To evaluate induction of LINE-1 hypermethylation in lymphocytes influenced by breast cancer cell lines

2.4. Identify and evaluate upregulated genes, containing intragenic LINE-1

2.5. Evaluate genes, containing intragenic LINE-1 for screening metastatic lymph nodes

3. Materials and methods

Strategies

We analyzed methylation level of LINE-1 by two main methods as shown in Figure 2. First, we used paraffin-embeded tissue (FFPE) of breast cancer, breast cancer surrounding tissue to measured LINE-1 methylation level. Second, we performed co-culture technique to detect the influence of cancer cell to LINE-1 methylation in cancer cells.

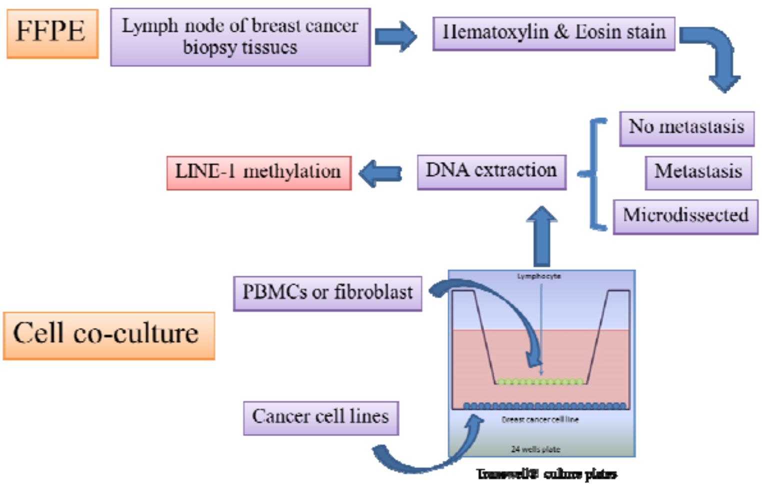

Figure 2. Flowcharts of main experiment

GSE data

Four GSE datasets were retrieved from the GenBank (www.ncbi.nlm.nih.gov) as follow; GSE10797(11), GSE9014(12), GSE5364(13) and GSE10810(14).

Lymph node and microdissected tissue

All samples will be immediately cut from the resected breast tissue, embedded in Tissue Tek® OCT medium (Sakura™, Tokyo, Japan), and frozen in liquid nitrogen. All patients will had no anti-inflammatory treatment, chemical, hormonal or radical therapy. The frozen tissues will be sectioned by a cryostat (Carl Zeiss Microimaging™, New York, USA) at 8 µm, mounted on glass slides and covered with PEN foil (2.5 µm thick; Carl Zeiss Microimaging™). The slice samples will be quickly fixed using a mixture of absolute ethanol and acetic anhydride (19:1), and stored at -80□C until use. Slides will be stained with hematoxylin and eosin (H&E) at room temperature for investigation to confirm histopathologically component by a pathologist and dehydrated for 5 sec each with 70, 80, 95 and then 100% ethanol. The breast cancer sections which included in this study will be consisted of at least 80 percent of tumor cells. After being air-dried, the sections will be microdissected using the LMD system with a 337-nm nitrogen ultraviolet (UV) laser (Zeiss PALM Microbeam LCM System, Carl Zeiss Microsystems™). The target cells dissected from a section will be dropped immediately into a microcentrifuge tube cap filled with 30 μl of RLT lysis buffer (Qiagen®, Hiden, Germany). The samples of noncancerous tissues will be selected from at least 5 cm away from cancer tissue, and pathologically composed of >80% normal breast tissue without cancerous and dysplastic cells. Laser capture microdissection will be used to collect approximately 1,500 cells for further experiment.

PBMCs preparation

PBMCs were purified using standard Ficoll-Paque gradient centrifugation according to the instructions of the manufacturer (Amersham Pharmacia, Uppsala, Sweden). Briefly, 4 ml of Ficoll-Paque gradient was pipetted into two 15-ml centrifuge tubes. The heparinized blood was diluted 1:1 in phosphate-buffered saline (PBS) and carefully layered over the Ficoll-Paque gradient (9 to 10 ml/tube). The tubes were centrifuged for 20 min at 1,020 g. The cell interface layer was harvested carefully, and the cells were washed twice in PBS (for 10 min at 640 g followed by 10 min at 470 g) and resuspended in RPMI 1640 medium with Glutamax supplemented with penicillin (50 U/ml)-streptomycin (50 g/ml) and 10 mM HEPES (complete RPMI medium) before counting.

Cells and co-culture conditions

The established human carcinoma cell lines which obtain from American Type Culture Collection (Rockville, MD) are including mammary carcinoma (MCF-7, ATCC-HBT22), head and neck squamous cell carcinoma (WSU-HN17) and cervical carcinoma (HeLa, ATCC-CCL-2). Normal human fibroblasts were isolated from normal breast tissue in the absence of tumoral lesion and retained a fibroblastic morphology more than 10 passages. All of them were grown up with DMEM medium supplemented with 10% FBS (Gibco BRL, Life Technologies) at 37 ^{o}C in a humidified atmosphere (95% air: 5% CO_2). The cell lines will be passaged twice a week, and the medium will be changed every other day. All cell lines will be performed mycoplasma-free test with the Boehringer Mannheim BM-Cyclin test (F. Hoffmann-La Roche Ltd.). The cells, grown in culture flasks (CytoOne T225 flask, USA Scientific®.Inc), will be harvested at 60-65% confluence using 0.05% Trypsin, 0.5 mM EDTA, and washed in a phosphate buffer saline (PBS).

Indirect co culture experiments associating cancer cells with PBMCs or fibroblast were performed in Transwell® culture plates (Costar, Dutscher, Brumath, France) allowing paracrine exchanges between both cell types. The cancer cells were seeded in 24-well culture plates ($5x10^4$ cells/well) and allowed to attach overnight in DMEM serum-free medium, whereas PBMCs or fibroblasts were plated in permanent membrane culture inserts which is 6.5-mm diameter; tissue culture treated polycarbonate membranes, 0.4-mm pore size ($1x10^5$ cells/well). Culture inserts containing PBMCs or fibroblasts were then placed in the wells containing cancer cells. Both PBMCs and fibroblasts were co-cultivated for 4 and 8 hours to harvest and determine DNA methylation.

DNA extraction

Cells from the tissue culture and breast biopsy tissue were centrifuged at 4 ^{o}C 2,500 rpm, 15 minutes. Cell pellet were collected and discarded supernatant. Wash cell pellet in sterile phosphate buffer saline solution and centrifuged at 4 ^{o}C 2,500 rpm, 15 minutes. Cell pellet were added with 1 ml of extraction buffer with 10% SDS and proteinase K 0.5 mg/ml. The mixture were incubated at 50 ^{o}C, 72 hours. Phenol-chloroform solution were added into the digest cell pellets or tissues mixture. After that, the mixtures were centrifuged at 4 ^{o}C 14000 g for 15 minutes. Collect the upper phase and add 10 M ammonium acetate, absolute ethanol for DNA precipitation. The air-dry DNA were suspended in distill water and applied for COBRA LINE-1 to measure the LINE-1 methylation.

<u>Quantitaive Combine Bisulfite Restriction Analysis for LINE-1 (qCOBRA LINE-1)</u>

All DNA samples were converted by bisulfite reaction using sodium bisulfate as previously described. Unmethylated cytosine at CpG island were changed into uracil while methylated cytosine were not be changed. A total of 1 μg DNA samples were denatured in 0.22 M NaOH at 37 ^{o}C, 10 minutes and added 10 mM hydroquinone (Sigma-Aldrich, Singapore) with 3 M sodium bisulfited (pH 5.0) incubated at 50 ^{o}C, 16-20 hours. After that, DNA was recovered using the Wizard DNA Clean-Up Kit (Promega, Madison, WI) follow by the manufacturer's protocol. DNA samples were eluted by warm water and precipitated with sodium acetate in ethanol. Then, Bisulfited DNA pellets were resuspended in distills water. One microliter of bisulfited DNA were subjected into 45 cycles of PCR process using LINE-1 forward primer (5′-CCGTAAGGGGTTAGGGAGTTTTT-3′) and LINE-1 reverse primer (5′-RTAAAACCCTCCRAACCAAATATAAA-3) with annealing temperature 50 °C. The amplified products were digested with 2 U of *TaqI* and *TasI* restriction endonuclease in buffer III (MBI Fermentas®, Glen Burnie, MD) at 65 °C, overnight. The digested products were identified by 8% non-denaturing polyacrylamide gel electrophoresis and stained with SYBR green (SYBR® Green JumpStart™ Taq ReadyMix™, Sigma-Aldrich® .Co.LLC). All samples will be process in duplicate.

According to LINE-1 analysis and calculation, the amplified products were classified into 3 types depended on the methylation pattern of the 2 CpG dinucleotides. There are hypermethylated loci (mCmC), partial methylated loci (uCmC and mCuC) and hypomethylated loci (uCuC). After enzyme digestion, four sizes of products were detected for COBRA LINE-1 (160 bp, 98 bp, 80 bp and 62 bp). Then, the band intensities were measured by a phosphoimager using ImageQuant Software (Molecular Dynamics, GE Healthcare®, Slough, UK).

Next, the percentage of LINE-1 methylation pattern will be calculated as follow; First, the intensity of each band were divided by bp of DNA length; %160/160 = A, %98/94 = B, %80/78 = C, and %62/62 = D. After that, the percentage of methylation were calculated as following formula; mC = 100×(C+A)/(C+A+A+B+D), mCuC = 100×(A)/(((C–D+B)/2)+A+D), uCmC = 100×(D-B)/(((C–D+B)/2)+A+D), uCuC = 100×B/(((C–D+B)/2)+ A+D) and mCmC = 100×((C–D+B)/2)/(((C–D+B)/2)+D+A). The same DNA preparations from HeLa (Cervical cancer), DauDi (B-cell lymphoma) and JurKat (T-cell lymphoma) cell lines were used as a positive control in the experiment and for inter-assay adjustments.

Bioinformatics (CU-DREAMX)

GEO dataset were selected from NCBI microarray database including GSE10797, GSE9014, GSE5364 and GSE10810. GSE10797 and GSE9014 comparing gene expression between stromal cell from invasive breast cancer and stromal from normal adjacent tissue. GSE 5364 and GSE10810 reveal expression data from breast cancer cell and normal adjacent tissue. All GEO datasets were analyzed expression level of gene containing LINE-1 with CU-DREAMX program which calculated *p*-value and odd ratio.

Immunohistochemistry

Three-micrometer-thick sections of formalin-fixed, paraffin-embedded tissue specimens will be deparaffinized and dehydrated. After antigen retrieval by heating in an autoclave for 10 min at 120°C, the sections will be incubated with 2% normal bovine serum to block any non-specfic reaction. Then the sections will be incubated with an antihuman monoclonal antibody against specific candidate gene (Dilution 1:1000) at 4°C overnight and followed by incubation with a biotinylated secondary antibody (antigoat IgG, 1:200; Vector® Laboratories, Burlingame, CA) and Vectastain Elite ABC reagent (Vector® Laboratories) at room temperature for 30 min each. The sections will be treated with 3,3′-diaminobenzidine tetrahydrochloride, followed by counterstaining with hematoxylin. Tissue specimens which had detected positive immunoreactivity for candidate gene will be used as a positive control at staining.

Statistical analysis

Statistical analyses were determined by using SPSS (Statistical Package for the Social Sciences) software for Windows version 17.0.1 (SPSS Inc., Chicago, IL). The data were expressed in mean ± SEM and independent sample *t*-test were performed to calculate significant differences among normal, breast cancer adjacent tissue, PBMCs control and PBMCs after co-culture. All *p*-values were obtained by two sided and *p*-values less than 0.05 were observed to statistical significant.

4. Results

The results from CU-DREAM Ex program show significantly *p*-value in all selected GEO datasets. When comparing between stromal cell from invasive breast cancer and normal, upregulated gene containing LINE-1 are significant different (GSE10797; p = 3.08 x 10^{-8}, GSE9014; p = 1.34 x 10^{-8}). However, downregulated gene containing LINE-1 are significant only comparing between breast cancer cell and adjacent normal tissue (GSE5364; p = 1.11 x 10^{-7}, GSE10810; p = 8.09 x 10^{-10}). From strategic of LINE-1, intragenic LINE-1 can regulate gene expression when the CpG methylations of LINE-1 were change. Intragenic LINE-1 hypermethylation can cause gene up regulation and hypomethylation condition lead to gene down regulation. Consequently, the result of GEO dataset (shown in figure 3.) implied that LINE-1 methylation occurred in stromal cell surrounded by cancer cell was higher than normal stromal cell. Moreover, the methylation in cancer cell might be lower than adjacent normal tissue.

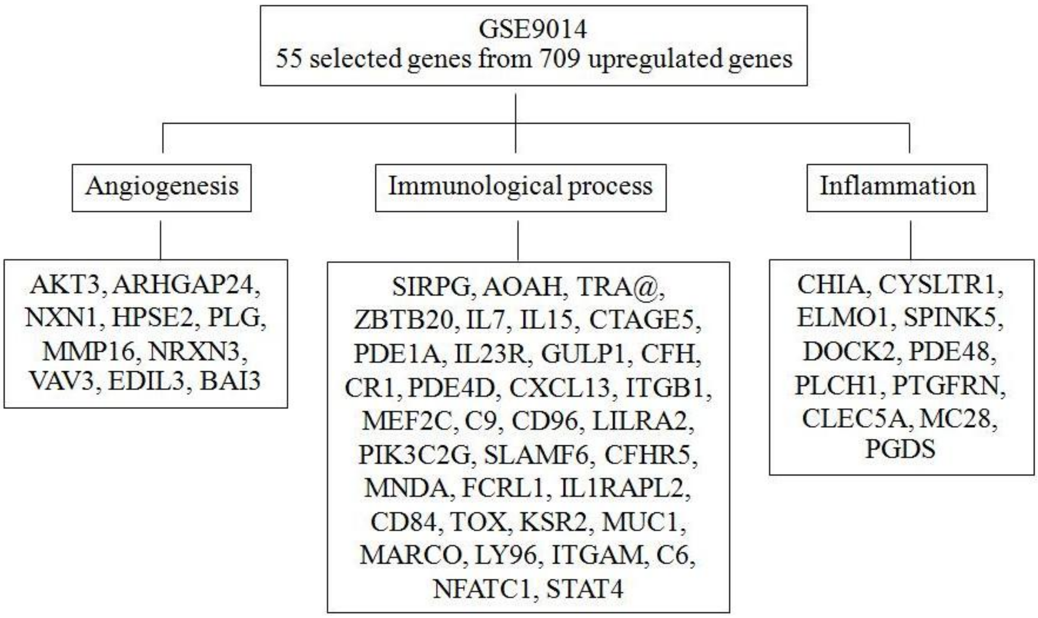

Geo Dataset	Case	Control	Down regulated		Up regulated	
			Odd Ratio	*P*-value	Odd Ratio	*P*-value
GSE10797	Stromal cells from invasive breast cancer	Stromal cells from healthy normal	0.52	8.36E-03	1.68	3.08E-08
GSE9014	invasive breast cancer, stromal cells	Normal adjacent stromal cells	0.72	1.52E-06	1.39	1.34E-08
GSE5364	Breast cancer sample	Adjacent normal breast tissue	1.51	1.11E-07	0.6	6.24E-09
GSE10810	Invasive breast cancer	Adjacent normal breast tissue	1.64	8.09E-10	0.66	3.17E-06

Figure 3. The results from CU-DREAM Ex program show genes containing LINE-1 expression are up regulate in stromal cells from invasive breast cancer. All of up regulated gene containing LINE-1 can classified into 3 major groups including angiogenesis, inflammation and immunological process.

When we observed LINE-1 methylation level in breast cancer lymph node as shown in Figure 4 and Table 1, we found that the methylation level were different between breast cancer cell and adjacent tissue (*p*-value = 0.0148). The LINE-1 methylation were increased from No metas, Metas LN- and Matas LN+ group, respectively. The *P*-value in each group were observed (No metas: Metas LN+ = 0.002, No metas: Metas LN- =0.106, Metas LN- : Metas LN+ =0.008)

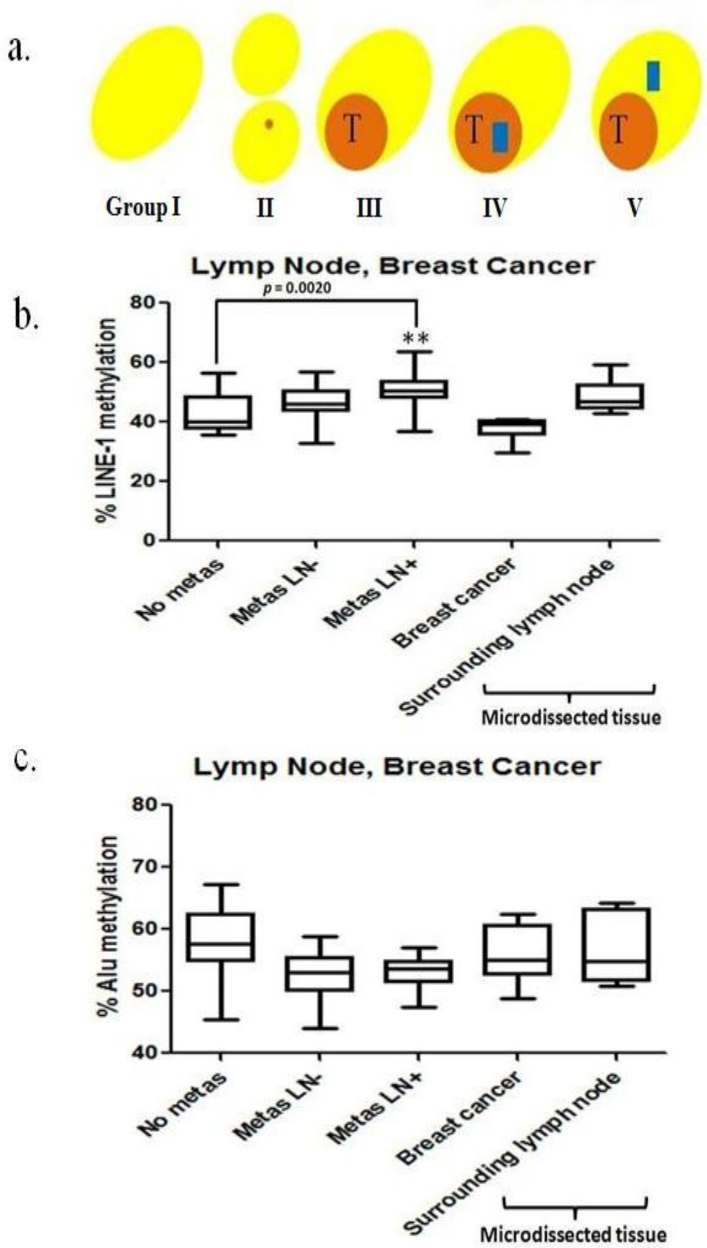

Figure 4. Show the results of LINE-1 methylation in lymph node. a) demonstrated figure in each group. b) The percentage of LINE-1 methylation in lymph node show increasing level from no metas, metas LN- and metas LN+, respectively. c) The percentage of Alu methylation in the same group of lymph node which not found significant result.

We also measured LINE-1 methylation level in surrounding adipose tissue of breast cancer. The results showed higher level of LINE-1 methylation along the distance from the cancer tissue (Figure 5).

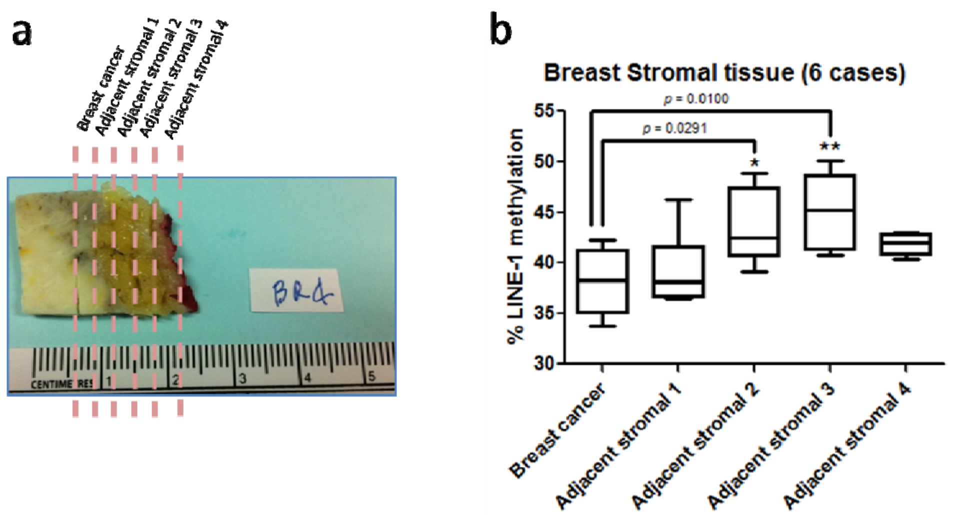

c

% LINE-1 methylation (mC)	Breast cancer	Adjacent stromal 1	Adjacent stromal 2	Adjacent stromal 3	Adjacent stromal 4
Average ± SD	38.16 ± 3.62	39.29 ± 3.77	43.53 ± 3.69	45.20 ± 4.05	41.87 ± 1.13

Figure 5. LINE-1 methylation in surrounding adipose tissue of breast cancer. a) Illustration of surrounding adipose tissue separation in different distances from tumor tissue. b and c) LINE-1 hypermethylation in the adjacent stromal tissue.

Next, we observed LINE-1 methylation change (%^{m}C) with indirect co-culture. PBMCs after co-culture in 4 and 8 hours with MCF-7 were shown LINE-1 hypermethylation when compare with control (*p*-value =0.0044 and 0.0240). This hypermethylation evidence was found in the indirect co-culture between MCF-7 and primary fibroblast (*p*-value =0.0288 and 0.8624). In Figure 6 and Table 1 show LINE-1 hypermethylation only occurred in co-culture with breast cancer cell line.

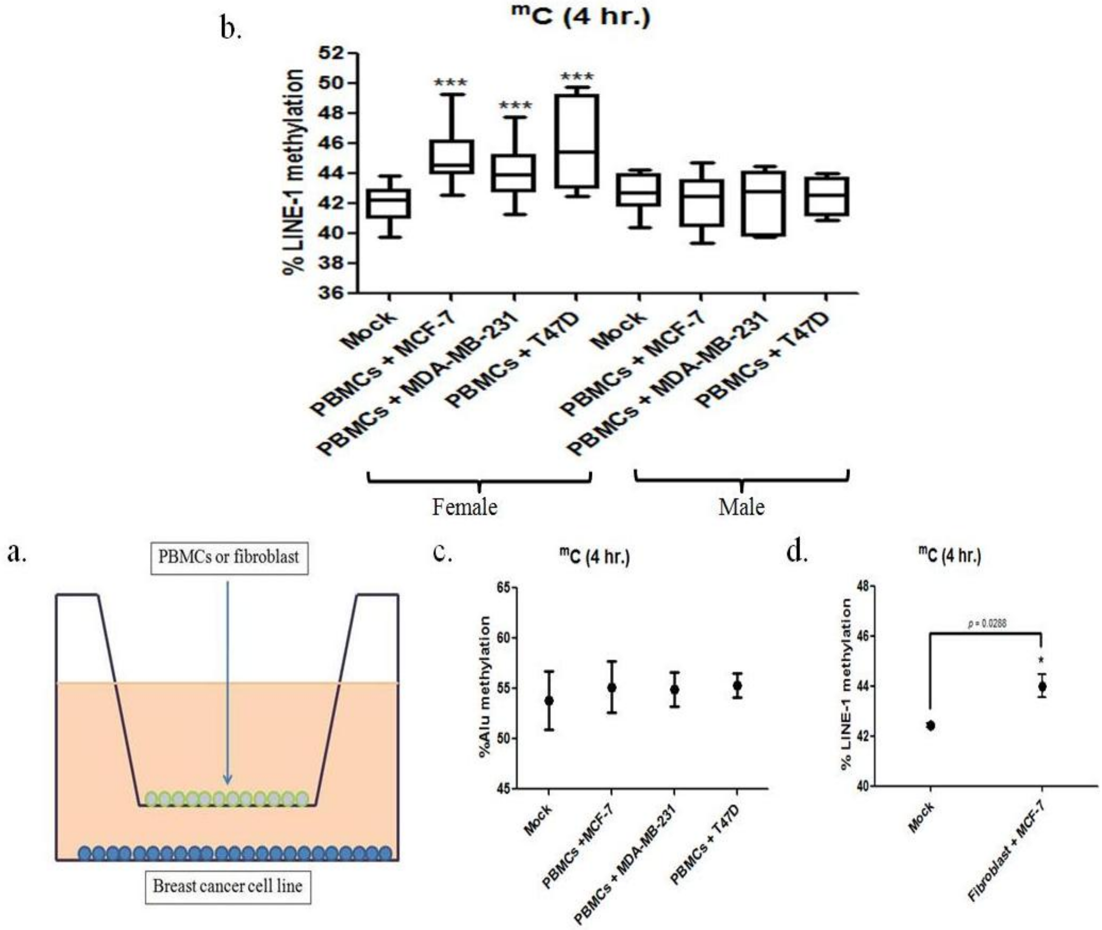

Figure 6. The percentage of LINE-1 methylation from PBMcs when performed indirect co-culture including a) Schematic of indirect co-culture composed of lower layer which is breast cancer cell lines and upper layer which is PBMCs or fibroblast. b) The results of LINE-1 methylation from 4 hr. indirect co-culture PBMCs found LINE-1 hypermethylation only female PBMCs indirect co-culture with breast cancer cell lines. c) Show Alu methylation of 4hr. indirect co-culture PBMCs with breast cancer cell line which found no significant. d) LINE-1 hypermethylation also occurred in 4hr indirect co-culture fibroblast with breast cancer cell line.

Table 1. Detail data of LINE-1 and Alu methylation levels

Sample		N	LINE-1 methylation (%± S.D.)	Alu methylation (%± S.D.)
Breast cancer, lymph node				
	Group 1……No metas…………………	12	42.65±6.63	58.24±6.03
Match	Group 2……Metas, LN-…………………	26	46.36±5.18	52.72±3.63
	Group 3……Metas, LN+………………	26	50.55±5.08	53.12±2.50
Match	Microdissected breast cancer	6	37.81±4.19	55.91±4.81
	Microdissected surrounding lymph node	6	48.55±5.74	56.62±5.66
Head & Neck cancer, lymph node				
	Group 1……No metas…………………	16	49.61±5.64	N/A
Match	Group 2……Metas, LN-…………………	25	45.57±5.13	N/A
	Group 3……Metas, LN+………………	25	40.21±4.18	N/A
Match	Microdissected head and neck cancer	-	N/A	N/A
	Microdissected surrounding lymph node	-	N/A	N/A
Cell Co-culture				
Female PBMCs control		21	42.02±1.23	N/A
Female PBMC:MCF-7		21	45.16±1.98	N/A
Female PBMC:MDA-MB-231		12	44.12±1.96	N/A
Female PBMC:T47D		9	46.23±3.02	N/A
Female PBMC:WSU-HN 17		14	41.65±1.89	N/A
Female PBMC:HeLa		14	40.27±2.21	N/A
Male PBMCs control		7	42.68±1.31	N/A
Male PBMC:MCF-7		7	42.27±1.84	N/A
Male PBMC:MDA-MB-231		7	42.16±1.93	N/A
Male PBMC:T47D		4	42.49±1.28	N/A
Male PBMC:WSU-HN 17		4	41.68±1.62	N/A
Male PBMC:HeLa		4	41.24±1.19	N/A
Fibroblast Control		3	42.43±0.14	N/A
Fibroblast:MCF-7		3	44.00±0.80	N/A
Fibroblast:WSU-HN 17		3	42.27±1.57	N/A
Fibroblast:HeLa		3	42.33±1.72	N/A

Afterthat, we used the CU-DREAM Ex data of GSE 9014 and selected candidate genes from the up-regulation criteria. We selected from gene function including inflammation, angiogenesis and immunological process. Five of them with high p-value were select as candidate genes to performed immunohistochemistry including ALK-1, MUC-1, Prolactin, Collagen type IV and Ubiquitin. However, the positive result was found only in MUC-1 immunohistochemistry staining (shown in figure 7). The MUC-1 positive cells were found only in Metas LN- which not found in No metas. Both group show negative for breast cancer cells when performed pan-cytokeratin staining. CD138+ were used as a marker for plasma cells and the result found CD138+ positive in both group. Moreover, some of positive cells are MUC-1 positive and CD138+ positive which implied that positive cells is MUC-1 positive plasma cells.

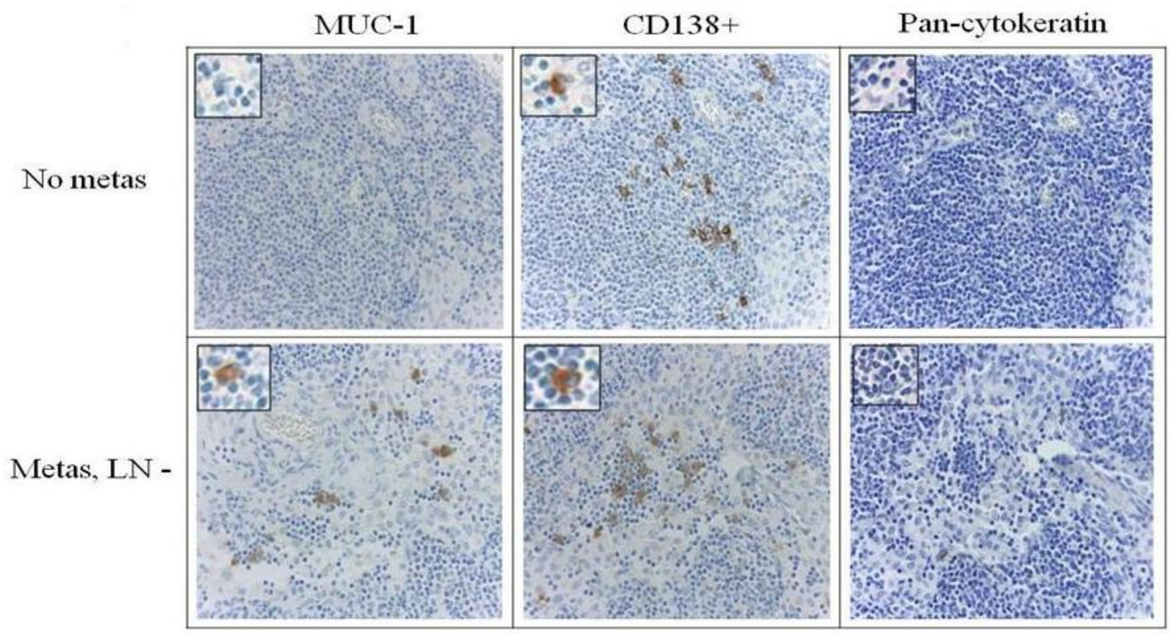

Figure 7. Immunohistochemistry of No metas and Metas LN- lymph node. MUC-1 positive cells were found only in metas LN-. CD138+ is a maker for plasma cells which found in both group and some of them are MUC-1 positive cells. Pan-cytokeratin is marker for breast cancer which negative in both group.

Finally, MUC-1 positive cells were calculated in percentage of positive cells per lymph node. The results displayed the capacity of MUC-1 positive plasma cell in discrimination between no metas lymph node between and metas LN- group. (Table 2)

Percentage of MUC-1 positive plasma cell				
	CD138+	CD138−, MUC-1+	% of MUC-1+	Average±SD
No metas (5 nodes)	43	2	4.65	5.74±3.01
	56	6	10.71	
	35	2	5.71	
	40	2	5.00	
	38	1	2.63	
Metas LN- (5 nodes)	54	41	75.93	80.74±6.15
	48	40	83.33	
	71	63	88.73	
	60	44	73.33	
	51	42	82.35	
Metas LN+ (5 nodes)	45	31	68.89	77.41±9.56
	66	49	74.24	
	48	33	68.75	
	39	34	87.18	
	75	66	88.00	

Table 2. Immunohistochemistry staining MUC-1 positive plasma cells in three lymph node groups.

5. Discussion and conclusion

In general, cancer cells composes of multiple components from both tumor cells and host stromal cells. Recently, many researches notify that tumor stromal cells play important roles in tumor initiation, progression, and metastasis (15). There are some stromal cells which can involve in breast cancer progression such as T lymphocyte (infiltrating lymphocyte) and macrophage (tumor-associated macrophage) (16) and cancer-associated fibroblasts (15, 17). However the mechanism of stromal cell induction by cancer cells still unknown. Here, we found the epigenetic change, the LINE-1 hypermethylation which specific to breast cancer stromal tissue.

In case of hypermethylation of CpG island, genes can causes inactivation of tumor-associated genes early in carcinogenesis. Early studies suggest that this could be a consequence of deregulation of the methylation mechanism such as over expression of DNMT1, 3A and 3B in cancer cell lines, which cause an increase in CpG island methylation (18, 19). Recently, demethylation of CpG island genes leads to the implication of alternative transcripts and overexpression of oncogenes (20).

Normally, LINE-1 hypomethylation is responsible for genome-wide hypomethylation. LINE-1 methylation change can regulate gene expression especially for intragenic LINE-1 (9). When LINE-1 methylation levels were reduced in some conditions (chemical treatment or carcinogenesis), a significant number of LINE-1 RNA were increase (Figure 9). The LINE-1 RNA-genomic mRNA complex will bind to AGO2 which lead to RNA degradation process. Afterthat, gene containing LINE-1 will down-regulate. The degree of this repression correlated with the intragenic LINE-1 methylation level (partial-, complete-methylation). During cancerous tissue development, the system interaction as microenvironment between cancer cells and surrounding stromal cells is occurred.

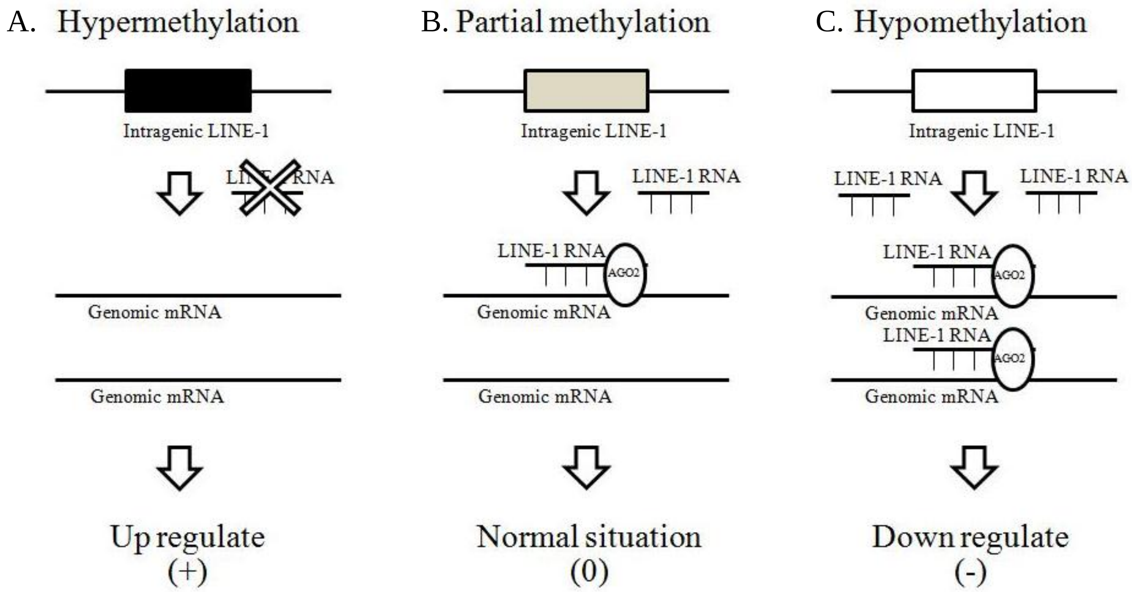

Figure 9. Intragenic LINE-1 can regulate gene expression. The LINE-1 RNA-genomic mRNA complex was bound to AGO2 which lead to RNA degradation process and mRNA production is not occurred a) upregulated gene expression occurred by hypermethylation of intragenic LINE-1 b) partial methylation of intragenic LINE-1 can transcript LINE-1 RNA which complementary to genomic mRNA c) LINE-1 RNA were increase in hypomethylation of intragenic LINE-1 which lead to down regulated gene expression.

We observed that breast cancer cells can promote LINE-1 methylation of normal surrounding cells including fibroblast, PBMC and adipose tissue. This event not occurred in both H&N cancer and cervical cancer. Therefore, there should be some mechanisms that need further investigation for the breast cancer- microenvironment interaction especially, focus to gene-containing LINE-1 and LINE-1 methylation. Interestingly, we were not found any LINE-1 methylation change of normal surrounding cells in male. That should be explanation by female hormone impaction such as estrogen. In this point, our ongoing study will approve the influence of estrogen to gene-containing LINE-1 transcription. In this study we also found some application. The Muc-1 which is one of gene-containing LINE-1 was observed to be overexpression in breast cancer surrounding plasma cells. Although, we stilled not know the definite mechanism, but this first evidence may help us to gain questions for our further study. Finally, we expect to apply Muc-1 positive plasma cells as a prognosis prediction in histologically negative lymph node of breast cancer.

In conclusion, our studies demonstrated

- Breast cancer cells can promote LINE-1 methylation of normal surrounding cells in female.
- Breast cancer cells cannot promote LINE-1 methylation of normal surrounding cells in male.
- H&NSCC and cervical cancer cannot promote LINE-1 hypermethylation in normal surrounding cells.
- Upregulated gene containing LINE-1 of breast cancer surrounding cells involve in carcinogenesis including angiogenesis, inflammation and immunological process
- Plasma cells in metastatic cancer express MUC-1 has a potential application for micrometastatic cancer detection in lymph node.

6. References

1. Jemal A, Bray F, Center MM, Ferlay J, Ward E, Forman D. Global cancer statistics. CA Cancer J Clin. 2011;61(2):69-90.

2. Bird A. DNA methylation patterns and epigenetic memory. Genes Dev. 2002 ;16:6-21.

3. Shames DS, Minna JD, Gazdar AF. DNA methylation in health, disease, and cancer. Curr Mol Med. 2007;7:85-102.

4. Mutirangura A. Quantitative PCR analysis for methylation level of genome: clinical implications in cancer. Asian Biomedicine. 2007;1:121-8.

5. Kazazian HH, Jr. and Moran JV. The impact of L1 retrotransposons on the human genome. Nature genetics. 1998; 19: 19-24.

6. B. Lander ES, Linton LM, Birren B, Nusbaum C, Zody MC, Baldwin J, Devon K, Dewar K, Doyle M, FitzHugh W, Funke R, Gage D, Harris K, Heaford A, Howland J, Kann L, Lehoczky J, LeVine R, McEwan P, McKernan K, Meldrim J, Mesirov JP, Miranda C, Morris W, Naylor J, Raymond C, Rosetti M, Santos R, Sheridan A, Sougnez C, Stange-Thomann N, Stojanovic N, Subramanian A, Wyman D, Rogers J, Sulston J, Ainscough R, Beck S, Bentley D, Burton J, Clee C, Carter N, Coulson A, Deadman R, Deloukas P, Dunham A, Dunham I, Durbin R, French L, Grafham D, Gregory S, Hubbard T, Humphray S, Hunt A, Jones M, Lloyd C, McMurray A, Matthews L, Mercer S, Milne S, Mullikin JC, Mungall A, Plumb R, Ross M, Shownkeen R, Sims S, Waterston RH, Wilson RK, Hillier LW, McPherson JD, Marra MA, Mardis ER, Fulton LA, Chinwalla AT, Pepin KH, Gish WR, Chissoe SL, Wendl MC, Delehaunty KD, Miner TL, Delehaunty A, Kramer JB, Cook LL, Fulton RS, Johnson DL, Minx PJ, Clifton SW, Hawkins T, Branscomb E, Predki P, Richardson P, Wenning S, Slezak T, Doggett N, Cheng JF, Olsen A, Lucas S, Elkin C, Uberbacher E, Frazier M. Initial sequencing and analysis of the human genome. Nature. 2001; 409: 860-921.

7. Kitkumthorn N, Mutirangura A. Long interspersed nuclear element-1 hypomethylation in cancer: biology and clinical application. Clin Epigenetics. 2011; 2: 315-330

8. Kitkumthorn N, Tuangsintanakul T, Rattanatanyong P, Tiwawech D, Mutirangura A. LINE-1 Methylation in the peripheral blood mononuclear cells of cancer patients. Clinica Chimica Acta. 413: 869-74, 2012

9. Aporntewan C, Phokaew C, Piriyapongsa J, Ngamphiw C, Ittiwut C, Tongsima S, Mutirangura A. Hypomethylation of intragenic LINE-1 represses transcription in cancer cells through AGO2. A. PLoS One. 2011 Mar 15; 6 :e17934.

10. Arporntewan C, Mutirangura A. Connection up- and down- regulation expression analysis of microarrays (CU-DREAM): a physiogenimic discovery tool. Asian Biomedicine. 2011; 5: 257-262.

11. Lee YS, Chen CH, Tsai CN, Tsai CL, Chao A, Wang TH. Microarray labeling extension values: laboratory signatures for Affymetrix GeneChips. Nucleic Acids Res. 2009; 37: e61. Epub 2009 Mar 18.

12. Finak G, Bertos N, Pepin F, Sadekova S, Souleimanova M, Zhao H, Chen H, Omeroglu G, Meterissian S, Omeroglu A, Hallett M, Park M. Stromal gene expression predicts clinical outcome in breast cancer. Nat Med. 2008; 14: 518-27

13. Yu K, Ganesan K, Tan LK, Laban M. A precisely regulated gene expression cassette potently modulates metastasis and survival in multiple solid cancers. PLoS Genet 2008 18; 4: e1000129.

14. Pedraza V, Gomez-Capilla JA, Escaramis G, Gomez C. Gene expression signatures in breast cancer distinguish phenotype characteristics, histologic subtypes, and tumor invasiveness. Cancer 2010; 116: 486-96.

15. Kalluri R, Zeisberg M. Fibroblasts in cancer. Nat Rev Cancer. 2006; 6(5): 392-401.

16. Man YG, Magrane GG, Lininger RA, Shen T, Kuhls E, Bratthauer GL. Morphologically similar epithelial and stromal cells in primary bilateral breast tumors display different genetic profiles: implications for treatment. Appl Immunohistochem Mol Morphol. 2004; 12(4): 305-14.

17. Ostman A, Augsten M. Cancer-associated fibroblasts and tumor growth-bystanders turning into key players. Curr Opin Genet Dev. 2009; 19(1): 67-73.

18. Jones PA, Gonzalgo ML. Altered DNA methylation and genome instability: a new pathway to cancer? Proc Natl Acad Sci U S A. 1997; 94(6) :2103-5.

19. Lin H, Yamada Y, Nguyen S, Linhart H, Jackson-Grusby L, Meissner A, Meletis K, Lo G, Jaenisch R. Suppression of intestinal neoplasia by deletion of Dnmt3b. Mol Cell Biol. 2006; 26(8): 2976-83.

20. Lamprecht B, Bonifer C, Mathas S. Repeat-element driven activation of proto-oncogenes in human malignancies. Cell Cycle. 2010; 9(21): 4276-81.

Output

Output จากโครงการวิจัยที่ได้รับทุนจาก สกว.

1. ผลงานตีพิมพ์ในวารสารวิชาการนานาชาติ

- Kitkumthorn N, Keelawat S, Rattanatanyong P, Mutirangura A. LINE-1 and Alu Methylation Patterns in Lymph Node Metastasis of Head and Neck Cancers. Asian Pac J Cancer Prev. 2012;13(9):4469-75.
- Puttipanyalears C, Subbalekha K, Mutirangura A, Kitkumthorn N. Aluhypomethylation in smoke-exposed epithelia and oral squamous carcinoma. Asian Pac J Cancer Prev. 2013; 14: 5495-5501.
- Senthong A, Kitkumthorn N, Rattanatanyong R, Khemapech N, Triratanachart S, Mutirangura A. Differences in LINE-1 Methylation between Endometriotic Ovarian Cyst and Endometriosis-Associated Ovarian Cancer. IntJ Gyn Cancer. 2014; 24: 36-42.
- Muangsub T, Samsuwan J, Tongyoo P, Kitkumthorn N, Mutirangura A. Analysis of methylation microarray for tissue specific detection. Gene.2014; 553: 31-41.
- Puttipanyalears C, Buranapraditkun S, Keelawat S, Kitkumthorn N, Mutirangura A. LINE-1 Hypermethylation in Breast Cancer Stromal Cells and Application for Micrometastatic Cancer Detection, In preparation

2. การนำผลงานวิจัยไปใช้ประโยชน์ในเชิงวิชาการ

มีการสร้างนักวิจัย

1. นายเจริญชัย พุฒิปัญญาเลิศ
นิสิตปริญญาเอกสาขาชีวเวชศาสตร์ บัณฑิตวิทยาลัย จุฬาลงกรณ์มหาวิทยาลัย
2. นายทัชพล เมืองทรัพย์
นิสิตปริญญาโท สาขาวิทยาศาสตร์การแพทย์ บัณฑิตวิทยาลัย จุฬาลงกรณ์มหาวิทยาลัย
3. ร้อยตำรวจเอกหญิง จรัญญา สามสุวรรณ
นิสิตปริญญาโท สาขาพันธุศาสตร์ คณะวิทยาศาตร์ จุฬาลงกรณ์มหาวิทยาลัย

3.ผลงานอื่น ๆ

การเสนอผลงานในที่ประชุม

- Puttipanyalears C, Buranapraditkul S, Kitkumthorn N, Mutiarngura A, LINE-1 Hypermethylation in Metastatic Lymph Node and Breast Cancer Supporting Tissue. Poster presentation in The 7th Princess Chulabhorn International Science Congress 29 November-3 December 2012 at Shangarila Hotel, Bangkok.
- Puttipanyalears C, Buranapraditkul S, Kitkumthorn N, Mutiarngura A, LINE-1 Hypermethylation in Metastatic Lymph Node and Breast Cancer Supporting Tissue. Poster presentation in The 2nd International Anatomical Sciences and Cell Biology Conference 6-8 December 2012 at Chiangmai Grand View Hotel, Chiangmai.
- Samsuwan J, Muansub T, Kitkumthorn N, Mutirangura A. Brain Specific Tissue Detection by Site-Specific CpG Methylation. Poster presentation in the 5th Asian Forensic Sciences Network (AFSN), 11 – 14 November 2013 at the Resorts World Sentosa Convention Centre, Singapore.
- Kitkumthorn N, Bumalee D, Rattanatanyong P, Mutirangura A. Detection of DNA Methylatiom in Clinical Applications. Keynote lecture in The 8th International Dental Collaboration of the Mekong River Region Congress, 5-6 December 2013 at Phnom Penh Hotel, Phnom Penh, Cambodia.
- Kitkumthorn N, Muangsub T, Samsuwan J, Tongyoo P, Mutirangura A. Methylation Microarray Analysis for Tissue Specific DNA Detection. Poster presentation in the 7th General Assembry and General Conference of Asian Pacific Organization for Cancer Prevention, March 20-23, 2014 at Academia Sinica, Taipei, Taiwan.
- Kitkumthorn N, Mutirangura A. Detection of DNA Methylatiom in Clinical Applications. Oral presentation in The 12th Dental Faculty Consortium of Thailand Acadermic Meeting and Research Presentation, 1-3 July 2014 at Cholapreuk Hotel and Resort, NakhonNayok, Thailand.
- Kitkumthorn N, Detection of DNA Methylation in Clinical Applications. Invited speaker in The 4th japan-Thailand-Korea Joint Symposium on 30th October, 2014 at School of Dentistry, Soul national University, Soul, Repulic of Korea

รางวัลที่ได้รับ

-รางวัลนักวิจัยที่มีผลงานวิจัยที่มีคุณภาพได้รับการอ้างอิงสูงที่สุดในรอบ 5 ปีที่ผ่านมา ประจำปี 2557 จากคณะทันตแพทยศาสตร์ มหาวิทยาลัยมหิดล

- รางวัลนักวิจัยที่มีผลงานวิจัยที่มีคุณภาพได้รับการอ้างอิงสูงที่สุดในรอบ 5 ปีที่ผ่านมา ประจำปี 2558 จากคณะทันตแพทยศาสตร์ มหาวิทยาลัยมหิดล

- รางวัลวิจัยอันดับ 2 ในงานประชุมวิชาการครบรอบวันสถาปนา โรงพยาบาลตำรวจ ประจำปี 2557 โดยร้อยตำรวจเอกหญิง จรัญญา สามสุวรรณ

- รางวัลระดับดี ในการประกวดผลงานวิจัย ของนิสิตระดับบัณฑิตศึกษา หลักสูตรวิทยาศาสตร์ดุษฎีบัณฑิต ประจำปี 2558 จาก ฝ่ายบัณฑิตศึกษา คณะแพทยศาสตร์ จุฬาลงกรณ์มหาวิทยาลัย โดย นายเจริญชัย พุฒิปัญญาเลิศ

Appendix

RESEARCH ARTICLE

LINE-1 and Alu Methylation Patterns in Lymph Node Metastases of Head and Neck Cancers

Nakarin Kitkumthorn[1], Somboon Keelawat[2]*, Prakasit Rattanatanyong[3], Apiwat Mutirangura[3]

Abstract

Background: The potential use of hypomethylation of Long INterspersed Element 1 (LINE-1) and Alu elements (Alu) as a biomarker has been comprehensively assessed in several cancers, including head and neck squamous cell carcinoma (HNSCC). Failure to detect occult metastatic head and neck tumors on radical neck lymph node dissection can affect the therapeutic measures taken. Objective: The aim of this study was to investigate the LINE-1 and Alu methylation status and determine whether it can be applied for detection of occult metastatic tumors in HNSCC cases. Methods: We used the Combine Bisulfite Restriction Analysis (COBRA) technique to analyse LINE-1 and Alu methylation status. In addition to the methylation level, LINE-1 and Alu loci were classified based on the methylation statuses of two CpG dinucleotides in each allele as follows: hypermethylation ($^{m}C^{m}C$), hypomethylation ($^{u}C^{u}C$), and 2 forms of partial methylation ($^{m}C^{u}C$ and $^{u}C^{m}C$). Sixty-one lymph nodes were divided into 3 groups: 1) non-metastatic head and neck cancer (NM), 2) histologically negative for tumor cells of cases with metastatic head and neck cancer (LN), and 3) histologically positive for tumor cells (LP). Results: Alu methylation change was not significant. However, LINE-1 methylation of both LN and LP was altered, as demonstrated by the lower LINE-1 methylation levels ($p<0.001$), higher percentage of $^{m}C^{u}C$ ($p<0.01$), lower percentage of $^{u}C^{m}C$ ($p<0.001$) and higher percentage of $^{u}C^{u}C$ ($p<0.001$). Using receiver operating characteristic (ROC) curve analysis, %$^{u}C^{m}C$ and %$^{m}C^{u}C$ values revealed a high level of AUC at 0.806 and 0.716, respectively, in distinguishing LN from NM. Conclusion: The LINE-1 methylation changes in LN have the same pattern as that in LP. This epigenomic change may be due to the presence of occult metastatic tumor in LN cases.

Keywords: Long INterspersed element-1s (LINE-1s) - Alu elements - DNA methylation - lymph nodes - occult tumor

Asian Pacific J Cancer Prev, **13 (9)**, 4469-4475

Introduction

DNA methylation of the human cancer genome is usually lower (hypomethylation) than in representative normal cells (Chalitchagorn, 2004; Hoffmann, 2005; Esteller, 2011; Kitkumthorn, 2011). The methylated CpG dinucleotides in 5'UTR of the two most abundant interspersed repetitive sequences, Long INterspersed Element-1 (LINE-1 or L1) and Alu elements, are frequently evaluated as representative of the genome-wide methylation levels. Genome-wide hypomethylation, which is characterized by reduced methylation levels of LINE-1 and Alu, is often present in many malignancies (Kitkumthorn, 2011). The epigenomic changes are associated with genomic instability and altered gene expression (Hoffmann, 2005; Kongruttanachok, 2010; Aporntewan, 2011). Both LINE-1 and Alu hypomethylation are also associated with advanced tumor stage, higher histological grade, poorer prognosis and tumor metastasis (Cho, 2007; Choi, 2007; Shuangshoti, 2007; Tangkijvanich, 2007; Pattamadilok, 2008; Iramaneerat, 2011; Kitkumthorn, 2011; Nopavichai, 2012).

Each LINE-1 locus has a distinct methylation level and pattern (Phokaew, 2008; Singer, 2012). To improve the efficiency of detecting cancer DNA and to measure the overall methylation level, we recently classified LINE-1s into 4 groups based on the methylation statuses of 2 CpG dinucleotides in each LINE-1 sequence. These 4 classes were hypermethylation ($^{m}C^{m}C$), hypomethylation ($^{u}C^{u}C$), and 2 forms of partial methylation ($^{m}C^{u}C$ and $^{u}C^{m}C$) (Pobsook, 2011; Kitkumthorn, 2012). We found that differences in the LINE-1 methylation pattern could be observed even if the overall levels were unchanged. Furthermore, partial methylation contributed to differences in the overall methylation levels between various normal tissue types, oral epithelium and white blood cells (Pobsook, 2011). Finally, for cancer DNA

*[1]Department of Oral and Maxillofacial Pathology, Faculty of Dentistry, Mahidol University, [2]Department of Pathology, [3]Center of Excellencein Molecular Genetics of Cancer and Human Diseases, Department of Anatomy, Faculty of Medicine, Chulalongkorn University, Bangkok, Thailand *For correspondence: trcskl@gmail.com*

detection, $\%^{u}C^{u}C$ is more sensitive and specific than the methylation level (Pobsook, 2011; Kitkumthorn, 2012).

Head and neck squamous cell carcinoma (HNSCC) is one of the most serious health problems, ranking as the sixth most common cancer worldwide (Bennett, 2008). Metastasis from these cancers can be fatal (Manikantan, 2012). The 5-year survival rate is less than 50% for patients with a single unilateral lymph node metastasis and less than 25% for patients with bilateral metastases (Zhang, 2007). Genome-wide hypomethylation has also been found to be involved in the carcinogenesis of these cancers. In a limited cohort of 6 tumor samples, we demonstrated LINE-1 hypomethylation in HNSCC versus histologically normal mucosal tissues (Chalitchagorn, 2004). This result has been confirmed by Smith et al., who determined that 67% of HNSCCs are hypomethylated compared to normal mucosal specimens (Smith, 2007). Furthermore, the latter study also demonstrated a relationship between increasing tumor stage and the degree of hypomethylation-that is, the mean levels of genome-wide methylation are reduced in the Stage IV lesions compared to the Stage I-III diseases (Smith, 2007). Moreover, in a recent study, we found that tumors at metastatic sites presented significant decreases in methylation compared with the primary lesions (Nopavichai, 2012).

Despite the important role of pathologists in cancer-staging evaluations (one of which is the diagnosis of lymph node metastasis), there are some limitations of the routine histological examination for identifying occult metastatic tumor cells. Failure to detect occult tumor cells may be due to inadequate tissue sampling or the inattention of pathologists to minuscule tumor-cell groups. These actions can cause inaccurate tumor staging and lead to improper therapeutic management (Gu, 2002; Coello, 2004; Imoto, 2006; Broglie, 2011; Rahbari, 2012). Many studies have developed methods for detecting occult tumor cells or DNA, including serial section staining, immunohistochemistry, PCR and RT-PCR-based methods (Tsavellas, 2001; Riethdorf, 2008; Wada, 2008; Shimizu, 2012); however, their conclusions have been less satisfactory. In this study, we aimed to determine whether LINE-1 and Alu methylation measurements are effective biomarkers for the detection of occult metastatic HNSCC and whether these measurements can provide a supportive method for diagnosing nodal metastases from HNSCC as an alternative to routine pathological examination.

Materials and Methods

Recruited subjects

Sixty-one lymph nodes were included in this study. All specimens were retrieved from the Department of Pathology, Faculty of Medicine, Chulalongkorn Hospital. All of the primary cancer tissue was collected from patients with diagnosed squamous cell carcinoma. Lymph node samples were derived from radical neck dissections and were classified into 3 groups: 1) lymph nodes from cases with non-metastatic head and neck cancer (NM, n=15), 2) lymph nodes from cases with metastatic head and neck cancer but histologically negative for tumor cells (LN, n=23), and 3) lymph nodes from cases with metastatic head and neck cancer and histologically positive for tumor cells (LP, n=23). The NM and LN groups were confirmed to be histologically free of cancer cells, whereas the LM group was diagnosed as having metastatic malignant cells by two pathologists (NK and SK). The lymph nodes in groups 2 and 3 (LN and LM) belonged to the same group of patients. The patients' demographic data, clinical stages and histological grades were reviewed from each patient's chart and are presented.

DNA extraction and bisulfite modification

Formalin-fixed, paraffin-embedded lymph node tissues were sliced into 3-5 sections (each of them 5 μm thick) and were then left unstained. Another section was stained with hematoxylin and eosin for pathological confirmation. After deparaffinization with xylene, the DNA was isolated using Tris/SDS and proteinase K and left at 50°C overnight, followed by phenol/chloroform extraction and ethanol precipitation. The isolated genomic DNA was eluted and then used for bisulfite treatment. Bisulfite modification of the genomic DNA was performed using previously published methods (Chalitchagorn, 2004). In brief, 200 ng of DNA was dissolved in 50 μl of distilled water, followed by denaturation in 5.5 μl of 2 M NaOH for 10 min at 37°C. Then, 30 μl of 10 mM hydroquinone (Sigma-Aldrich, Singapore) and 520 μl of 3 M sodium bisulfite (pH 5.0) were added, mixed and incubated at 50°C for 16 h. The bisulfite-treated DNA was purified using the Wizard DNA clean-up kit (Promega, Madison, WI) according to the manufacturer's protocols. After this step, the DNA was eluted with 50 μl of warm water, desulfonated with 5.5 μl of 3 M NaOH for 5 min and precipitated (with NH4OAC- EtOH) using glycogen as a carrier. Finally, the bisulfite-treated DNA was resuspended in 20 μl of water and stored at -20°C until needed for use.

Combined Bisulfite Restriction Analysis (COBRA) of LINE-1 and Alu

For COBRALINE-1, the bisulfate-treated DNA was subjected to 40 PCR cycles with LINE-1-F (5'-CCGTAAGGGGTTAGGGAGTTTTT-3') and LINE-1-R (5'-RTAAAACCCTCCRAACCAAATATAAA-3') primers at an annealing temperature of 50°C. For COBRAAlu, the bisulfite-treated DNA was subjected to 40 cycles of PCR with two primers, Alu-F (5'-GGCGCGGTGGTTTACGTTTGTAA-3') and Alu-R (5'-TTAATAAAAACGAAATTTCACCATATTAACCAAAC-3') at an annealing temperature of 53°C. After PCR amplification, the LINE-1 amplicons (160 bp) were digested with TaqIand TasI in NEB buffer 3 (New England Biolabs, Ontario, Canada) while the Aluamplicons (117 bp) were digested with TaqI in TaqI buffer (MBI Fermentas, Burlington, Canada). Both digestion reactions were incubated at 65°C overnight. The LINE-1- and Alu-digested products were then electrophoresed on an 8% non-denaturing polyacrylamide gel and stained with the SYBR green nucleic-acid gel stain (Gelstar, Lonza, USA). The intensities of both COBRA PCR fragments were measured using a phosphoimager with ImageQuant Software (Molecular Dynamics, GE Healthcare, Slough, UK). Distilled water was used as a negative control. DNA samples from HeLa, Jurkat, and Daudi cell lines were used as positive controls in every experiment to standardize the interassay variation. All experiments were performed in duplicate.

LINE-1 methylation analysis

The COBRALINE-1 amplicons generated 4 bands based on the methylation status of the 2 CpG dinucleotides as follows: $^{m}C^{u}C$, 160 bp; $^{u}C^{u}C$, 98 bp; 1 methylated CpG (^{m}C, 80 bp); and 1 unmethylatedCpG (^{u}C, 62 bp) (Figure 1A). The LINE-1 methylation level of each pattern was calculated according to previous methods (Kitkumthorn, 2012) to determine the precise percentage of CpG dinucleotides.

Briefly, the calculation was performed using the following steps. First, the intensity of each band was separated by the length (bp) of the double-stranded DNA as follows: %160/160=A, %98/94=B, %80/78=C and %62/62 =D. Second, the LINE-1 methylation levels were computed using the following formulas: percentage of overall methylated loci ($\%^{m}C$)=100×(C+A)/(C+2A+B+D), $\%^{m}C^{m}C$=100×((C-D+B)/2)/(((C-D+B)/2)+D+A), $\%^{u}C^{u}C$=100×B/(((C-D+B)/2)+A+D), $\%^{m}C^{u}C$=100×(A)/(((C-D+B)/2)+A+D) and $\%^{u}C^{m}C$=100×(D-B)/((C-D+B)/2)+A+D).

Alu methylation analysis

The COBRAAlu produced 3 bands according to the methylation status: $^{u}C^{u}C$, 117 bp; two partially methylated sequences, $^{m}C^{u}C$ and $^{u}C^{m}C$ (74 and 75 bp, respectively); and methylated loci (^{m}C, 42 and 43 bp) (Figure 1B). The Alu methylation level of each pattern was calculated to obtain the exact percentage number.

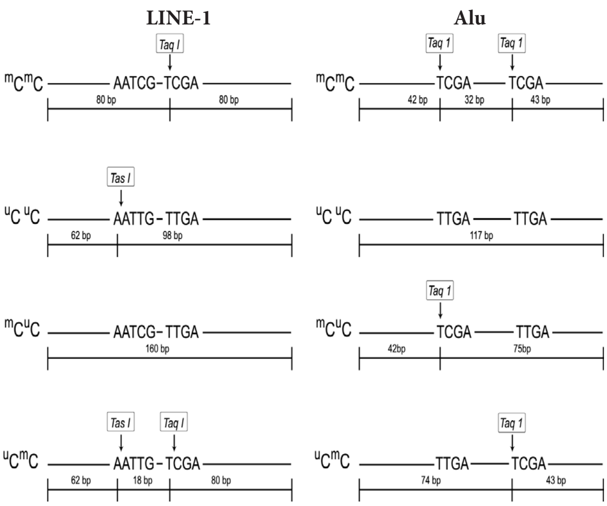

Figure 1. LINE-1 and Alu Methylation Patterns. COBRALINE-1 and COBRAAlu possess four possible methylation patterns: hypermethylated loci ($^{m}C^{m}C$), hypomethylated loci ($^{u}C^{u}C$), and 2 partially methylated loci ($^{m}C^{u}C$ and $^{u}C^{m}C$). TaqI is a restriction enzyme that is specific to methylated cytosine, whereas TasIis specific to unmethylated cytosine. a) The various methylation patterns of the digested LINE-1 PCR product yielded four differently sized digested products of 160 bp, 98 bp, 80 bp and 62 bp. b) The various methylation patterns of the Alu PCR products yielded four differently sized digested products of 117 bp, 74/75 bp, 42/43 bp and 32 bp.

The calculation was performed as follows: Initially, the intensity of each band was divided by the length (bp) of the double-stranded DNA: %117/117=A, %74 and 75/74.5=B, %42 and 43/43.5=D, and D-B=C (C=hypermethylated loci,$^{m}C^{m}C$). Then, the Alu methylation level in each pattern was calculated as follows: $\%^{m}C$=100x(2C+2B)/(2A+2B+2C)=100x(2D)/(2A+2D), $\%^{m}C^{m}C$=100xC(A+B+C), $\%^{u}C^{u}C$=100xA(A+B+C) and percentage of partially methylated loci ($\%^{u}C^{m}C+\%^{m}C^{u}C$) =100xB/(A+B+C).

Statistical Analysis

All statistical analyses were conducted using SPSS software for Windows version 17.0 (SPSS Inc., Chicago, IL). An independent sample t-test was performed to determine the difference between the NM and LN groups and between the NM and LM groups, whereas the paired t-test was used to evaluate the LN and LM groups. All p-values were two sided. The p-values that were less than 0.05 were considered statistically significant. A receiver operating characteristic (ROC) analysis was performed to verifythe ability of the COBRALINE-1 and COBRAAlu methylation status to differentiate between lymph nodes with or without occult metastatic tumor.

Results

Overall LINE-1 and Alu methylation

As shown in Table 1, Table 1 and Figure 2, the percentage of overall LINE-1 methylation (^{m}C) among

Table 1. Each Pattern and *p*-value

	$\%^{m}C$	$\%^{m}C^{m}C$	$\%^{m}C^{u}C$	$\%^{u}C^{m}C$	$\%^{u}C^{u}C$
LINE-1 methylation levels (mean%±S.D.) and p-value:					
NM (N=15)	46.42±5.38	22.86±9.22	20.03±6.44	27.10±11.57	30.01±9.21
LN (N=23)	46.01±5.13	22.89±6.70	27.17±5.70	19.08± 7.78	30.86±5.65
LP (N=23)	40.21±4.31	19.88±5.81	32.09±6.38	9.21± 8.10	39.47±6.78
p-value:					
NM vs. LN	0.817	0.991	0.001	0.016	0.728
NM vs. LP	<0.001	0.278	<0.001	<0.001	0.001
LN vs. LP	<0.001	0.136	0.007	<0.001	<0.001

	$\%^{m}C$	$\%^{m}C^{m}C$	$\%^{m}C^{u}C+\%^{u}C^{m}C$	$\%^{u}C^{u}C$
Alu methylation levels (mean%±S.D.) and p-value:				
NM (N=15)	57.09±3.42	22.74±5.67	34.35±6.53	42.91±3.42
LN (N=23)	56.01±5.49	18.45±6.43	37.56±5.62	43.99±5.49
LP (N=23)	53.08±5.56	15.13±9.83	38.36±7.42	46.92±5.56
p-value				
NM vs. LN	0.498	0.042	0.116	0.498
NM vs. LP	0.017	0.010	0.097	0.017
LN vs. LP	0.073	0.112	0.636	0.073

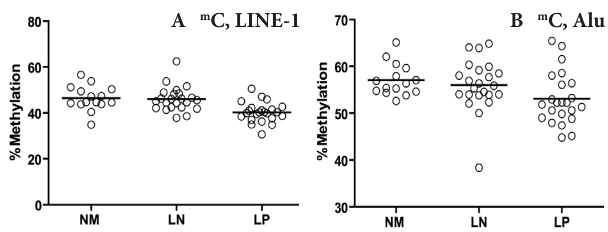

Figure 2. Comparison between the Percentages of the Overall LINE-1 and Alu Methylation Levels Among the NM, LN and LP Groups. Black horizontal bars represent the mean. '^{m}C' represents the overall levels of methylation.

the 3 groups demonstrated a stepwise decrease from NM to LN to LP, respectively. The p-values of the differences between NM and LP and between LN and LP were <0.001. However, when compared between NM and LN, the p-value was insignificant (p=0.817). The same trend was also found in Alu, i.e., the overall methylation level (^{m}C) among the 3 groups tended to decline from NM to LN to LP, respectively, though a significant difference was only observed between NM and LP (p=0.017).

Percentage of LINE-1 methylation in each pattern

The level of each LINE-1 methylation pattern and its p-value are presented in Table 1 and Figure 3. The value of %^{m}C^{m}C did not reveal significant differences among the 3 groups. However, %^{u}C^{u}C increased stepwise from NM to LN to LP; significant differences were found between NM and LP (p=0.001) and between LN and LP (p<0.001). Interestingly, the levels of partial methylation were significantly different among the 3 groups. The value of %^{m}C^{u}C progressively increased from NM to LN to LP. The predictive value of the differences between each pair was as follows: NM:LN (p=0.001), NM:LP (p<0.001) and LN:LP (p=0.007). In contrast, %^{u}C^{m}C decreased stepwise from NM to LN to LP, with significant differences between NM and LN (p=0.016), NM and LP (p<0.001), and LN and LP (p<0.001).

Alu methylation in each pattern

The level of each Alu methylation pattern is presented in Table 3 and Figure 4. Similar to LINE-1, the percentage of ^{m}C^{m}C decreased stepwise from NM to LN to LP. The difference was statistically significant between NM and LN (p=0.042) and between NM and LP (p=0.010), but the methylation rate between LN and LP was insignificant (p=0.112). In contrast, although the percentage of ^{u}C^{u}C seemed to gradually increase from NM to LN to LP, the difference was only significant between NM and LP (p=0.017). Furthermore, no significant differences in the percentage of partially methylated Alu loci were observed.

Application of the levels of partially methylated LINE-1 loci to differentiate between the LN and NM groups

Next, we evaluated the benefit of this test for the detection of occult tumor. We selected some significant data points to develop a test by setting an optimal cut-off value and using it for the calculation of the sensitivity, specificity and area under the curve (AUC). Among the various patterns of LINE-1 and Alu methylation, %^{m}C^{u}C and % ^{u}C^{m}C values of LINE-1 methylationhad the highest potential to distinguish the LN group from the NM group (Figures 5A, 5C). The %^{m}C^{u}C value yielded the maximal AUC at 0.716. This pattern could detect the occult tumor with a cut-off value of 22.94%, sensitivity of 78.26% and specificity of 66.67% (Figure 5B). Whereas, %^{u}C^{m}C yielded the highest AUC at 0.806, with a cut-off value, sensitivity and specificity of 23.98%, 78.80% and 80.00%, respectively (Figure 5D). We also determined whether the combination of these two markers could improve the diagnostic power for the detection of occult tumor. In the case of screening tests such as fine needle aspiration (FNA), the test criteria of higher %^{m}C^{u}C or lower %^{u}C^{m}C exhibited a higher sensitivity (95.30%) but lower specificity (53.30%). In contrast, using the combination of higher %^{m}C^{u}C and lower%^{u}C^{m}C for the detection of occult tumor made the test more specific (93.30%) but less sensitive (61.28%).

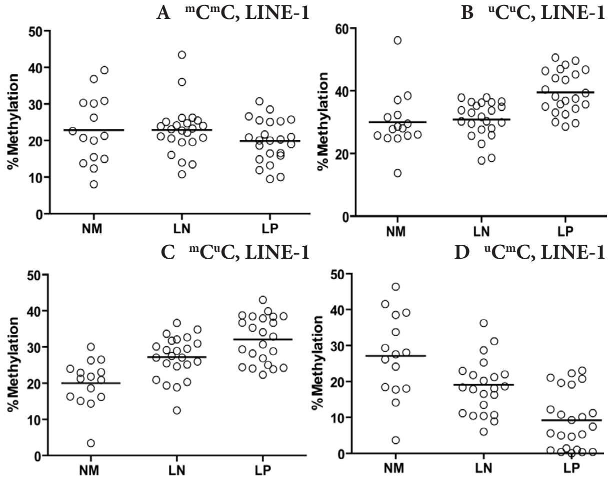

Figure 3. Comparison between the Percentages of LINE-1 Methylation Levels in Each Pattern Among the NM, LN and LP Groups. Black Horizontal bars Represent the Mean. '^{m}C^{m}C' and '^{u}C^{u}C' Represent the Hyper- and Hypomethylated LINE-1 Loci, Respectively; '^{m}C^{u}C' and '^{u}C^{m}C' Represent the Partially Methylated LINE-1 Loci.

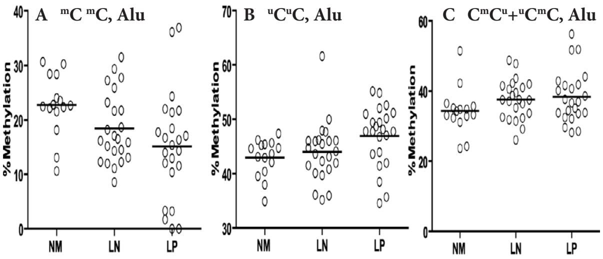

Figure 4. Comparison between the Percentages of Alu Methylation Levels Among the NM, LN and LP Groups. Black horizontal bars represent the mean. '^{m}C^{m}C' and '^{u}C^{u}C' represent the hyper- and hypomethylated Alu loci, respectively; '^{m}C^{u}C+^{u}C^{m}C' represents the total partially methylated Alu loci.

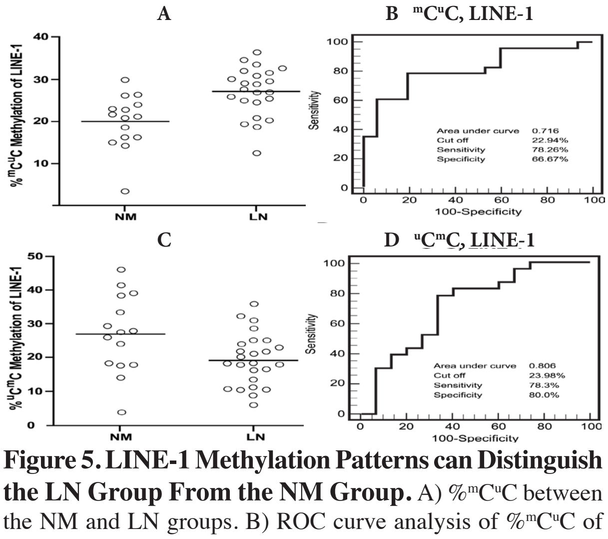

Figure 5. LINE-1 Methylation Patterns can Distinguish the LN Group From the NM Group. A) %^{m}C^{u}C between the NM and LN groups. B) ROC curve analysis of %^{m}C^{u}C of LINE-1 methylation and cancer detection. C) %^{u}C^{m}C between the NM and LN groups. D) ROC curve analysis of %^{u}C^{m}C of LINE-1 methylation and cancer detection.

Discussion

DNA methylation is one of the most commonly occurring epigenetic events in the mammalian genome and has demonstrated an important role in tumor progression (Kitkumthorn, 2011). These changes affect different types of repetitive DNA sequences, such as retrotransposons, endogenous retroviruses and satellites, in which the majority of the methylcytosines in the genome are found (Bird, 2002; Fazzari, 2004). Among these repetitive elements, LINE-1 retrotransposons comprise the largest component. They account for 20.1% of the entire human genome (Levy, 2007). Another example is the Alu-repetitive element, which makes up 13.1% of the human genome (Levy, 2007). Therefore, it is estimated that these two types of repetitive sequences together account for approximately one-third of DNA methylation and are suitable as surrogate markers for the genome-wide DNA methylation changes that are associated with multistep tumorigenesis in many types of cancers (Watanabe, 2010).

We used modified COBRALINE-1 and COBRAAlu techniques to conduct this study. These techniques were designed to detect 2 CpG dinucleotide sites, allowing us to determine not only the methylation level but also the methylation patterns of LINE-1 and Alu (Pobsook, 2011). At present, most quantitative methylation techniques, including pyrosequencing, can only measure the methylation level (usually from 3 CpG) and cannot distinguish specific LINE-1 and Alu methylation patterns. Moreover, overall methylation levels from this COBRA technique are proven to have linear correlations with the pyrosequencing technique (Jintaridth, 2010). Taken together, COBRALINE-1 and COBRAAlu are advanced and useful techniques for quantifying the methylation status of LINE-1 and Alu in genomic DNA.

Various molecular markers have been proposed for investigating the presence of occult tumor metastases in histologically negative lymph nodes; these markers include P53 mutations (Ahrendt, 2002), K-ras mutations (Ahrendt, 2002), mRNAs of specific genes (Riethdorf, 2008) and the methylation of specific gene promoters (Harden, 2003). However, the targets for amplification of these markers exist as only 2 copies per cell and provided low efficacy when evaluating DNA from paraffin embedded tissues. In our study, we used interspersed repetitive sequences, including LINE-1 and Alu, as targets. The measurement of these markers has the advantage of increasing the sensitivity of detection of occult tumor metastases.

Our results confirmed that both LINE-1 and Alu demonstrated decreased methylation levels in the lymph nodes that contained metastatic disease compared to the cases without lymph node metastasis (N0). We also found that in the same group of patients with positive nodal status, negative nodes also demonstrated some evidence of hypomethylation, the level of which was intermediate between the cases with negative nodal status and the matched cases with true positive nodes. This phenomenon may be due to the effect of occult metastatic tumor, which is possibly not detected in routine pathological examination.

In this study, neither LINE-1 nor Alu methylation levels were correlated with the clinical stage or histological grade (data not shown), which was in agreement with the previous study (Smith, 2007). This finding may have been because our tumor samples were not retrieved using a microdissection procedure; therefore, the mixed cell types of the tumor and adjacent lymph node affected these results.

We also observed that the percentages of the $^{m}C^{u}C$ and $^{u}C^{m}C$ loci of LINE-1 were potentially suitable as supplement measures to detect lymph node metastasis because these measurements yielded the strongest differentiation power between the 3 groups of lymph nodes. By setting cut-off values for these two loci and applying them in combination, we can develop a test useful for distinguishing the lymph nodes that are positive for metastatic tumor. To obtain high sensitivity (as is yielded by FNA for screening metastatic lymph nodes), the test criteria of %$^{m}C^{u}C$ higher than 22.94% or %$^{u}C^{m}C$ lower than 23.98% is proposed. In contrast, if the test requires high specificity (i.e., to support a definitive diagnosis), the criteria of %$^{m}C^{u}C$ higher than 22.94% and %$^{u}C^{m}C$ lower than 23.98% should be applied. We do not recommend that this test be used for confirmation because, in our opinion, the histopathological examination should remain the gold standard for a definitive diagnosis. To integrate this test into clinical practice, an algorithm is proposed for the management approach in the routine radical neck dissection of lymph nodes (Figure 6).

In conclusion, our study clearly demonstrated the difference in the hypomethylation of both LINE-1 and Alu between the lymph nodes with metastatic HNSCC and the cases with negative nodes. We also found that the negative nodes from cases with metastatic nodal status demonstrated some tendency toward hypomethylation, which, in our opinion, implied occult metastatic tumor. Apart from confirming the occurrence of hypomethylation in HNSCC that has been reported in previous studies (Smith, 2007), our findings also suggest the potential use of this technology as an ancillary tool for detecting occult metastatic tumor in lymph node metastases; however, tumor cells are not detected by routine pathological

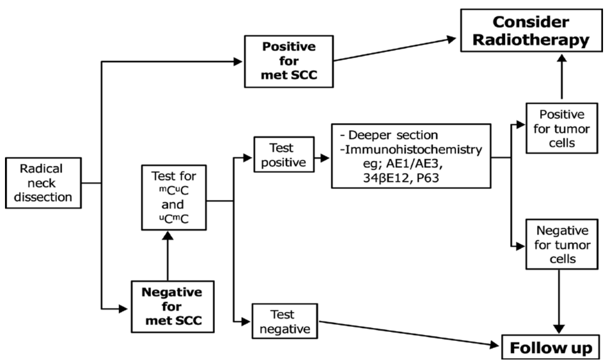

Figure 6. Proposed Algorithm for the Diagnosis and Management of Radical Neck Dissection with Integration of $^{m}C^{u}C$ and $^{u}C^{m}C$ into the Approach. *met SCC, metastatic squamous cell carcinoma; IHC, immunohistochemistry, **Test positive =%$^{m}C^{u}C$ higher than 22.94% and %$^{u}C^{m}C$ lower than 23.98%, Test negative =%$^{m}C^{u}C$ lower than 22.94% or %$^{u}C^{m}C$ higher than 23.98%.

examination. This technique may also be helpful for the diagnosis of metastatic diseases in fine-needle-aspiration cytology specimens. Despite a strong possibility for use in future clinical practice, these data are still post diagnosis evaluation. Further study in prediagnosis set up is warranted before this technique can be employed as a part of a laboratory investigation.

Acknowledgements

We thank the staff of the Department of Pathology, Faculty of Medicine, Chulalongkorn University,Bangkok for their assistance in collecting the samples. This study was financially supported by Research Chair Grant 2011 from the National Science and Technology Development Agency (NSTDA), Thailand, Grant no RSA5580013 from Thailand Research Fund and the Four Seasons Hotel Bangkok's 4th Cancer Care charity fun run in coordination with the Thai Red Cross Society and Chulalongkorn University.

References

Ahrendt SA, Yang SC, Wu L, et al (2002). Molecular assessment of lymph nodes in patients with resected stage I non-small cell lung cancer: preliminary results of a prospective study. *J Thorac Cardiovasc Surg*, **123**, 466-73.

Aporntewan C, Phokaew C, Piriyapongsa J, et al (2011). Hypomethylation of intragenic LINE-1 represses transcription in cancer cells through AGO2. *PLoS One*, **6**, 17934.

Bennett KL, Karpenko M, Lin MT, et al (2008). Frequently methylated tumor suppressor genes in head and neck squamous cell carcinoma. *Cancer Res*, **68**, 4494-9.

Bird A (2002). DNA methaile SR, Stoeckli SJ (2011). Long-term experience in sentinel node biopsy for early oral and orophylation patterns and epigenetic memory. *Genes Dev*, **16**, 6-21.

Broglie MA (2012). Haryngeal squamous cell carcinoma. *Ann Surg Oncol*, **18**, 2732-8.

Chalitchagorn K, Shuangshoti S, Hourpai N, et al (2004). Distinctive pattern of LINE-1 methylation level in normal tissues and the association with carcinogenesis. *Oncogene*, **23**, 8841-6.

Cho NY, Kim BH, Choi M, et al (2007). Hypermethylation of CpG island loci and hypomethylation of LINE-1 and Alu repeats in prostate adenocarcinoma and their relationship to clinicopathological features. *J Pathol*, **211**, 269-77.

Choi IS, EstecioMR, Nagano Y, et al (2007). Hypomethylation of LINE-1 and Alu in well-differentiated neuroendocrine tumors (pancreatic endocrine tumors and carcinoid tumors). *Mod Pathol*, **20**, 802-10.

Coello MC, Luketich JD, Litle VR, Godfrey TE (2004). Prognostic significance of micrometastasis in non-small-cell lung cancer. *Clin Lung Cancer*, **5**, 214-25.

Esteller M (2011). Epigenetic changes in cancer. *F1000 Biol Rep*, **3**, 9.

Fazzari MJ, Greally JM (2004). Epigenomics: beyond CpG islands. *Nat Rev Genet*, **5**, 446-55.

Gu CD, Osaki T, Oyama T, et al (2002). Detection of micrometastatic tumor cells in pN0 lymph nodes of patients with completely resected nonsmall cell lung cancer: impact on recurrence and Survival. *Ann Surg*, **235**, 133-9.

Harden SV, Tokumaru Y, Westra WH, et al (2003). Gene promoter hypermethylation in tumors and lymph nodes of stage I lung cancer patients. *Clin Cancer Res*, **9**, 1370-5.

Hoffmann MJ, Schulz WA (2005). Causes and consequences of DNA hypomethylation in human cancer. *Biochem Cell Biol*, **83**, 296-321.

Imoto S, Ochiai A, Okumura C, Wada N, Hasebe T (2006). Impact of isolated tumor cells in sentinel lymph nodes detected by immunohisto chemical staining. *Eur J Surg Oncol*, **32**, 1175-9.

Iramaneerat K, Rattanatunyong P, Khemapech N, Triratanachat S, Mutirangura A (2011). HERV-K hypomethylation in ovarian clear cell carcinoma is associated with a poor prognosis and platinum resistance. *Int J Gynecol Cancer*, **21**, 51-7.

Jintaridth P, Mutirangura A (2010). Distinctive patterns of age-dependent hypomethylation in interspersed repetitive sequences. *Physiol Genomics*, **41**, 194-200.

Kitkumthorn N, Mutirangura A (2011). Long interspersed nuclear element-1 hypomethylation in cancer: biology and clinical application. *Clin Epigenet*, **2**, 315-30.

Kitkumthorn N, Tuangsintanakul T, Rattanatanyong P, Tiwawech D, Mutirangura A (2012). LINE-1 methylation in the peripheral blood mononuclear cells of cancer patients. *Clinica Chimica Acta*, **413**, 869-74.

Kongruttanachok N, Phuangphairoj C, Thongnak A, et al (2010). Replication independent DNA double-strand break retention may prevent genomic instability. *Mol Cancer*, **9**, 70.

Levy S, Sutton G, Ng PC, et al (2007). The diploid genome sequence of an individual human. *PLoS Biol*, **5**, 254.

Manikantan K, Dwivedi RC, Sayed SI, Pathak KA, Kazi R (2012). Current concepts of surveillance and its significance in head and neck cancer. *Ann R Coll Surg Engl*, **93**, 576-82.

Nopavichai C, Sanpawat A, Kantabandit P, Mutirangura A, Shuangshoti S (2012). Changes in LINE-1 methylation level in cancers during metastasis. *Asian Biomedicine*, **6**, 307-12.

Pattamadilok J, Huapai N, Rattanatanyong P, et al (2008). LINE-1 hypomethylation level as a potential prognostic factor for epithelial ovarian cancer. *Int J Gynecol Cancer*, **18**, 711-7.

Phokaew C, Kowudtitham S, Subbalekha K, Shuangshoti S, Mutirangura A (2008). LINE-1 methylation patterns of different loci in normal and cancerous cells. *Nucleic Acids Res*, **36**, 5704-12.

Pobsook T, Subbalekha K, Sannikorn P, Mutirangura A (2011). Improved measurement of LINE-1 sequence methylation for cancer detection. *Clin Chim Acta*, **412**, 314-21.

Rahbari NN, Bork U, Motschall E, et al (2012). Molecular detection of tumor cells in regional lymph nodes is associated with disease recurrence and poor survival in node-negative colorectal cancer: a systematic review and meta-analysis. *J Clin Oncol*, **30**, 60-70.

Riethdorf S, Wikman H, Pantel K (2008). Review: Biological relevance of disseminated tumor cells in cancer patients. *Int J Cancer*, **123**, 1991-2006.

Shimizu Y, Takeuchi H, Sakakura Y, et al (2012). Molecular Detection of Sentinel Node Micrometastases in Patients with Clinical N0 Gastric Carcinoma with Real-time Multiplex Reverse Transcription-Polymerase Chain Reaction Assay. *Ann Surg Oncol*, **19**, 469-77.

Shuangshoti S, Hourpai N, Pumsuk U, Mutirangura A (2007). Line-1 hypomethylation in multistage carcinogenesis of the uterine cervix. *Asian Pac J Cancer Prev*, **8**, 307-9.

Singer H, Walier M, Nusgen N, et al (2012). Methylation of L1Hs promoters is lower on the inactive X, has a tendency of being higher on autosomes in smaller genomes and shows inter-individual variability at some loci. *Hum Mol Genet*, **21**, 219-35.

Smith IM, Mydlarz WK, Mithani SK, Califano JA (2007). DNA global hypomethylation in squamous cell head and neck cancer associated with smoking, alcohol consumption and stage. *Int J Cancer*, **121**, 1724-8.

Tangkijvanich P, Hourpai N, Rattanatanyong P, et al (2007). Serum LINE-1 hypomethylation as a potential prognostic marker for hepatocellular carcinoma. *Clin Chim Acta*, **379**, 127-33.

Tsavellas G, Patel H, Allen-Mersh TG (2001). Detection and clinical significance of occult tumour cells in colorectal cancer. *Br J Surg*, **88**, 1307-20.

Wada N, Imoto S (2008). Clinical evidence of breast cancer micrometastasis in the era of sentinel node biopsy. *Int J Clin Oncol*, **13**, 24-32.

Watanabe Y, Maekawa M (2010). Methylation of DNA in cancer. *Adv Clin Chem*, **52**, 145-67.

Zhang X, Hunt JL, Shin DM, Chen ZG (2007). Down-regulation of S100A2 in lymph node metastases of head and neck cancer. *Head Neck*, **29**, 236-43.

RESEARCH ARTICLE

Alu Hypomethylation in Smoke-Exposed Epithelia and Oral Squamous Carcinoma

Charoenchai Puttipanyalears[1], Keskanya Subbalekha[2]*, Apiwat Mutirangura[1], Nakarin Kitkumthorn[3]*

Abstract

Background: Alu elements are one of the most common repetitive sequences that now constitute more than 10% of the human genome and potential targets for epigenetic alterations. Correspondingly, methylation of these elements can result in a genome-wide event that may have an impact in cancer. However, studies investigating the genome-wide status of Alu methylation in cancer remain limited. Objectives: Oral squamous cell carcinoma (OSCC) presents with high incidence in South-East Asia and thus the aim of this study was to evaluate the Alu methylation status in OSCCs and explore with the possibility of using this information for diagnostic screening. We evaluated Alu methylation status in a) normal oral mucosa compared to OSCC; b) peripheral blood mononuclear cells (PBMCs) of normal controls comparing to oral cancer patients; c) among oral epithelium of normal controls, smokers and oral cancer patients. Materials and Methods: Alu methylation was detected by combined bisulfite restriction analysis (COBRA) at 2 CpG sites. The amplified products were classified into three patterns; hypermethylation ($^{m}C^{m}C$), partial methylation ($^{u}C^{m}C$+$^{m}C^{u}C$), and hypomethylation ($^{u}C^{u}C$). Results: The results demonstrate that the %$^{m}C^{m}C$ value is suitable for differentiating normal and cancer in oral tissues (p=0.0002), but is not significantly observe in PBMCs. In addition, a stepwise decrease in this value was observed in the oral epithelium from normal, light smoker, heavy smoker, low stage and high stage OSCC (p=0.0003). Furthermore, receiver operating characteristic (ROC) curve analyses demonstrated the potential of combined %^{m}C or %$^{m}C^{m}C$ values as markers for oral cancer detection with sensitivity and specificity of 86.7% and 56.7%, respectively. Conclusions: Alu hypomethylation is likely to be associated with multistep oral carcinogenesis, and might be developed as a screening tool for oral cancer detection.

Keywords: Alu element - hypomethylation - oral cancer - smoke-exposed epithelia

Asian Pac J Cancer Prev, **14 (9)**, 5495-5501

Introduction

Oral squamous cell carcinoma (OSCC) is the most frequent malignant neoplasm of the oral cavity which represents approximately 3% of all malignancies affecting humans (Yasusei et al., 2004; Song et al., 2011). OSCC accounts for more than five hundred thousand newly diagnosed cases every year worldwide (Massimo et al., 1995; Massimo et al., 2012). Generally, the highest incidence rates of oral cancer are found in South-East Asia, and Central and Eastern Europe for both males and females (Ahmedin et al., 2011). Because of its high mortality and low cure rate, OSCC represents a major global public health and socioeconomic problem (Massimo et al., 2012). At present, OSCC still lacks reliable diagnostic and prognostic molecular markers.

Cancers including OSCC are now known to develop and progress through a series of genetic and epigenetic alterations (Lingen et al., 2011; Saintingny et al., 2011). While on one hand genetic aberrations constitute irreversible changes (increased copy number) or mutations in the DNA coding sequences resulting in overexpression/increased activity or inactivation, of key oncogenes and tumor suppressor genes, respectively (Lingen et al., 2011; Saintigny et al., 2011). On the other hand, promoter hypermethylation of tumor suppressor gene and genome-wide hypomethylation are the main features commonly associated epigenetics events (Chalitchagorn et al., 2004; Kitkumthorn and Mutirangura, 2011; Song et al., 2011). Of interest though, both types of alterations are now thought to occur in the transition of normal oral epithelium to premalignant lesion and to overt carcinomas (Diez-Perez et al., 2011; Lingen et al., 2011). Furthermore, with recent data suggesting that smoking related oral premalignant conditions might be associated with genome-wide hypomethylation (Demarini, 2004; Ian et al., 2007; Subbalekha et al., 2009) further investigation can likely afford the possibility of identifying novel molecular markers of OSCC.

Genome-wide hypomethylation can occur on

*[1]Department of Anatomy, Faculty of Medicine, [2]Department of Oral and Maxillofacial Surgery, Faculty of Dentistry, Chulalongkorn University, [3]Department of Oral and Maxillofacial Pathology, Faculty of Dentistry, Mahidol University, Bangkok, Thailand *For correspondence: Skeskanya@gmail.com, Nakarinkit@gmail.com*

interspersed repetitive sequences (IRS) and are dispersed throughout the genome. Long Interspersed Element 1 (LINE-1) and Alu accounting for the majority of IRS can likely represent key targets for genome-wide methylation that can lead to abnormal epigenetic events and consequently cancer. However, while the methylation status of LINE-1 is now reported to be widespread in many cancers, corresponding analysis of Alu methylation remains sparse and unclear (Debra et al., 2007; Moore et al., 2008; Hou et al., 2010; Wilhelm et al., 2010; Pobsook et al., 2011).

Fundamentally, Alu elements are Short Interspersed Elements (SINEs), widely dispersed with a notably high copy number (~500,000 copies) and accounting for ~10% of the human genome (Rubin et al., 1980). Thus, Alu elements can represent likely targets for genome-wide methylation (Xiang et al., 2010; Nakkuntod et al., 2011). In general though, Alu elements are normally methylated and transcriptionally inactive, but in certain stress-induced conditions, for example cellular heat shock, can lead to demethylation (hypomethylation) of CpG islands and activate Alu transcription (Peter et al., 2008). Although Alu transcripts are not protein encoding, nonetheless they can regulate associated gene expression, affecting processes such gene recombination, chromosome translocation, nucleosome formation and genome evolution that impacts genomic instability (Alexandros et al., 2008; Ana et al., 2009; Kristy et al., 2009).

While reduction in Alu methylation levels have been observed in several cancers (breast, colon, stomach, liver, lung, ovarian, urinary bladder, prostate gland) (Choi et al., 2007; 2009; Rodriguez et al., 2008; Watts et al., 2008; Yoo et al., 2008; Bollati et al., 2009; Daskalos et al., 2009; Lee et al., 2009; Park et al., 2009; Cho et al., 2010; Hehuang et al., 2010; Hou et al., 2010; Kwon et al., 2010; Xiang et al., 2010; Yoshida et al., 2011), those occurring in OSCC have not been reported. Here, we evaluated and compared levels and pattern of Alu methylation levels in formalin-fixed and paraffin-embedded (FFPE) specimens of normal and OSCC ,and in peripheral blood mononuclear cells (PBMCs). Furthermore, we compared this emerging data with that of oral rinse samples from control patients and those with OSCC with known smoking habit that may provide new knowledge of Alu methylation in the pathogenesis of oral cancer.

Materials and Methods

Samples

In this study, samples were retrieved from 3 patient cohorts collected during January-December 2011. The demographics of these patient samples were collected from the available answer from questionnaires and records (Table 1). The patient cohorts that were used in this study include:

Cohort 1

FFPE archived cases (9 OSCC and 22 normal oral mucosa) were derived from the Faculty of Dentistry, Chulalongkorn University. From each retrieved case, 3-5 sections of approximately 5 μm-thickness, were prepared onto clean microscopic glass slides. One section underwent haematoxylin and eosin (H&E) staining, which than used for confirmatory histopathological evaluation by a pathologist (NK). All oral cancer samples consisting of at least 80% tumor cells were included for analysis.

Table 1. Demographic Data of All Sample Groups

Sample groups	N	Male:Female	Age (Average±SD)
Paraffin-embedded tissue			
Normal	22	6:16	47.59±13.87
Oral cancer	9	5:4	64.33±14.76
PBMCs			
Normal	31	14:17	48.28±11.78
Oral cancer	36	16:20	63.03±11.58
Oral rinse			
Normal (Non-smoker)	42	12:31	48.37±11.65
Light smoker	42	36:6	41.09±8.06
Heavy smoker	24	19:5	55.21±9.66
Oral cancer	43	21:22	60.40±12.95
Low stage (I+II)	14	5:9	63.79±11.68
High stage (III+IV)	29	16:13	58.76±13.41

Cohort 2

The PBMCs were derived from 36 patients with OSCC (36) and normal controls (31) and patients. The collection was carried out at three centers (Rajavithi Hospital, Bangkok; Buddhachinaraj Hospital, Bangkok; Faculty of Dentistry, Chulalongkorn University, Bangkok). Patients who had prior chemotherapy or radiotherapy were excluded. From each patient, six mL of blood was collected in heparinized tube, which than after underwent Ficoll-Hypaque centrifugation to separate the PBMCs which were used as source for DNA extraction.

Cohort 3

A total of 153 oral rinse samples were collected. Sample groups included normal, which was essentially sub-divided into non-smoker (42) and light to heavy smokers (66). The remaining group constituted samples from patients with histopathologically confirmed OSCC (43). Oral rinse from OSCC patients was collected prior to any treatment. All oral rises was done with 10 mL of sterile 0.9% normal saline solution and after gargling for 15 sec, solutions underwent centrifugation, and the cell pellet underwent DNA extraction within 24 hours of collection (see below). Total oral cancers were classified into 2 groups depended on patient pathological status including low and high stage oral cancer.

All participating subjects in cohorts 2 and 3 were given a self-administered questionnaire to collect medical history and information on smoking, prior to sample collection. Smoking consumption as number of years smoked, number of cigarettes smoked daily, age at which patient started smoking and the numbers of years since quitting, were carefully recorded. However, total smokers were divided into light and heavy smoker groups base on the average mean of pack/year value as previously described (Godtfredsen et al., 2004). After completing the questionnaire, patients underwent clinical examination by an oral surgeon (KS) and confirmation of patient histopathology by a pathologist (NK), prior to oral

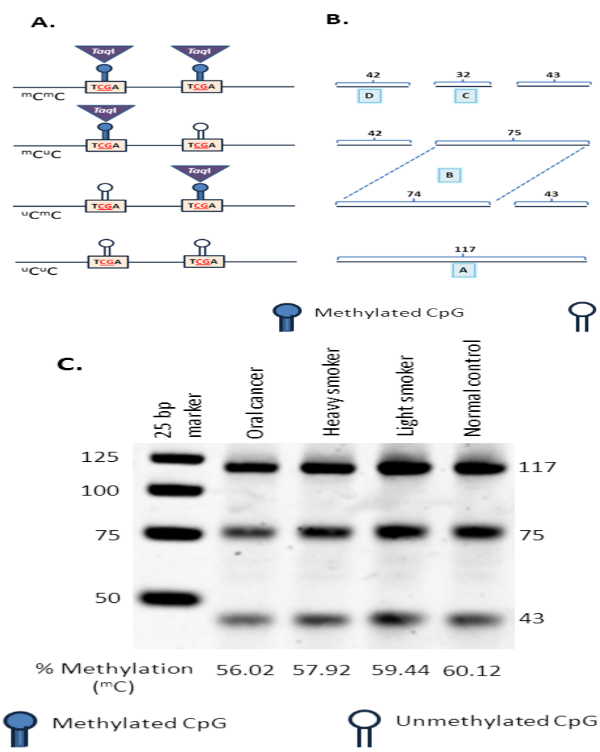

Figure 1. Alu Methylation Pattern in COBRA Alu Method. Amplified products digested with *TaqI* are represented in 3 patterns; hypermethylation ($^{m}C^{m}C$) 42/43 base pair (bp), partial methylation ($^{m}C^{u}C$+$^{u}C^{m}C$) 74/75 bp and hypomethylation ($^{u}C^{u}C$) 117 bp. **A)** *TaqI* can digest only methylated CpG; **B)** different pattern of amplified product after *TaqI* digestion including A, B, C, and D which used calculate % methylation; and **C)** Gel electrophoresis showing 3 size of *TaqI* digested amplified product (117bp, 75 bp and 43 bp) in the indicated groups of oral rinse samples

rinse was collection. All samples were obtained under a protocol approved by the Ethics Committee, Faculty of Dentistry, Chulalongkorn University, Thailand (approval number: 7/2010) and signed informed consent.

DNA extraction

Cells from oral rinses and PBMCs were centrifuged at 4°C at 2500 rpm for 15 min. Next, the supernatant from oral rinse samples was discarded and the resulting cell pellets resuspended in sterile PBS. For PBMCs, after standard Ficoll-Hypaque centrifugation, the layer corresponding to PBMCs was removed and placed in PBS for washing. Washed cells were centrifuged at 4°C at 2,500 rpm for 15 min and the resulting pellet underwent DNA extraction with 1 mL of extraction buffer supplemented with 10% SDS and proteinase K 0.5 mg/mL. For FFPE tissue sections, these first underwent de-paraffination in xylene prior to lysing the tissue off the slide with 1 mL of extraction buffer and than transferring the extracts to a clean eppendorf tube. All the lysed extracts were first incubated at 50°C for 72h, and then 0.5 mL of phenol-chloroform solution was added to each before mixing thoroughly. After, the mixtures were centrifuged at 4°C at 14000g for 15 min and for each sample, the resulting clear upper phase was carefully removed and transferred to a clean eppendorff tube and the DNA precipitated by adding 10M ammonium acetate and absolute ethanol. The precipitated DNA was than centrifuged at 14000g, washed with 70% ethanol and after air drying, the pellet was re-suspended in distill water and used for COBRA Alu anaysis.

Combined bisulfite restriction analysis of Alu (COBRA Alu)

All DNA samples were converted to bisulfite DNA by using sodium bisulfate as previously described (Chalitchagorn et al., 2004). Briefly, a total of 1 μg of DNA of each sample first underwent denaturation in 0.22 M NaOH at 37°C for 10 min and after the addition of 10 mM hydroquinone (Sigma-Aldrich, Singapore) and 3M sodium bisulfite (pH 5.0) samples underwent an additional incubation at 50°C for 16-20h. After, DNA was recovered using the Wizard DNA Clean-Up Kit (Promega, Madison, WI) following the manufacturer's protocol. DNA samples were eluted from the columns by distilled water and precipitated with sodium acetate and 100% ethanol as indicated previously. Then, COBRA Alu was performed as previously described (Kitkumthorn et al., 2012; Sirivanichsunthorn et al., 2013). Briefly, the modified DNA pellets were resuspended in distilled water 1 μL of this was subject to 45 cycles of PCR using forward (GGCGCGGTGGTTTACGTTTGTAA) and reverse (TTA ATAAAAACGAAATTTCACCATATTAACCAAAC) primers with an annealing temperature of 53°C. After, all amplified products were than digested with 2U of *TaqI* in *TaqI* buffer (MBI Fermentas, Glen Burnie, MD) overnight at 65°C. The digested products were identified by 8% non-denaturing polyacrylamide gel electrophoresis and visualized with SYBR green.

Alu methylation analysis and calculation

The amplified products of DNA samples from the 3 patient cohorts were classified into 3 types depended on the methylation pattern of the 2 CpG dinucleotides. These are the hypermethylated ($^{m}C^{m}C$), partial methylated ($^{u}C^{m}C$ and $^{m}C^{u}C$) and hypomethylated loci ($^{u}C^{u}C$). After enzyme digestion, three product size (117bp, 75bp, 43bp) depending on the methylation status of the loci are generally detected as shown in Figure 1. Then, band intensities can be measured and quantitated by a phosphoimager using ImageQuant Software (Molecular Dynamics, GE Healthcare, Slough, UK). Next, the percentage of each methylation pattern can be calculated using the following; First, the intensity of each band is divided by bp of DNA length; %117/117=A, %75(74)/74.5=B, %42(43)/42.5=D and C (represent of $^{m}C^{m}C$)=D-B. After that, the percentage of methylation was calculated as following formula; $^{m}C=100\times(2D)/(2A+2D)$, $^{m}C^{m}C=100\times C/(A+B+C)$, $^{u}C^{m}C+^{m}C^{u}C=100\times B/(A+B+C)$ and $^{u}C^{u}C=100\times A/(A+B+C)$.

DNA extracted from HeLa, DauDi and JurKat cell lines were used as positive controls in the experiments and for inter-assay adjustments.

Statistical analysis

Statistical analysis was performed using SPSS software for Windows version 17.0 (SPSS Inc., Chicago, IL). Analysis of variance (ANOVA) and independent

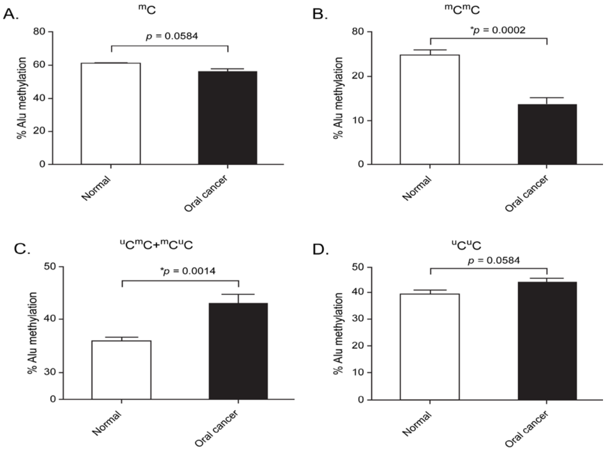

Figure 2. Comparisons of COBRA Alu Methylation Levels in FFPE Derived Normal Oral Mucosa and Oral Cancer Tissue

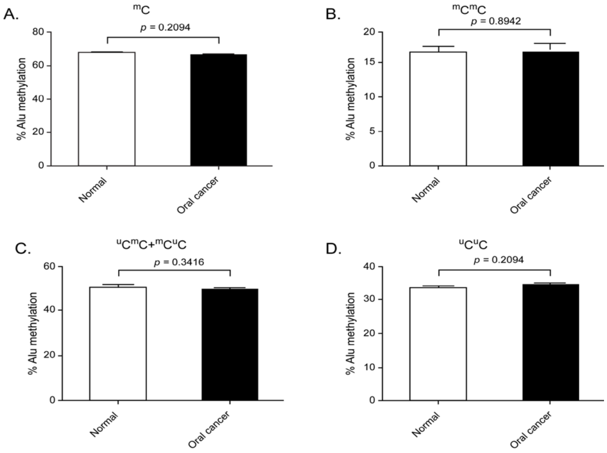

Figure 3. Comparison of Alu Methylation Levels in PBMCs from Normal and Oral Cancer Patients

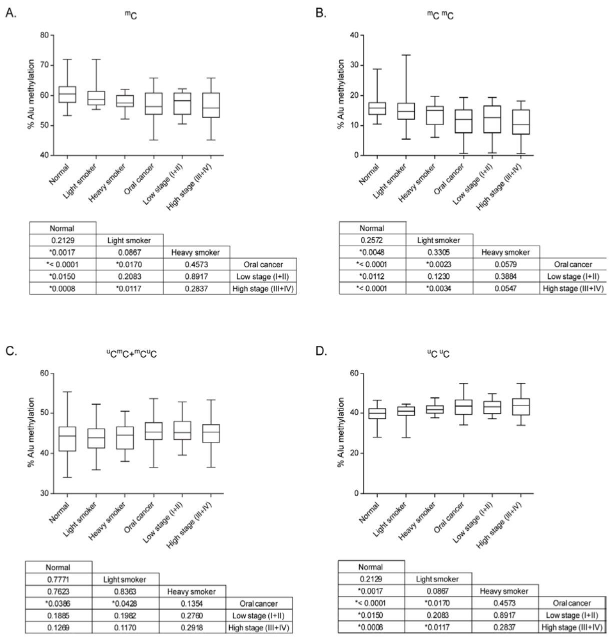

A.

Normal			
0.2129	Light smoker		
*0.0017	0.0867	Heavy smoker	
*< 0.0001	*0.0170	0.4573	Oral cancer
*0.0150	0.2083	0.8917	Low stage (I+II)
*0.0008	*0.0117	0.2837	High stage (III+IV)

B.

Normal			
0.2572	Light smoker		
*0.0048	0.3305	Heavy smoker	
*< 0.0001	*0.0023	0.0579	Oral cancer
*0.0112	0.1230	0.3884	Low stage (I+II)
*< 0.0001	*0.0034	0.0547	High stage (III+IV)

C.

Normal			
0.7771	Light smoker		
0.7623	0.8363	Heavy smoker	
*0.0386	*0.0428	0.1354	Oral cancer
0.1885	0.1982	0.2760	Low stage (I+II)
0.1269	0.1170	0.2918	High stage (III+IV)

D.

Normal			
0.2129	Light smoker		
*0.0017	0.0867	Heavy smoker	
*< 0.0001	*0.0170	0.4573	Oral cancer
*0.0150	0.2083	0.8917	Low stage (I+II)
*0.0008	*0.0117	0.2837	High stage (III+IV)

Figure 4. Comparisons of Alu Methylation Levels in Oral Rinses from Normal Controls, Light Smokers, Heavy Smokers, Total Oral Cancer, Low Stage Oral Cancer and High Stage Oral Cancer

sample t-test was performed to calculate significant differences in normal oral epithelium and oral cancer epithelium. All p values were obtained by two sided and values <0.05 were considered to be statistically significant. A receiver-operating characteristic (ROC) curve was used to test the feasibility of the COBRA Alu method of analysis of methylation status could distinguish between normal oral mucosa and oral cancer.

Results

Alu methylation status comparing normal oral mucosa and oral cancer tissues

In this analysis, we observed the frequency of each Alu methylation pattern compare between normal oral mucosa and oral cancer FPPE tissue samples. The results as shown in Table 1 and Figure 2 (A-D), indicate that overall methylation levels (^{m}C) in oral cancer, was lower than normal oral mucosa (p=0.0584). Moreover, when same comparison was done using $\%^{m}C^{m}C$ values, this difference was significantly lower in oral cancer tissue (p<0.0002). In contrast, the partial methylation levels and the $\%^{u}C^{u}C$ values in oral cancer tissues was higher than normal oral mucosa with p value=0.0014 and 0.0584. Overall, the data suggest that Alu hypomethylation were found in oral cancer tissue especially when observed in $\%^{m}C^{m}C$ value.

Comparisons of Alu methylation status between PBMCs from normal and oral cancer patients

As our previous analysis indicated that there was a clear difference in the methylation levels between normal oral mucosa and oral cancer tissue, we questioned if we would find a similar trend in PBMCs isolated from independent groups of normal and oral cancer patients. As shown when performing this analysis, Alu methylation levels and pattern were found to be only different between the two groups of PBMCs (p=0.2094; Figure 3). However, the decrease of methylation level was not found in the comparison of $\%^{m}C^{m}C$ and $\%^{u}C^{m}C+^{m}C^{u}C$.

Comparison of Alu methylation status in oral rinse samples from normal, light smoker, heavy smoker and oral cancer patients

Since our analysis using PBMCs showed only a marginal difference between normal and oral cancer patients, we sought to address if DNA from oral rinse may hold value. Cellular material from oral rinse from normal, smokers (light and heavy) and oral cancer patients was used to extract DNA and perform methylation analysis. The overall methylation level and the p value decreased respectively, from normal oral epithelium, light smoker (p=0.2129), heavy smoker (p=0.0017) and oral cancer (p<0.0001). Moreover, the ^{m}C level decreased from low stage (stage I and II) to high stage (stage III and IV) oral cancer (p=0.0150 and p=0.0008), respectively (Table 2). Conversly, hypomethylation pattern is observed to be highly elevated in patients with oral cancer and those who exposed smoking related carcinogens than in normal oral epithelium. However, no significant difference in the analysis of partial methylation pattern was observed. (Figure 4).

Table 2. Percentage of Alu Methylation Levels in All Sample Groups

Sample groups		Level (Average±SD)			
		^{m}C	$^{m}C^{m}C$	$^{u}C^{m}C+^{m}C^{u}C$	$^{u}C^{u}C$
Paraffin-embedded tissue	Normal	60.62±5.65	24.63±6.79	35.99±3.04	39.38±5.65
	Oral cancer	56.46±4.77	13.65±4.57	42.81±5.16	43.54±4.77
PBMCs	Normal	66.68±3.52	16.25±6.11	50.43±5.26	33.32±3.52
	Oral cancer	65.56±3.67	16.48±7.89	49.08±6.16	34.44±3.67
Oral rinse	Normal (Non-smoker)	60.41±3.37	16.44±3.93	43.97±4.30	39.59±3.37
	Light smoker	59.48±3.39	15.26±5.40	44.22±3.73	40.52±3.39
	Heavy smoker	57.81±2.52	13.53±3.80	44.28±3.13	42.19±2.52
	Oral cancer	56.58±4.84	11.08±5.27	45.50±3.43	43.42±4.84
	Low stage (I+II)	57.42±3.69	11.56±5.63	45.86±3.59	42.58±3.69
	High stage (III+IV)	56.17±5.31	10.84±5.18	45.33±3.40	43.83±5.31

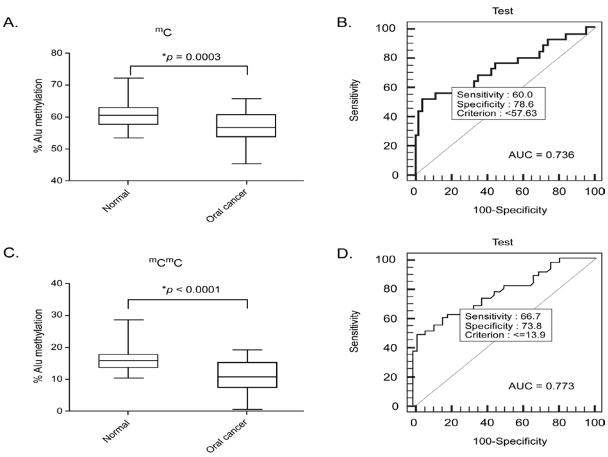

Figure 5. ROC Curve Analysis of Pair Data between Normal and Oral Cancer. Combined sensitivity (^{m}C or $^{m}C^{m}C$) calculated by 100%-[false negative ^{m}C×false negative $^{m}C^{m}C$] and combined specificity (^{m}C or $^{m}C^{m}C$) calculated by Specificity ^{m}C×Specificity $^{m}C^{m}C$. (AUC represent for Area under curve)

Receiver Operating Characteristic (ROC) curve analysis of ^{m}C and $^{m}C^{m}C$ methylation pattern

Since our data suggested that ^{m}C and $^{m}C^{m}C$ show the highest significant value, we chose to further analysis this sub-set. We selected methylation and hypermethylation results to perform ROC curve to assess if this was able to discriminate normal and oral cancer tissues. As shown in Figure 5, ^{m}C pattern demonstrated a sensitivity and specificity of 60.0% and 78.6%, respectively. In the same way, 66.7% sensitivity and 73.8% specificity was observed for the $^{m}C^{m}C$ pattern. However, sensitivity and specificity determined individually for ^{m}C and $^{m}C^{m}C$ are not suitable for use as tool for oral cancer detection. Fortunately, the combination of these two markers did improve the diagnostic power of the oral cancer detection (86.68% sensitivity and 56.68% specificity). With a high percentage of sensitivity, the methylation level of ^{m}C or $^{m}C^{m}C$ in oral rinse sample has high potential for use as a screening tool for oral cancer detection from the oral rinse specimen.

Discussion

In this study, we have used COBRA Alu analysis, which is highly capable of detecting methylation levels of Alu elements at 2 CpG loci. This alone is the key advantage of this technique, providing information on multiple CpG loci rather than 1. For example, in the FFPE derived tissue, we not only found hypomethylation in both of the CpG loci ($^{m}C^{m}C$), we were also able to examine the increase in $^{u}C^{u}C$ pattern which we determined to hold grater significance.

Since a previous study reported that Alu hypomethylation was correlated with aging when assessed in PBMCs (Jintaridth and Mutirangura, 2010), we chose to follow this approach for oral cancer, since it is not as invasive as tissue biopsy. Although our data did show that methylation was datable, the result of methylation patterns showed no significant changes. Nonetheless, decreasing trend in methylation level and increasing hypomethylation loci same as paraffined-embeded tissue were noted. The results are far from conclusive and this might have occurred by the possibility that the PBMCs could be with a high proportion of normal PBMCs and with very few circulating cancer cell DNA in the patient sample.

Finally, we observed notable differences in oral rinse samples which its self represents an excellent cost-effective and non-invasive technique for sample collection. We also investigated the component of potentially malignant condition arising from a smoking habit. Our results demonstrate a significant reduction in Alu methylation level in oral rinse samples from non-smoker, light smoker, heavy smoker and cancer patients (Figure 4). The level of Alu methylation is noted to be stepwise decrease concordant with the potentially malignant changes of the oral epithelium. Although the majority of the oral rinse contains cells from the normal oral epithelium, in smokers and cancer patients the oral rinse can likely include dysplastic/cancer squamous cells (Subbalekha et al., 2009; Wangsri et al., 2012). The DNA from dysplastic/cancer cells is capable to show reduced the Alu methylation level. This observation is confirmed by the Alu methylation level in high stage cancer is lower than low stage cancer, and collectively demonstrating the sensitivity of the COBRA Alu method of analysis.

The association between smoking status and Alu hypomethylation in tumors suggest that tobacco exposure may be causing genome-wide damage and contributing in epigenetic events including Alu methylation status. Smoking has been associated to promote methylation of several genes in different cancer, for example, SFRP in head and neck squamous cell carcinoma (HNSCC) (Marsit et al., 2006) and TSLC1/IGSF4 in non-small cell lung cancer (Kikuchi et al., 2006). Although smoking has not been previously shown directly to cause genome-wide hypomethylation, there are reports suggesting that smoking can be associated with vitamin B12 reduction, which is required for the normal synthesis of S-adenyl-methionine (Gabriel et al., 2006), an important protein involved in methyl-transferase pathway. This may provide a clue in better understanding the association between Alu hypomethylation and smoking.

The result of this study clearly demonstrates that Alu methylation level and pattern in oral cancer was readily datable in oral rinse sample than in tissues or PBMCs. Here, we proposed to use the sample from oral rinse technique for developing a test for oral cancer detection. Supporting this is that when we performed ROC curve to evaluate the sensitivity and specificity for this test, we observe high sensitivity in combined ^{m}C or $^{m}C^{m}C$ methylation pattern, implying that, this technique may be suitable for oral cancer screening. However, some limitations of this study could be concerned. Firstly, in case of OSCC with ulcer, the results may disturbed by some blood cells contamination. Secondly, our experiment had limited sample size and unmatched age of the participants among normal, smoker and oral cancer patients. Therefore, further investigation should be age consideration and larger sample size evaluation. In conclusion, Alu methylation might be beneficial method for screening oral cancer in oral rinse sample.

References

Ahmedin J, Freddie B, Melissa MC, et al (2011). Global cancer statistics. *CA Cancer J Clin*, **61**, 69-90.

Alexandros D, Georgios N, George X, et al (2008). Hypomethylation of retrotransposable elements correlates with genomic instability in non-small cell lung cancer. *Int J Cancer*, **124**, 81-7.

Ana CF, Flavia CS, Nathalia de S, et al (2009). Estimating genomic instability mediated by Alu retroelements in breast cancer. *Genet Mol Biol*, **32**, 25-31.

Bollati V, Fabris S, Pegoraro V, et al (2009). Differential repetitive DNA methylation in multiple myeloma molecular subgroups. *Carcinogenesis*, **30**, 1330-5.

Chalitchagorn K, Shuangshoti S, Hourpai N, et al (2004). Distinctive pattern of LINE-1 methylation level in normal tissues and the association with carcinogenesis. *Oncogene*, **23**, 8841-6.

Cho YH, Yazici H, Wu HC, et al (2010). Aberrant promoter hypermethylation and genomic hypomethylation in tumor, adjacent normal tissues and blood from breast cancer patients. *Anticancer Res*, **30**, 2489-96.

Choi IS, Estecio MR, Nagano Y, et al (2007). Hypomethylation of LINE-1 and Alu in welldifferentiated neuroendocrine tumors (pancreatic endocrine tumors and carcinoid tumors). *Modern Pathology*, **20**, 802-10.

Choi SH, Worswick S, Byun HM, et al (2009). Changes in DNA methylation of tandem DNA repeats are different from interspersed repeats in cancer. *Int J Cancer*, **125**, 723-9.

Daskalos A, Nikolaidis G, Xinarianos G, et al (2009). Hypomethylation of retrotransposable elements correlates with genomic instability in non-small cell lung cancer. *Int J Cancer*, **124**, 81-7.

Debra TH, Carmen JM, Andres H, et al (2007). Global DNA methylation level in whole blood as a biomarker in head and neck squamous cell carcinoma. *Cancer Epidemiol Biomarkers Prev*, **16**, 108-14.

Demarini DM (2004). Genotoxicity of tobacco smoke and tobacco smoke condensate: a review. *Mutation Res*, **567**, 447-74.

Diez-Perez R, Campo-Trapero J, Cano-Sanchez J, et al (2011). Methylation in oral cancer and pre-cancerous lesions. *Oncology Reports*, **25**, 1203-9.

Gabriel HE, Crott JW, Ghandour H, et al (2006). Chronic cigarette smoking is associated with diminished folate status, altered folate form distribution, and increased genetic damage in the buccal mucosa of healthy adults. *Am J Clin Nutrition*, **83**, 835-41.

Godtfredsen NS, Lucht H, Prescott E, et al (2004). A prospective study linked both alcohol and tobacco to Dupuytren's disease. *J Clin Epidemol*, **57**, 858-63.

Hehuang X, Min W, Maria de FB, et al (2010). Epigenomic analysis of Alu repeats in human ependymomas. *PNAS*, **107**, 6952-7.

Hou L, Wang H, Sartori S, et al (2010). Blood leukocyte DNA hypomethylation and gastric cancer risk in a high-risk Polish population. *Int J Cancer*, **127**, 1866-74.

Ian MS, Wojciech KM, Suhail KM, et al (2007). DNA global hypomethylation in squamous cell head and neck cancer associated with smoking, alcohol consumption and stage. *Int J Cancer*, **121**, 1724-8.

Jintaridth P, Mutirangura A (2010). Distinctive patterns of age-dependent hypomethylation in interspersed repetitive sequences. *Physiol Genomics*, **41**, 194-200.

Kikuchi S, Yamada D, Fukami T, et al (2006). Hypermethylation of the TSLC1/IGSF4 promoter is associated with tobacco smoking and a poor prognosis in primary nonsmall cell lung carcinoma. *Cancer*, **106**, 1751-8.

Kitkumthorn N, Keelawat S, Rattanatanyong P, et al (2012). LINE-1 and Alu methylation patterns in lymphnode metastases of head and neck cancers. *Asian Pac J Cancer Prev*, **13**, 4469-75.

Kitkumthorn N, Mutirangura A (2011). Long interspersed nuclear element-1 hypomethylation in cancer: biology and clinical applications. *Clin Epigenetics*, **2**, 315-30.

Kristy LR, Baili Z, Keith AB, et al (2009). Genome-wide hypomethylation in head and neck cancer is more pronounced in HPV-negative tumors and is associated with genomic instability. *PLoS One*, **4**, 4941.

Kwon HJ, Kim JH, Bae JM, et al (2010). DNA methylation changes in ex-adenoma carcinoma of large intestine. *Virchows Arch*, **457**, 433-41.

Lee HS, Kim BH, Cho NY, et al (2009). Prognostic implications of and relationship between CpG island hypermethylation and repetitive DNA hypomethylation in hepatocellular carcinoma. *Clin Can Res*, **15**, 812-20.

Lingen MW, Pinto A, Mendes RA, et al (2011). Genetics/epigenetics of oral premalignancy: current status and future research. *Oral Disease*, **17**, 7-22.

Marsit CJ, McClean MD, Furniss CS, et al (2006). Epigenetic inactivation of the SFRP genes is associated with drinking, smoking and HPV in head and neck squamous cell carcinoma. *Int J Cancer*, **119**, 1761-6.

Massimo C, Halina P, John FE, et al (1995). Tyrosine phosphorylation as a marker for aberrantly regulated growth-promoting pathways in cell lines derived from head and neck malignancies. *Int J Cancer*, **61**, 98-103.

Massimo M, Maria S, Gennaro I, et al (2012). Epigenetic disregulation in oral cancer. *Int J Mol Sci*, **13**, 2531-3.

Moore LE, Pfeiffer RM, Poscablo C, et al (2008). Genomic DNA hypomethylation as a biomarker for bladder cancer susceptibility in the Spanish Bladder Cancer Study: a case–control study. *Lancet Oncol*, **9**, 359-66.

Nakkuntod J, Avihingsanon Y, Mutirangura A, et al (2011).

Hypomethylation of LINE-1 but not Alu in lymphocyte subsets of systemic lupus erythematosus patients. *Clinica Chimica Acta*, **412**, 1457-61.

Park SY, Yoo EJ, Cho NY, et al (2009). Comparison of CpG island hypermethylation and repetitive DNA hypomethylation in premalignant stages of gastric cancer, stratified for Helicobacter pylori infection. *J Pathol*, **219**, 410-6.

Peter DM, Ryan DW, Celso AE, et al (2008). Human Alu RNA is a modular transacting repressor of mRNA transcription during heat shock. *Molecular Cell*, **29**, 499-509.

Pobsook T, Subbalekha K, Sannikorn P, et al (2011). Improved measurement of LINE-1 sequence methylation for cancer detection. *Clinica Chimica Acta*, **412**, 314-21.

Rodriguez J, Vives L, Jorda M, et al (2008). Genome-wide tracking of unmethylated DNA Alu repeats in normal and cancer cell. *Nucleic Acids Res*, **36**, 770-84.

Rubin CM, Houck CM, Deininger PL, et al (1980). Partial nucleotide sequence of the 300-nucleotide interspersed repeated human DNA sequences. *Nature*, **284**, 372-4.

Saintigny P, Zhang L, Fan YH, et al (2011). Gene expression profiling predicts the development of oral cancer. *Cancer Prev Res (Philadelphia)*, **4**, 218-29.

Sirivanichsuntorn P, Keelawat S, Danuthai K, et al (2013). LINE-1 and Alu hypomethylation in mucoepidermoid carcinoma. *BMC Clin Pathol*, **13**, 10.

Song F, Qiong-lan T, Ying-jin L, et al (2011). A review of clinical and histological parameters associated with contralateral neck metastases in oral squamous cell carcinoma. *Int J Oral Sci*, **3**, 180-91.

Subbalekha K, Pimkhaokham A, Pavasant P, et al (2009). Detection of LINE-1s hypomethylation in oral rinses of oral squamous cell carcinoma patients. *Oral Oncol*, **45**, 184-91.

Wangsri S, Subbalekha K, Kitkumthorn N, et al (2012). Patterns and possible roles of LINE-1 methylation changes in smoke-exposed epithelia. *PLoS One*, **7**, 45292.

Watts GS, Futscher BW, Holtan N, et al (2008). DNA methylation changes in ovarian cancer are cumulative with disease progression and identify tumor stage. *BMC Medical Genomics*, **1**, 47-59.

Wilhelm CS, Kelsey KT, Butler R, et al (2010). Implications of LINE1 methylation for bladder cancer risk in women. *Clin Cancer Res*, **16**, 1682-9.

Xiang S, Liu Z, Zhang B, et al (2010). Methylation status of individual CpG sites within Alu elements in the human genome and Alu hypomethylation in gastric carcinomas. *BMC Cancer*, **10**, 44-55.

Yasusei K, Shojiro K, Ikuko O, et al (2004). Invasion and metastasis of oral cancer cells require methylation of E-cadherin and/or degradation of membranous beta-catanin. *Clin Cancer Res*, **10**, 5455-63.

Yoo EJ, Park SY, Cho NY, et al (2008). Helicobacter pylori-infection-associated CpG island hypermethylation in the stomach and its possible association with polycomb repressive marks. *Virchows Arch*, **452**, 515-24.

Yoshida T, Yamashita S, Takamura-Enya T, et al (2011). Alu and Satalpha hypomethylation in Helicobacter pylori-infected gastric mucosae. *Int J Cancer*, **128**, 33-9.

Differences in LINE-1 Methylation Between Endometriotic Ovarian Cyst and Endometriosis-Associated Ovarian Cancer

Ajaree Senthong, MD, Nakarin Kitkumthorn, PhD,† Prakasit Rattanatanyong, BSc,‡ Nipon Khemapech, MD,* Surang Triratanachart, MD,§ and Apiwat Mutirangura, MD, PhD‡*

Background: Endometriosis in endometriosis-associated ovarian cancer (EAOC) refers to lesions that can derive from endometriotic ovarian cysts (ECs) that form in the ovarian endometrium with the potential to transform into full-blown ovarian cancer. Hypomethylation of long interspersed element-1 (LINE-1 or L1) is a common epigenomic event in several cancers and is strongly associated with ovarian cancer progression.

Objectives: To evaluated alterations in LINE-1 methylation between EC, ovarian endometrioid adenocarcinoma (OEA), EAOC, and ovarian clear cell carcinoma (OCC).

Methods/ Materials: First, LINE-1 methylation status in 19 normal endometrium, 29 EC, 35 OCC, and 22 OEA tissues from unrelated samples were compared. Then, specific areas of eutopic endometrium, contiguous endometriosis, and cancer arising from 16 EAOCs were collected by microdissection and analyzed for LINE-1 methylation status.

Results: The total LINE-1 methylation levels were significantly different among the endometrium, endometriosis, and ovarian cancer ($P < 0.001$). A stepwise decrease in LINE-1 methylation was observed in the following order: normal endometrium, EC, OEA, and OCC. Interestingly, endometriosis in EAOC of both OEA ($P = 0.016$) and OCC ($P = 0.003$) possessed a higher percentage of LINE-1 unmethylated loci than EC.

Conclusion: Our data implicate that LINE-1 hypomethylation is an early molecular event involved in OEA and OCC malignant transformation. Precise measurements of LINE-1 methylation may help to distinguish EC and endometriosis in EAOC.

Key Words: Endometriosis-associated ovarian cancer (EAOC), Methylation, Long interspersed element-1s (LINE-1s)

Received May 29, 2013, and in revised form September 11, 2013.
Accepted for publication September 15, 2013.

(*Int J Gynecol Cancer* 2014;24: 00–00)

*Gynecologic Oncology Unit, Department of Obstetrics and Gynecology, Faculty of Medicine, Chulalongkorn University; †Department of Oral and Maxillofacial Pathology, Faculty of Dentistry, Mahidol University; ‡Center of Excellence in Molecular Genetics of Cancer and Human Diseases, Department of Anatomy, Faculty of Medicine, Chulalongkorn University; and §Gynecologic Cytopathology Unit, Department of Obstetrics and Gynecology, Faculty of Medicine, Chulalongkorn University, Bangkok, Thailand.

ISSN: 1048-891X
DOI: 10.1097/IGC.0000000000000021

Address correspondence and reprint requests to Apiwat Mutirangura, MD, PhD, Center of Excellence in Molecular Genetics of Cancer and Human Diseases, Department of Anatomy, Faculty of Medicine, Chulalongkorn University, Bangkok 10330, Thailand. E-mail: mapiwat@chula.ac.th; apiwat.mutirangura@gmail.com.

This study was supported by a Research Chair Grant 2011 from the National Science and Technology Development Agency in Thailand at the Center of Excellence in Molecular Genetics of Cancer and Human Diseases at Chulalongkorn University and the Ratchadapiseksomphot Fund from the Faculty of Medicine at Chulalongkorn University.
NK was supported by Thailand Research Funds (RSA 5580013).
The remaining authors declare no conflicts of interest.

Endometriosis is a common gynecological disease that is an estrogen-dependent chronic disorder and is classically defined based on the presence of endometrial glands and stroma located outside the uterine cavity and musculature. The incidence of endometriosis is 7% to 15% in women of reproductive age and less than 2% in postmenopausal women.[1] The etiology of endometriosis is largely unclear, but one accepted mechanism for its development is retrograde menstruation.[2] Although endometriosis is considered a benign disease, endometriosis displays several common malignantlike features, including local and distant metastases, which can attach to adjacent tissues and consequently invade and damage them. The histopathological evidence of malignant transformation was first documented in 1925 by Sampson[3] who suggested 3 criteria for the diagnosis of endometriosis-associated ovarian carcinoma (EAOC). These criteria include evidence of endometriosis near the tumor, origination of the carcinoma in the endometriosis and not by invasion of tumor cells from an unknown source, and the presence of tissue resembling endometrial stroma surrounding characteristic glands. However, Scott et al[4] added a stricter criterion to better define EAOC that included the presence of an area demonstrating a transition from benign endometriosis to cancer by histopathological evaluation. In this regard, endometrioid and clear cell carcinomas are now the predominant histological subtypes of EAOC.[5–7] Other subtypes of malignant tumors also arise in association with endometriosis, and these are known as borderline serous or serous carcinomas; but the incidence is less frequent. Stern et al[8] collected cases of malignant ovarian and extraovarian endometriosis, and 63% of ovarian endometriotic cases were found to be clear cell or endometrioid carcinomas. Similarly, a study by Modesitt et al[9] reported that more than 52% of cancers arising in endometriotic ovarian cysts (ECs) were endometrioid and clear cell subtypes.

Epidemiologic studies also demonstrated a strong correlation between endometriosis and EAOC. A retrospective study of patients with a diagnosis of endometriosis approximately 11 years prior found that the rate of ovarian cancer was 1.8, and this risk increased to 4.2 for those with a long history of ovarian endometriosis exceeding 10 years or greater.[2]

A recent study by Wiegand et al[10] identified mutations in *ARID1A* gene in ovarian clear cell and endometrioid carcinomas. The authors also noted mutations in *ARID1A* and *BAF250a*, a chromatin remodeling complex, in both tumor types and contiguous atypical endometriosis but not in distant endometriotic lesions. These observations represent compelling molecular evidence that mutations in *ARID1A* are an early event in the transformation of endometriosis into cancer.

Long interspersed element-1 (LINE-1 or L1) is a non–retroviral-like retrotransposon that is dispersed in many loci throughout the human genome, and these elements are usually heavily methylated in normal tissues.[11] A reduction in LINE-1 methylation is a common epigenetic change in several key cancers[12,13] including advanced ovarian cancer.[14,15] The underlying causes of LINE-1 hypomethylation are essentially unknown, but recent data are now suggesting the influence of carcinogen and oxidative stress on this process.[16,17] Nonetheless, LINE-1 hypomethylation can promote cancer by altering gene expression and promoting genomic instability.[18–20] Crucial, however, LINE-1 hypomethylation in key cancers is detected not only in a progressive multistep carcinogenetic manner; this effect is also detectable in premalignant lesions.[16,21,22] Therefore, LINE-1 hypomethylation can be considered a potential biomarker for early cancer detection.

From our previous study, we found that LINE-1 methylation has different levels in each locus of genome.[23] For this reason, we classified the methylation statuses of LINE-1 loci using combined bisulfite restriction analysis (COBRA) to differentiate LINE-1 loci into 4 classes depending on the methylation status of two 5′ and 3′ CpG dinucleotides in the LINE-1 amplicon. These loci are hypermethylated ($^{m}C^{m}C$), hypomethylated ($^{u}C^{u}C$), or partially methylated ($^{m}C^{u}C$ and $^{u}C^{m}C$). Unlike the overall LINE-1 methylation levels, we had shown that the $^{u}C^{u}C$ loci (percent $^{u}C^{u}C$) is potentially more sensitive and specific in cancer DNA detection.[24–26] Furthermore, we have found that smoking, a premalignant condition, can alter methylation levels of partial methylated loci, thereby increasing the amount of hypomethylated and hypermethylated loci in oral carcinogenesis.[27]

In this current study, we evaluated LINE-1 methylation status in endometriosis from EAOC in ovarian clear cell carcinoma (OCC) and ovarian endometrioid adenocarcinoma (OEA) and compared the status to EC.

MATERIALS AND METHODS

Formalin-fixed, paraffin-embedded tissue specimens were obtained from patients who had undergone total hysterectomy or salpingo-oophorectomy and surgical staging of ovarian cancer with endometriosis-associated ipsilateral ovarian cancer (15 endometrioid and 15 clear cell cancers). Histopathological examination revealed the coexistence and continuity of the endometriosis and cancer in the patients with EAOC, fulfilling the criteria proposed by Sampson.[3] The patients were treated at King Chulalongkorn Memorial Hospital between January 2001 and January 2012. Additional tissues were obtained from 22 cases of OEA, 35 cases of OCC, and 29 cases of EC. Endometrial tissues from 19 cases diagnosed with benign conditions of the uterus, including leiomyoma and cervical intraepithelial neoplasia III without endometriosis, were collected as normal endometrium; and before analysis, all cases underwent histopathological evaluation by a gynecologic pathologist to ensure that there was no pelvic endometriosis or endometriotic cyst. The exclusion criteria included 2 primary cancers, neoadjuvant chemotherapy, incomplete surgical staging, and the lack of availability of paraffin-embedded specimens. None of these patients received any Gonadotropin releasing hormone (GnRH) analog or other hormonal medication or antibiotics during the 6 months before surgery. The histological diagnosis of each patient was reviewed by a gynecological pathologist following the criteria of the World Health Organization's classification.[28]

Among the 30 patients who were histologically confirmed as having EAOC, 14 patients were excluded because of inadequate tissue for DNA extraction. Finally, 16 remaining patients (9 patients with endometrioid carcinomas and 7 patients with clear cell carcinomas) were included in the study group. The demographic data of the patients included age, clinical stage, histological grade, pretreatment CA-125 level, surgical outcome, and follow-up time; and these were reviewed for each patient. The ethics committee of the Faculty of Medicine, Chulalongkorn University, Bangkok, Thailand, approved this study (Institutional Review Board No. 018/55).

DNA Extraction and Bisulfite Modification

Formalin-fixed, paraffin-embedded tissues were sliced into 3 to 5 sections (each one was 5-μm thick) and were left unstained. Another section was stained with hematoxylin and eosin for pathological confirmation. In the EAOC group, the microdissection technique was performed for separation of the 3 different tissues (normal endometrium, endometriosis, and ovarian cancer) and collected from each EAOC specimen (Fig. 1A). After deparaffinization with xylene, the DNA was extracted by proteinase K digestion and a standard phenol-chloroform extraction protocol. The isolated genomic DNA was next purified using distilled water and, after elution, used for bisulfite treatment. Bisulfite modification of DNA was performed by using the EZ DNA methylation kit (Zymo Research, ZYMO RESEARCH CORP, Orange, CA) according to the manufacturer's instructions.

Combined Bisulfite Restriction Analysis (COBRA) of LINE-1

The bisulfate-treated DNA was amplified for 40 cycles using primers with the following sequence: LINE-1 forward 5′-GTTAAAGAAAGGGGTGACGGT-3′ and LINE-1 reverse 5′-TAGATCGGTTTAAGAAACGGCGTATT-3′. Polymerase chain reaction (PCR) was performed at an annealing temperature of 50°C. After PCR amplification, the LINE-1 amplicons (92 base pairs [bp]) were digested with 2 units of *TaqI* and *TasI* in NEB buffer 3 (New England Biolabs, Ontario, Canada) in a final volume of 10 μL. The reactions were incubated overnight at 65°C and then electrophoresed on an 8% nondenaturing polyacrylamide gel and stained with the SYBR green nucleic acid gel stain (Gelstar, Lonza, Allendale, NJ). The intensities of both COBRA PCR fragments were measured using a phosphorimager with Image Quant Software (Molecular Dynamics, GE Healthcare, Slough, UK). Distilled water was used as a negative control. DNA samples from HeLa, Jurkat, and Daudi cell lines were used as positive controls in every experiment to standardize the interassay variation. All experiments were performed in duplicate.

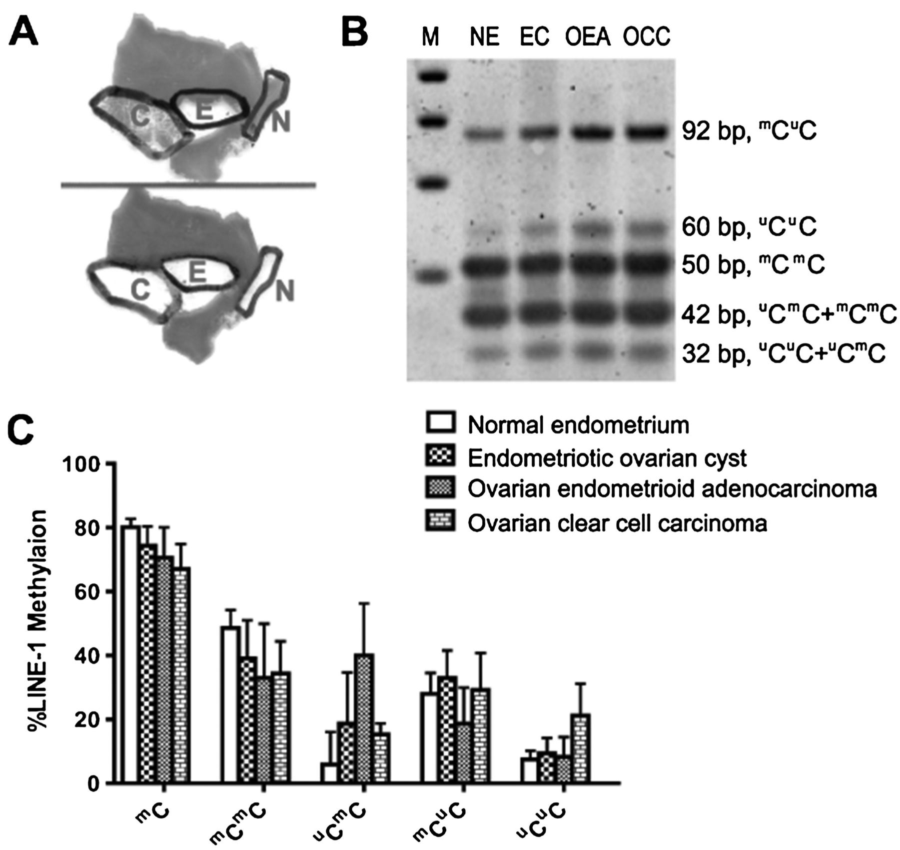

FIGURE 1. Methodology and graphical data of LINE-1 methylation levels. A, Demonstration of the microdissection technique: upper picture, EAOC before microdissection; lower picture, EAOC after microdissection. C, Cancer area; E, contiguous endometriosis; N, eutopic endometrium. B, Examples of COBRA polyacrylamide gel. EC, endometriotic ovarian cyst; M, 25-bp marker; NE, normal endometrium; OCC, ovarian clear cell carcinoma; OEA, ovarian endometrioid adenocarcinoma. C, Bar graph shows percentages of each LINE-1 methylation pattern in NE, EC, OEA, and OCC. ^{m}C represents the total methylation of the LINE-1s. $^{m}C^{m}C$ and $^{u}C^{u}C$ indicate hypermethylation and hypomethylation in the amplified region. $^{m}C^{u}C$ and $^{u}C^{m}C$ represent 2 forms of partial methylation.

TABLE 1. Methylation levels and patterns of LINE-1 in NE, EC, and ovarian cancer

	No. Patients	Age (Range, Median) (Years)	FFPE Storage Time (Range, Median) (Years)	LINE-1 Methylation Patterns (Mean ± SD)				
				Percent ^{m}C	Percent $^{m}C^{m}C$	Percent $^{u}C^{m}C$	Percent $^{m}C^{u}C$	Percent $^{u}C^{u}C$
Normal endometrium	19	(36–54.42)	(1–3.2)	80.12 ± 2.60	48.65 ± 5.50	15.87 ± 10.16	27.98 ± 6.56	7.50 ± 2.68
Proliferative phase	10	(41–54.44)	(1–3.2)	80.14 ± 3.18	48.81 ± 6.35	14.14 ± 11.01	29.50 ± 7.65	7.55 ± 2.45
Secretory phase	9	(36–51. 41)	(1–3.2)	80.08 ± 1.95	48.47 ± 4.75	17.79 ± 9.38	26.30 ± 4.98	7.45 ± 3.06
EC	29	(29–57.42)	(1–3.2)	74.30 ± 6.09	39.09 ± 11.90	18.67 ± 15.94	32.91 ± 8.63	9.32 ± 4.84
OEA	22	(32–92.56)	(2–5.4)	70.55 ± 9.52	32.97 ± 16.97	40.01 ± 16.26	18.74 ± 11.2	8.29 ± 6.19
OCC	35	Unavailable	Unavailable	67.10 ± 7.80	34.27 ± 10.10	15.331 ± 3.47	29.23 ± 11.5	21.17 ± 9.94

FFPE, Formalin-fixed, paraffin-embedded.

LINE-1 Methylation Analysis

The COBRA LINE-1 amplicons generate 4 bands based on the methylation status of the 2 CpG dinucleotides as follows: partial methylation ($^{m}C^{u}C$, 92 bp; $^{u}C^{m}C$, 32 and 18 bp), hypomethylation ($^{u}C^{u}C$, 32 and 60 bp), and hypermethylation ($^{m}C^{m}C$, 50 and 42 bp) as demonstrated in Figure 1B. The LINE-1 methylation level of each pattern was calculated to determine the precise percentage using the following steps as described below.

First, the intensity of each band was divided by the length (bp) of the double-stranded DNA as follows: 92/92 = A, 60/56 = B, 50/48 = C, 42/40 = D, 32/28 = E, and [(D + E) – (B + C)] / 2 = F.

Next, the frequency of each methylation pattern was calculated: % ^{m}C (total methylation) = [(A + 2C + F) × 100] / (2A +2 B + 2C + 2F); % $^{m}C^{m}C$ (hypermethylated loci) = [(C/2) × 100) / [(C / 2) + A + B + F]; % $^{u}C^{m}C$ (partial methylated loci) = (F × 100) / [(C / 2) + A + B + F]; % $^{m}C^{u}C$ (partial methylated loci) = (A × 100) / [(C / 2) + A + B + F]; and % $^{u}C^{u}C$ (hypomethylated loci) = (B × 100) / [(C / 2) + A + B + F].

Statistical Analysis

Analysis of variance was used to compare the methylation patterns of LINE-1 among normal endometrium, ovarian endometriosis, OCC, and OEA. A paired *t* test was used to analyze the tissue subtypes in paired samples of EAOC. An independent sample *t* test was performed to determine the difference in LINE-1 patterns between OCC, OEA, EC, and normal endometrium groups. All calculations were performed using the SPSS software for Windows, version 17.0 (SPSS Inc, Chicago, IL). The results were considered statistically significant when the P <0.05.

RESULTS

LINE-1 Methylation in 4 Different Tissues (Normal Endometrium, EC, OEA, and OCC)

In 19 normal endometrium samples containing 10 proliferative and 9 secretory phases (depending on the menstrual cycle), the percentage of LINE-1 methylation level did not show any significant differences (Table 1). Next, we evaluated differences in LINE-1 methylation levels and pattern among the 19 normal, 29 EC, 35 OCC, and 22 OEA samples from unrelated samples. The frequency of LINE-1 methylation in each group is shown in Table 1 and Figure 1C. The loss of LINE-1 methylation is indicated to occur in a multistep manner (normal > EC > OEA > OCC). The LINE-1 methylation level (% ^{m}C) decreased progressively from normal endometrium (80.12 ± 2.60%) to EC (74.30 ± 6.09), then to 2 types of cancers, OEA (70.55 ± 9.52) and OCC (67.10 ± 7.80%) (P < 0.0001; Table 1; Fig. 1C).

Key factors likely to affect the level of LINE-1 methylation include age and menstrual phase. However, in our current study, the age and menstrual factors were not significantly associated with the level of LINE-1 methylation across the different sample groups (data are not shown).

LINE-1 Methylation in EAOC and EC

Sixteen patients with EAOC were enrolled in the study. The mean age at the time of diagnosis was 48.3 years. Fourteen patients (87.5%) had early-stage ovarian cancer (stages I and II), and 2 patients (12.5%) had advanced stages of ovarian cancer (1 case at stage III, and 1 case at stage IV). All patients received optimal surgery (operative procedure is total abdominal hysterectomy with bilateral salpingo-oophorectomy and surgical staging; the macroscopic of gross tumor after surgery documented no residual tumor). The mean level of pretreatment CA 125 was 267.52 U/mL. The mean follow-up time was 3.5 years, and most patients were alive at this time; however, the status was unknown for 1 patient. The clinical background of the EAOC cases is shown in Table 2.

In a comparison study of subtypes with clear cell carcinomas and endometrioid adenocarcinomas, the frequency of each LINE-1 pattern was evaluated and is shown in Table 3. The percent of ^{m}C decreased from the eutopic endometrium to the contiguous endometriosis and cancers (both OEA and OCC). For OCC, a statistically significant difference was found between the eutopic endometrium and contiguous endometriosis ($P < 0.05$) and between the eutopic endometrium and OCC ($P < 0.01$). For OEA, hypomethylation was observed between eutopic endometrium and cancer ($P < 0.05$).

In OCC, in addition to percent ^{m}C, the percent $^{u}C^{u}C$ also increased among normal endometrium, contiguous endometriosis, and clear cell carcinoma (6.76 ± 2.03, 15.93 ± 5.50, and 34.53 ± 17.05, respectively) ($P < 0.01$). For OEA, the increase in unmethylated LINE-1 was also observed between the eutopic endometrium and cancer ($P < 0.05$).

Interestingly, LINE-1 methylation levels between EC and EAOC were noted to be different. As shown in Figure 4, the percent $^{u}C^{u}C$ in EC, EAOC-OEA, and EAOC-OCC was 9.32 ± 4.84, 14.23 ± 9.66, and 15.93 ± 5.50, respectively; and these differences were statistically different (EC and EAOC-OEA, $P = 0.016$; EC and EAOC-CL, $P = 0.003$).

DISCUSSION

Currently, LINE-1 hypomethylation has been detected in many keys cancers.[12,13] More importantly, this effect of hypomethylation also present as an epigenomic change in premalignant lesions of multistep carcinogenetic process of cervical intraepithelial,[16] biliary intraepithelial,[21] and intestinal metaplasia[22] malignancies. Here, we report for the first time the status of LINE-1 methylation in ovarian endometriosis and EAOC. This study found an overall decrease in LINE-1 methylation when the endometrium undergoes transformation to endometriosis and to ovarian cancer corresponding with an increase in unmethylated LINE-1 loci. Therefore, LINE-1 hypomethylation is an epigenomic process that evolves into endometriosis-associated ovarian carcinogenesis in a multistep manner.

A study in LINE-1 methylation in epithelial ovarian cancer showed that $^{u}C^{u}C$ may be associated with more advanced and aggressive phenotype.[14] Our study also found that the clear cell subtype (OCC) had a higher proportion of $^{u}C^{u}C$ loci than the endometrioid subtype, suggesting that $^{u}C^{u}C$ may be a promising biomarker for distinguishing between endometrioid and clear cell ovarian cancer. Basic

TABLE 2. Patients' characteristics in 16 EAOC cases

EAOC	Cell Type	Age (Years)	FIGO Stage	Pretreatment CA 125 (U/mL)	Surgical Outcome	Follow-Up Time (Years)	Clinical Outcome
1	Endometrioid	45	2C	165.1	Optimal	3	Alive
2	Endometrioid	50	1C	100.3	Optimal	3	Alive
3	Endometrioid	51	2C	187.5	Optimal	1	Alive
4	Endometrioid	41	1C	107.7	Optimal	1	Alive
5	Endometrioid	49	2C	50.2	Optimal	4	Alive
6	Endometrioid	43	1C	33.1	Optimal	1	Alive
7	Endometrioid	48	3C	2348.8	Optimal	3	Alive
8	Endometrioid	54	2C	140	Optimal	11	Alive
9	Endometrioid	50	1A	52.2	Optimal	8	Alive
10	Clear cell	38	1C	45.2	Optimal	6	Alive
11	Clear cell	50	1C	35.1	Optimal	5	Alive
12	Clear cell	37	4	397.3	Optimal	3	Alive
13	Clear cell	49	1A	205	Optimal	1	Alive
14	Clear cell	60	1C	310	Optimal	2	Not known
15	Clear cell	54	2C	44.1	Optimal	0.5	Alive
16	Clear cell	54	2C	58.7	Optimal	3	Alive

FIGO, International Federation of Gynecology and Obstetrics.

TABLE 3. Methylation levels and patterns of LINE-1 in EAOC of endometrioid and clear cell subtypes

EAOC	Age (Range, Median) (Years)	FFPE Storage Time (Range, Median) (Years)	Group	LINE-1 Methylation Patterns (Mean ± SD) Percent ^{m}C	Percent $^{m}C^{m}C$	Percent $^{u}C^{m}C$	Percent $^{m}C^{u}C$	Percent $^{u}C^{u}C$
Clear cell carcinoma (n = 7)	(41–53.49)	(1–4.2)	Eutopic endometrium	83.34 ± 4.38	54.79 ± 8.97	19.41 ± 10.19	19.04 ± 5.79	6.76 ± 2.03
			Contiguous endometriosis	74.92 ± 4.24	44.14 ± 7.90	15.86 ± 6.37	24.08 ± 7.83	15.93 ± 5.50
			Clear cell carcinoma	66.00 ± 8.54	41.78 ± 13.51	18.38 ± 22.62	27.57 ± 16.21	34.53 ± 17.05
Endometrioid adenocarcinoma (n = 9)	(38–60.50)	(1–11.3)	Eutopic endometrium	78.56 ± 1.57	47.04 ± 3.05	22.14 ± 8.59	20.79 ± 6.75	10.02 ± 2.59
			Contiguous endometriosis	76.41 ± 6.14	46.37 ± 11.77	16.49 ± 12.88	22.91 ± 7.55	14.23 ± 5.78
			Endometrioid adenocarcinoma	73.04 ± 5.73	43.08 ± 6.37	13.60 ± 9.36	23.66 ± 5.39	19.67 ± 9.66

knowledge suggests that clear cell carcinoma is a potentially aggressive cancer type that is resistant to chemotherapy and has a higher recurrence rate after treatment. Furthermore, $^{u}C^{u}C$ was significantly associated with poor progression and a lower overall survival rate.[14,15] Therefore, differentiating between these different subtypes of lesion may be useful for predicting treatment response and prognosis.

Moreover, this study showed that LINE-1 hypomethylation occurred in EC, and it may occur in EAOC before its transformation into cancer. Most EAOC studies have found that endometriosis is a neoplastic disease that serves as a precursor to ovarian cancer.[29] Additionally, our study found a significant difference in LINE-1 methylation between EC and EAOC. Because LINE-1 hypomethylation can promote carcinogenesis (by several mechanisms),[13,18–20] our data support the idea that the carcinogenic potential of EAOC likely outweighs that of EC.

In this study, we did not find any influence to LINE-1 methylation level when we evaluated the data by age and menstrual phase, suggesting that these confounding factors are likely not associated with the LINE-1 methylation levels.

Oxidative stress is another important factor that may associated to the ovarian carcinogenesis. The high concentration of the free iron was proved to associate with the induction of oxidative stress and may play a major role in malignant change of endometriotic cyst.[30] In addition, the increase of oxidative stress is associated with LINE-1 hypomethylation in the bladder cancer development.[17] Therefore, in EC and EAOC, the high level of oxidative stress could be associated with LINE-1 hypomethylation and involved in ovarian cancer development. This hypothesis should be confirmed in further studies.

In conclusion, LINE-1 hypomethylation occurs early in EAOC development. This finding indicates that epigenomic alterations might precede the development of ovarian cancer phenotypes. The precise measurement of LINE-1 methylation patterns may be useful in distinguishing EC and endometriosis from EAOC and as basis for development as a diagnostic biomarker. Finally, a better understanding of the epigenetic events in the multistep progression of EAOC may be crucial for further understanding of the molecular mechanisms of ovarian carcinogenesis.

ACKNOWLEDGMENTS

The authors thank Mrs Sarunya Numto and Mr Dusit Bumalee for providing the paraffin-embedded specimens.

REFERENCES

1. Olive DL, Schwartz LB. Endometriosis. *N Engl J Med*. 1993;328:1759–1769.
2. Brinton LA, Gridley G, Persson I, et al. Cancer risk after a hospital discharge diagnosis of endometriosis. *Am J Obstet Gynecol*. 1997;176:572–579.
3. Sampson JA. Endometrial carcinoma of ovary arising in endometrial tissue in that organ. *Arch Surg*. 1925;10:1–72.
4. Scott RB. Malignant changes in endometriosis. *Obstet Gynecol*. 1953;2:283–289.

5. Vercellini P, Parazzini F, Bolis G, et al. Endometriosis and ovarian cancer. *Am J Obstet Gynecol*. 1993;169:181–182.
6. Oral E, Ilvan S, Tustas E, et al. Prevalence of endometriosis in malignant epithelial ovary tumours. *Eur J Obstet Gynecol Reprod Biol*. 2003;109:97–101.
7. Vercellini P, Scarfone G, Bolis G, et al. Site of origin of epithelial ovarian cancer: the endometriosis connection. *BJOG*. 2000;107:1155–1157.
8. Stern RC, Dash R, Bentley RC, et al. Malignancy in endometriosis: frequency and comparison of ovarian and extraovarian types. *Int J Gynecol Pathol*. 2001;20:133–139.
9. Modesitt SC, Tortolero-Luna G, Robinson JB, et al. Ovarian and extraovarian endometriosis-associated cancer. *Obstet Gynecol*. 2002;100:788–795.
10. Wiegand KC, Shah SP, Al-Agha OM, et al. ARID1A mutations in endometriosis-associated ovarian carcinomas. *N Engl J Med*. 2010;363:1532–1543.
11. Feinberg AP, Tycko B. The history of cancer epigenetics. *Nat Rev Cancer*. 2004;4:143–153.
12. Chalitchagorn K, Shuangshoti S, Hourpai N, et al. Distinctive pattern of LINE-1 methylation level in normal tissues and the association with carcinogenesis. *Oncogene*. 2004; 23:8841–8846.
13. Kitkumthorn N, Mutirangura A. Long interspersed nuclear element-1 hypomethylation in cancer: biology and clinical application. *Clin Epigenetics*. 2011;2:315–330.
14. Pattamadilok J, Huapai N, Rattanatanyong P, et al. LINE-1 hypomethylation level as a potential prognostic factor for epithelial ovarian cancer. *Int J Gynecol Cancer.* 2008;18:711–717.
15. Iramaneerat K, Rattanatunyong P, Khemapech N, et al. HERV-K hypomethylation in ovarian clear cell carcinoma is associated with a poor prognosis and platinum resistance. *Int J Gynecol Cancer*. 2011;21:51–57.
16. Shuangshoti S, Hourpai N, Pumsuk U, et al. Line-1 hypomethylation in multistage carcinogenesis of the uterine cervix. *Asian Pac J Cancer Prev.* 2007;8:307–309.
17. Petchsung M, Boonla C, Amnattrakul P, et al. Long interspersed nuclear element-1 hypomethylation and oxidative stress: correlation and bladder cancer diagnostic potential. *PLoS One*. 2011;7:e37009.
18. Aporntewan C, Phokaew C, Piriyapongsa J, et al. Hypomethylation of intragenic LINE-1 represses transcription in cancer cells through AGO2. *PLoS One*. 2011;6:e17934.
19. Pornthanakasem W, Kongruttanachok N, Phuangphairoj C, et al. LINE-1 methylation status of endogenous DNA double-strand breaks. *Nucleic Acids Res*. 2008;36:3667–3675.
20. Kongruttanachok N, Phuangphairoj C, Thongnak A, et al. Replication independent DNA double-strand break retention may prevent genomic instability. *Mol Cancer*. 2010;9:70.
21. Kim BH, Cho NY, Shin SH, et al. CpG island hypermethylation and repetitive DNA hypomethylation in premalignant lesion of extrahepatic cholangiocarcinoma. *Virchows Arch*. 2009; 455:343–351.
22. Park SY, Yoo EJ, Cho NY, et al. Comparison of CpG island hypermethylation and repetitive DNA hypomethylation in premalignant stages of gastric cancer, stratified for *Helicobacter pylori* infection. *J Pathol*. 2009;219:410–416.
23. Phokaew C, Kowudtitham S, Subbalekha K, et al. LINE-1 methylation patterns of different loci in normal and cancerous cells. *Nucleic Acids Res*. 2008;36:5704–5712.
24. Pobsook T, Subbalekha K, Sannikorn P, et al. Improved measurement of LINE-1 sequence methylation for cancer detection. *Clin Chim Acta*. 2011;412:314–321.
25. Kitkumthorn N, Tuangsintanakul T, Rattanatanyong P, et al. LINE-1 methylation in the peripheral blood mononuclear cells of cancer patients. *Clin Chim Acta*. 2012;413:869–874.
26. Sirivanichsuntorn P, Keelawat S, Danuthai K, et al. LINE-1 and Alu hypomethylation in mucoepidermoid carcinoma. *BMC Clin Pathol*. 2013;13:10.
27. Wangsri S, Subbalekha K, Kitkumthorn N, et al. Patterns and possible roles of LINE-1 methylation changes in smoke-exposed epithelia. *PLoS One*. 2012;7:e45292.
28. Tavassoli FA, Devilee P, eds. *Pathology and Genetics of Tumours of the Breast and Female Genital Organs*. Lyon, France: IARC Press; 2003:114–115.
29. Varma R, Rollason T, Gupta JK, et al. Endometriosis and the neoplastic process. *Reproduction*. 2004;127:293–304.
30. Yamaguchi K, Mandai M, Toyokuni S, et al. Contents of endometriotic cysts, especially the high concentration of free iron, are a possible cause of carcinogenesis in the cysts through the iron-induced persistent oxidative stress. *Clin Cancer Res*. 2008;14:32–40.

Gene 553 (2014) 31–41

Contents lists available at ScienceDirect

Gene

journal homepage: www.elsevier.com/locate/gene

Analysis of methylation microarray for tissue specific detection

Tachapol Muangsub [a], Jarunya Samsuwan [b], Pumipat Tongyoo [c], Nakarin Kitkumthorn [d,*], Apiwat Mutirangura [a]

[a] Center of Excellence in Molecular Genetics of Cancer and Human Diseases, Department of Anatomy, Faculty of Medicine, Chulalongkorn University, Bangkok 10330, Thailand
[b] Department of Forensic Biochemistry, Institute of Forensic Medicine, Police General Hospital, Royal Thai Police, Bangkok 10330, Thailand
[c] Inter-Department Program of Biomedical Sciences, Faculty of Graduate School, Chulalongkorn University, Bangkok 10330, Thailand
[d] Department of Oral and Maxillofacial Pathology, Faculty of Dentistry, Mahidol University, Bangkok 10400, Thailand

A R T I C L E I N F O

Article history:
Received 4 August 2014
Received in revised form 8 September 2014
Accepted 29 September 2014
Available online 1 October 2014

Keywords:
Methylation microarray
Tissue specific methylation
GPL8490
CpG loci

A B S T R A C T

The role of human DNA methylation has been extensively studied in genomic imprinting, X-inactivation, and disease. However, studies of tissue-specific methylation remain limited. In this study, we use bioinformatics methods to analyze methylation data and reveal loci that are exclusively methylated or unmethylated in individual tissues. We collect 39 previously published DNA methylation profiles using an Illumina® HumanMethylation 27 BeadChip Kit containing 22 common tissues and involving 27,578 CpG loci across the human genome. We found 86 positions of tissue specific methylation CpG (TSM) that encompass 34 hypermethylated TSMs (31 genes) and 52 hypomethylated TSMs (47 genes). Tissues were found to contain 1 to 25 TSM loci, with the majority in the liver (25), testis (18), and brain (16). Fewer TSM loci were found in the muscle (8), ovary (7), adrenal gland (3), pancreas (2–4), kidney, spleen, and stomach (1 each). TSMs are predominantly located 0–300 base pairs in the 3′ direction after the transcription start site. Similar to known promoters of methylation, hypermethylated TSM genes suppress transcription, while hypomethylated TSMs allow gene transcription. The majority of hypermethylated TSM genes encode membrane proteins and receptors, while hypomethylated TSM genes primarily encode signal peptides and tissue-specific proteins. In summary, the database of TSM loci produced herein is useful for the selection of tissue-specific DNA markers as diagnostic tools, as well as for the further study of the mechanisms and roles of TSM.

1. Introduction

The objective of this study is to identify gene promoters that are exclusively methylated or unmethylated in particular tissues. This information is beneficial for molecular diagnostic applications, and a better understanding of tissue-specific DNA methylation is important to the understanding of cellular differentiation and organ developmental processes.

Although currently only limited information is available, identifying the sources of DNA has been useful for diagnostic purposes. For example, the quantitative measurement of Epstein Bar viral (EBV) DNA in nasopharyngeal carcinoma (NPC) patients' plasma is a useful tumor marker for monitoring treatment (Lin et al., 2004). The success of this method is a result of the discovery of EBV DNA in NPC patients' circulation and the conclusion that EBV DNA present in serum was derived from the tumor (Mutirangura et al., 1998). A second example is the use of SHP1 (SH2 domain containing phosphatase) promoter 2 epithelial specific methylation to detect and quantify lung cancer DNA in plasma and lymph nodes (Vinayanuwattikun et al., 2011, 2013). *SHP1P2* exclusively methylates in epithelial tissue (Ruchusatsawat et al., 2006); therefore, methylated *SHP1P2* DNA is scarcely presented in lymph nodes and plasma. Consequently, the presence of methylated *SHP1P2* DNA in the lymph nodes or plasma of lung cancer patients is indicative of lung cancer, and the quantitative measurement of methylated *SHP1P2* DNA has proven to be useful in determining patient prognoses (Vinayanuwattikun et al., 2011, 2013). In addition to cancer, many disease-associated conditions such as tissue damage and viral infection can lead to the leakage of DNA into bodily fluids. Therefore, tissue-specific methylation DNA should be broadly useful for the identification of the tissue sources of diseases and for monitoring disease severity.

CpG methylation is a crucial epigenetic modification that controls gene expression and maintains genomic integrity (Aporntewan et al., 2011; Kitkumthorn and Mutirangura, 2011). The position of methylated CpGs is important for controlling gene expression. Promoter methylation, methylation 5′ to the transcriptional start site, usually leads to

Abbreviations: TSM, tissue specific methylation; EBV, Epstein Bar virus; SHP1, SH2 domain containing phosphatase; GEO, Gene Expression Omnibus; CU-DREAM, Connection Up- and Down-Regulation Expression Analysis of Microarrays; TSS, transcription start site; CGI, CpG island.

* Corresponding author at: Department of Oral and Maxillofacial Pathology, Faculty of Dentistry, Mahidol University, Bangkok, Yothi Road, Rajthawee District, Bangkok 10400, Thailand.
E-mail address: Nakarinkit@gmail.com (N. Kitkumthorn).

http://dx.doi.org/10.1016/j.gene.2014.09.060

heterochromatin formation and the suppression of gene expression (Jones and Takai, 2001; Cedar and Bergman, 2012). In contrast, gene body methylation is commonly associated with up-regulation of the associated gene through the down-regulation of intragenic small RNA (Maunakea et al., 2010; Aporntewan et al., 2011). However, the locations and roles of tissue specific methylation have not been intensively characterized.

The roles and mechanisms of CpG methylation in genomic imprinting, X-inactivation, and tumor suppressor gene promotion in cancer have been extensively studied (Jones and Takai, 2001; Phutikanit et al., 2010; Cedar and Bergman, 2012; Weisenberger, 2014). Although there have been several reports of the discovery of tissue specific methylation CpG (TSM) loci (Shiota et al., 2002; Ohgane et al., 2008; Yagi et al., 2008; Byun et al., 2009; Frumkin et al., 2011; How Kit et al., 2012), our understanding of the mechanisms and roles of TSM is still limited. Tissue development and cell differentiation can be considered multistep processes. Each organ changes as an individual develops from an embryo, to a fetus, an adolescent, an adult, and an aging individual. Furthermore, cell differentiation is an active process during each stage of development (Rakyan et al., 2010; Cedar and Bergman, 2012). Identifying tissue specific methylation will aid future studies in exploring the mechanisms and roles of this epigenetic modification.

Many technologies to detect DNA methylation in the genome have been developed recently (Sulewska et al., 2007; Bibikova et al., 2009; Jin et al., 2010; Phutikanit et al., 2010). The methylation microarray is one such technique. This technique was designed for the large-scale detection of methylation with high throughput and rapid results for DNA methylation profiling across the whole genome. A widely used commercial microarray for DNA methylation profiling is the Infinium HumanMethylation27 BeadChip from Illumina Inc. (Sun et al., 2011; Wang et al., 2012). This microarray quantitatively targets 27,578 CpG sites targeting approximately 14,000 genes in the human genome with the capacity to analyze 12 simultaneous samples (Bibikova et al., 2009). In this study, we analyzed Infinium HumanMethylation27 data that was reported in the NCBI Gene Expression Omnibus (GEO, http://www.ncbi.nlm. nih.gov/geo/) (Zhu et al., 2008) and in Bibikova et al. (Bibikova et al., 2009). We collected methylation data from each human tissue and organized this data into a methylation database. We then analyzed the methylation sites for their distribution, locations, and association with gene expression.

2. Materials and methods

2.1. DNA methylation database

The strategy of this experiment is summarized in Fig. S1. DNA methylation microarray data was collected from the GEO dataset in NCBI's database (http://www.ncbi.nlm.nih.gov/gds/) and a previous publication, Bibikova et al. (Bibikova et al., 2009). These data are presented in a GEO format that contains: GSE (series or experiment), GPL (platform or microarray), and GSM (sample or population). The NCBI's GEO dataset is the largest public database for microarray experiment data. The accessed keyword GPL8490 (Illumina® HumanMethylation27 BeadChip Kit, Illumina Inc., San Diego, CA, USA) from this platform was used for a methylation microarray. Ending on the 31st of Dec 2012, 172 GSE series were archived. Subsequently, we have considered normal human tissue data which have available and complete microarray data and excluded data from cell lines, stem cells, cancer, infected tissue, and non-human tissue. Finally, normal tissue data from 39 GSE series were included in this study.

The 39 GSE series used consisted of: GSE19711 (Teschendorff et al., 2010), GSE20067 (Teschendorff et al., 2010), GSE20080 (Teschendorff et al., 2010), GSE20712 (Dedeurwaerder et al., 2011), GSE21232 (Volkmar et al., 2012), GSE22249 (Dedeurwaerder et al., 2011), GSE22595 (Koch et al., 2011), GSE22867 (Etcheverry et al., 2010), GSE25062 (Hinoue et al., 2012), GSE25706 (Ko et al., 2010), GSE25869 (Kwon et al., 2011), GSE26033 (Pai et al., 2011), GSE26126 (Kobayashi et al., 2011), GSE26989 (Campan et al., 2011), GSE27130 (Kim et al., 2011), GSE27284 (Navab et al., 2011), GSE27899 (Hasler et al., 2012), GSE28746 (Bocklandt et al., 2011), GSE29490 (Kibriya et al., 2011), GSE30229 (Langevin et al., 2012), GSE30601 (Zouridis et al., 2012), GSE30760 (Teschendorff et al., 2012; Zhuang et al., 2012), GSE31788 (Matsusaka et al., 2011), GSE31835 (Roberson et al., 2012), GSE31979 (Fackler et al., 2011), GSE32867 (Selamat et al., 2012), GSE33065 (Hill et al., 2011), GSE33510 (Lauss et al., 2012), GSE34008 (Volkmar et al., 2012), GSE34355 (Wu et al., 2012), GSE35146 (Sanders et al., 2012), GSE36002 (Kresse et al., 2012), GSE36166 (Jacobsen et al., 2012), GSE36194 (Gibbs et al., 2010; Hernandez et al., 2011, 2012), GSE36353 (Fonseca et al., 2012), GSE36637 (Guenin et al., 2012), GSE37988 (Shen et al., 2012), GSE41037 (Horvath et al., 2012), and GSE42510 (Haas et al., 2013). The mean methylation level of each population sample from each selected GSE series and from the data from Bibikova et al. (Bibikova et al., 2009) was calculated by the Connection Up- and Down-Regulation Expression Analysis of Microarrays (CU-DREAM) program (Aporntewan and A., 2011). These calculated methylation values were collected in Microsoft Excel to produce a human organ DNA methylation database (Table S1 and S2).

2.2. Bioinformatics analysis

Since the GPL8490 platform observed 27,578 CpG loci, we were able to create 27,578 graphs of CpG loci by using an in-house R script (Fig. S2). We calculated the difference between the minimum methylation level of a particular organ and the maximum methylation level of the remaining organs for hypermethylation pattern. On the contrary, the difference between the maximum methylation level of a particular organ and the minimum methylation level of the remaining organs was calculated for hypomethylation pattern. Initially, the cut-off values for the difference in methylation level used were 0.6 and 0.5. However, only 6 and 20 graphs (CpG loci) passed the 0.6 and 0.5 cut-off values, respectively. Later, we used a less stringent cut-off at 0.4, resulting in 86 graphs (CpG loci) that were suitable for further analysis.

The details of each CpG locus were retrieved from the Illumina probe ID in the GPL8490-65 platform database available in http://www.ncbi.nlm.nih.gov/geo/query/acc.cgi?acc=GPL8490. We organized and recorded these data in Microsoft Excel, and analyzed the locations of these loci in the genome by descriptive analysis. The distribution of each loci are retrieved form GPL8490-65 platform database, including analysis of intra/intergenic, exon/intron, CpG island ((CGI)/non-CGI) and their distances from the transcription start site (TSS). The function of each TSM gene, except for *TUBA6*, *C10orf59*, and *ELA1*, was investigated by DAVID bioinformatics (http://david.niaid.nih.gov).

An association between methylation level and expression value was observed. The expression data used were imported from GSE7307 (normal and diseased human tissues were profiled for gene expression using the Affymetrix U133 plus 2.0 array: http://www.ncbi.nlm.nih.gov/geo/query/acc.cgi?acc=GSE7307). As with the methylation database, we collected data from normal human organs including the adrenal gland, brain, cervix, heart, kidney, liver, lung, muscle, ovary, pancreas, prostate gland, spleen, stomach, and testis.

2.3. Comparison of TSM gene expression values between specific tissues

Using a student's T-test, we compared the expression values of each TSM gene in each tissue. The *p*-values were recorded as follows: ≤ 0.5, ≤ 0.1 and ≤ 0.01.

2.4. Validation in autopsy samples

Methylation level of Cg03096975 of *EML2* which is methylated only in the brain tissue was selected to validate in two autopsy cases. Fifteen organs including the brain, kidney, lung, liver, spleen, pancreas, heart,

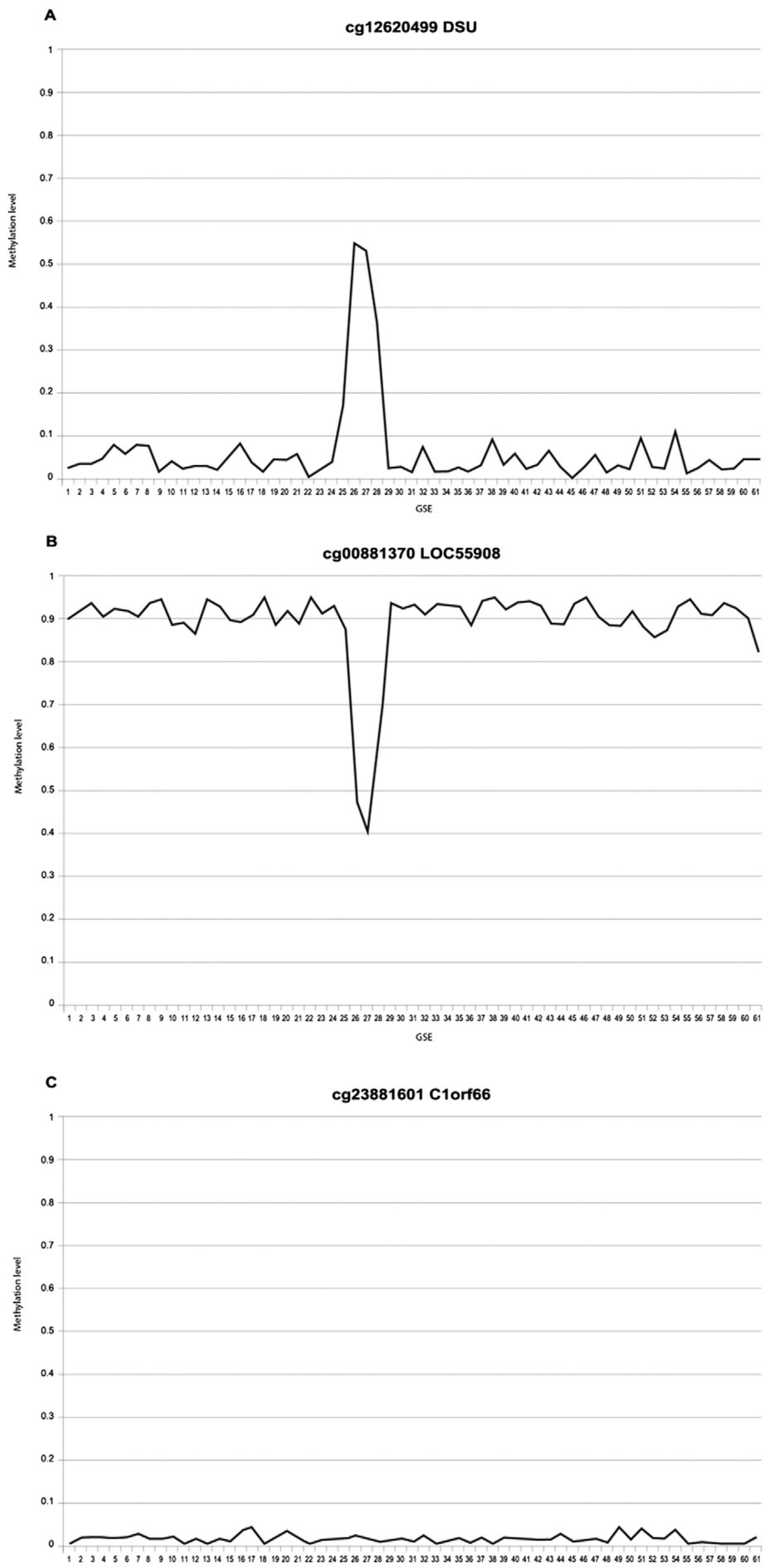

A
cg12620499 DSU
Methylation level
GSE
B
cg00881370 LOC55908
Methylation level
GSE
C
cg23881601 C1orf66
Methylation level
GSE

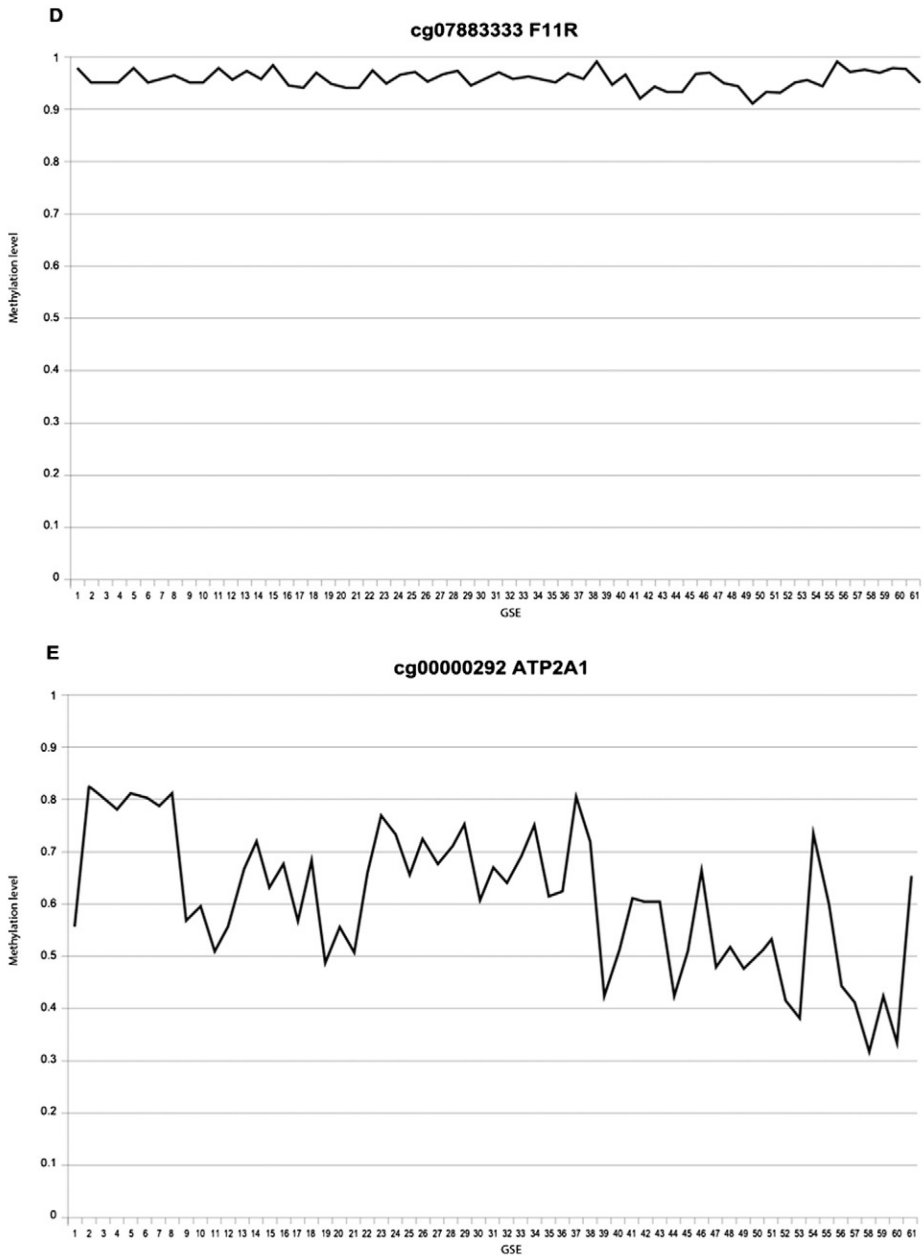

Fig. 1. Five graph patterns of CpG loci. All Y-axes represent methylation levels, and all X-axes represent the 61 codes of each tissue from each GSE in the methylation database as follows: 1—GSE36002 bone (Kresse et al., 2012), 2—GSE25706 bone marrow (Ko et al., 2010), 3—GSE19711 peripheral blood mononuclear cell (PBMC) (Teschendorff et al., 2010), 4—GSE20067 PBMC (Teschendorff et al., 2010), 5—GSE26989 PBMC (Campan et al., 2011), 6—GSE34008 PBMC (Volkmar et al., 2012), 7—GSE30229 PBMC (Langevin et al., 2012), 8—GSE41037 PBMC (Horvath et al., 2012), 9—Bibikova M. et al., brain (Bibikova et al., 2009), 10—GSE22867 brain (Etcheverry et al., 2010), 11—GSE34355 brain (Wu et al., 2012), 12—GSE36194 brain cerebellum (Gibbs et al., 2010; Hernandez et al., 2011, 2012), 13—GSE36194 brain frontal cortex (Gibbs et al., 2010; Hernandez et al., 2011, 2012), 14—Bibikova M. et al., lung (Bibikova et al., 2009), 15—GSE32867 lung (Selamat et al., 2012), 16—GSE35146 lung (Sanders et al., 2012), 17—Bibikova M., et al. breast (Bibikova et al., 2009), 18—GSE20712 breast (Dedeurwaerder et al., 2011), 19—GSE22249 breast (Dedeurwaerder et al., 2011), 20—GSE31979 breast, microdissected (Fackler et al., 2011), 21—GSE31979 breast, organoid (Fackler et al., 2011), 22—GSE33065 breast (Hill et al., 2011), 23—Bibikova M. et al., heart (Bibikova et al., 2009), 24—GSE26033 heart (Pai et al., 2011), 25—GSE42510 heart (Haas et al., 2013), 26—Bibikova M. et al., liver (Bibikova et al., 2009), 27—GSE26033 liver (Pai et al., 2011), 28—GSE37988 liver (Shen et al., 2012), 29—Bibikova M. et al., spleen (Bibikova et al., 2009), 30—Bibikova M. et al., stomach (Bibikova et al., 2009), 31—GSE25869 stomach (Kwon et al., 2011), 32—GSE30601 stomach (Zouridis et al., 2012), 33—GSE31788 stomach (Matsusaka et al., 2011), 34—Bibikova M. et al., colon (Bibikova et al., 2009), 35—GSE25062 colon (Hinoue et al., 2012), 36—GSE27130 colon (Kim et al., 2011), 37—GSE27899 colon (Hasler et al., 2012), 38—GSE29490 colon (Kibriya et al., 2011), 39—Bibikova M. et al., kidney (Bibikova et al., 2009), 40—GSE26033 kidney (Pai et al., 2011), 41—Bibikova M. et al., pancreas (Bibikova et al., 2009), 42—GSE21232 pancreatic islet cells (Volkmar et al., 2012), 43—GSE36353 adrenal gland (Fonseca et al., 2012), 44—Bibikova M. et al., prostate gland (Bibikova et al., 2009), 45—GSE26126 prostate gland (Kobayashi et al., 2011), 46—GSE20080 cervix (Teschendorff et al., 2010), 47—GSE30760 cervix (Teschendorff et al., 2012; Zhuang et al., 2012), 48—GSE36637 cervix (Guenin et al., 2012), 49—Bibikova M. et al., ovary (Bibikova et al., 2009), 50—Bibikova M. et al., testis (Bibikova et al., 2009), 51—GSE31835 skin (Roberson et al., 2012), 52—Bibikova M. et al., skeletal muscle (Bibikova et al., 2009), 53—GSE36166 muscle (Jacobsen et al., 2012), 54—GSE28746 oral epithelium (Bocklandt et al., 2011), 55—GSE33510 urothelium (Lauss et al., 2012), 56—GSE22595 fibroblast, arm (Koch et al., 2011), 57—GSE22595 fibroblast, abdomen (Koch et al., 2011), 58—GSE22595 fibroblast leg (Koch et al., 2011), 59—GSE22595 fibroblast, ear (Koch et al., 2011), 60—GSE22595 fibroblast, breast (Koch et al., 2011), and 61—GSE27284 fibroblast, lung (Navab et al., 2011). An example of each type is shown as (A) a single organ hypermethylated locus, (B) a single organ hypomethylated locus, (C) a universal hypomethylated locus, (D) a universal hypermethylated locus, or (E) a miscellaneous methylated pattern locus.

stomach, skin, gall bladder, small intestine, bone marrow, muscle, aorta and nerve were collected and approved for both macroscopic and microscopic appearances. After DNA extraction and bisulfite modification as previously described (Chalitchagorn et al., 2004), DNA from each case was sequenced at this position. The study protocol in autopsy cases was proved by the ethic committee of The

Table 1
Tissue specific methylation (TSM) loci.

Organs	Tissue specific methylation loci		
	Hypermethylated	Hypomethylated	Total
Adrenal gland	2	1	3
Brain	5	11	16
Kidney	0	1	1
Liver	7	18	25
Muscle	0	8	8
Ovary	0	7	7
Pancreas	2	0	2
Pancreas & Langerhans cell	3	1	4
Spleen	0	1	1
Stomach	1	0	1
Testis	14	4	18
Total	34	52	86

Institute of Forensic Medicine Police General Hospital, Royal Thai Police, Bangkok, Thailand.

3. Results

We collected and analyzed published TSM databases to identify TSM loci that are hypermethylated or hypomethylated in a single organ. Positions of TSM loci were analyzed in relation to transcriptional start sites (TSSs) and CpG Islands (CGIs). Finally, the expression patterns and functions of these TSM genes were studied (Fig. S1).

3.1. TSM database

The TSM database used contains data from 22 normal human organs: bone, bone marrow, blood, brain, lung, breast, heart, liver, spleen, stomach, colon, kidney, pancreas, adrenal gland, prostate gland, cervix, skin, muscle, oral epithelium, urothelium, ovary and testis. After the construction of 27,578 graphs of CpG loci, we classified the graphs into 5 TSM patterns dependent on the observed differences between organs (Fig. 1). A locus that was heavily methylated in one organ would be classified as a single organ hypermethylated locus. A single organ hypomethylated locus is a locus that is hypomethylated in only one organ. Other loci were classified as all-organ hypermethylated, all-organ hypomethylated, and miscellaneous methylated pattern loci. An example of each type was demonstrated in Fig. 1 as follows: (1) Fig. 1A: Cg12620499 of *DSU* represented a single organ hypermethylated locus, (2) Fig. 1B: Cg00881370 of *LOC55908* represented a single organ hypomethylated locus, (3) Fig. 1C: Cg23881601 of *C1orf66C* represented a universal hypomethylated locus, (4) Fig. 1D: Cg07883333 of *F11R* represented a universal hypermethylated locus, and (5) Fig. 1E: Cg00000292 of *ATP2A1* represented a miscellaneous methylated pattern locus. We used only single organ hypermethylated and single organ hypomethylated loci for further analyses. Both Cg sites in Fig. 1A and B were specific to liver tissue with the difference value of 0.48 and 0.42, which passed our criteria, respectively.

Finally, we had 86 TSM loci consisting of 34 single organ hypermethylated loci and 52 hypomethylated loci (Tables 1, S1 and S2).

3.2. Distribution of single organ TSM loci

We analyzed loci from the adrenal gland, brain, kidney, liver, muscle, ovary, pancreas and Langerhans cells, spleen, stomach, and testis. The three organs with the highest frequencies of loci were the liver (25 CpG loci), testis (18 CpG loci), and brain (16 CpG loci). Fewer TSM loci were found in the muscle (8 CpG loci), ovary (7 CpG loci), adrenal gland (3 CpG loci), pancreas (2–4 CpG loci), kidney, spleen, and stomach (1 each) (Tables 1–3).

Table 2
Hypermethylated TSM loci.

Tissue	Gene	Probe ID	SourceSeq
Adrenal gland	*CTSZ*	cg13021192	GGATCCAGAGCGGGAGCCGGCGCGGGATCTGGGACTCGGAGCGGGATCCG
Adrenal gland	*TNFRSF10C*	cg27090216	CGCGCACGAACTCAGCCAACGATTTCTGATAGATTTTTGGGAGTTTGACC
Brain	*EML2*	cg03096975	GTCTGGGTCCCAGGGGTTGGGTGAAACCTGAGATCTAAGCCCCGGGAGCG
Brain	*SP100*	cg05091653	AAAATAAACACTCCAGGGTAAACACCTGGCTTACTTTTAAACATCAGACG
Brain	*TUBA6*	cg12073537	CGGACTCCTTGGTAGTCTGTTAGTGGGAGATCCTTGTTGCCGTCCCTTCG
Brain	*IL10RB*	cg17506742	CGCAACTAGGCTGCTGCTGCCGTCGATTCTGTAACAGGAGAAAGCCCCAT
Brain	*TRIM38*	cg21844956	CGTCTTCAGAAGAAATTCTGTGTGGCTTCAAGAGACTGATCAAATTGTGA
Liver	*ESR1*	cg02720618	GGAGGTGTTTTCCCCCACAAATAACTGCTGCTTTGTCTGGTTTTCCAACG
Liver	*ESR1*	cg20253551	CGCCTTTCCTGCAGCCCCACGGCCAGCAGGTGCCCTACTACCTGGAGAAC
Liver	*DSU*	cg12620499	GCTGAGAACCGTGTGCTGCTGCTGCGGGTGCGAGTGCTTGGAGGAGCGCG
Liver	*IGF2AS*	cg04112019	ATTGGAATCCCCCGAGGATCAAGGGCTAATTGTTGAGCTCAAGCTTCCCG
Liver	*IGF2AS*	cg10501065	CGGGTCACAATAATTTTCTTGGACGTTAATTTCCGGGGACGTCAAAACAC
Liver	*TIAM1*	cg04807655	CTAAGTCAGGGACCGAGACGCAAACATAGACACAAGGATGCACAAGCACG
Liver	*PTK7*	cg21663580	CGCGCCGCAGGTCTGTCCGGCATCGGGCCCCAAACCAGCAACTCTTACCT
Pancreas	*MXD3*	cg02693857	GCACTTTTGTTACAAAGTAACTGACACGGTGCAACAAACACAGGGGCCCG
Pancreas	*ZNF681*	cg05520656	TCTCACCATTTCTAGGTTTCCGGGGGACCTGGCGTCTTAGCTATGGATCG
Pancreas & islet	*ACE*	cg02131967	CGGCCTCCGGCTCGATCTTCCCAGCCCGACCCCCCGGAGCCTCCCGCCTC
Pancreas & islet	*FRY*	cg16941656	GGTGGGGTCTTCCTCGGTTGCGTACCTGGCTGGAGCCGAGCTGGTGGGCG
Pancreas & islet	*BTBD6*	cg23034818	GGTGGACCTGCTTGTTTGGCCATTTGCATTCCGGAGTCTGCCTCTGGCCG
Stomach	*C10orf59*	cg06812977	CGCTCTTTGGTTCCGTGCTCCCTGGGCCGACCTGGGCCCTGAGCTTTCCT
Testis	*SLC25A22*	cg02973416	CCGAGGTGAAGGTTACGAGTCCCTGAGGATCTGTGGGTGTGAGCCAGCCG
Testis	*WFDC1*	cg04195127	CGGGATTTCTCGGCCAGCCTCGCAGGCAATGCCCGTTTCCAGATATTCTT
Testis	*FAM63A*	cg06433658	CGCTCCGGGCCCTGACTACAAGCTGGTTTTCAAAGGAAGTTTGTGGTTTT
Testis	*P2RX7*	cg07602200	CGTGGAAGAACCACTTAATGGTGCCATAATTCATGCTCTGGATCCGAGTG
Testis	*OASL*	cg11301598	GTGTGCTATACAGTTCCTGCATCAGTGCCATCTCTGTCCCGAGAGTACCG
Testis	*GRIN2D*	cg11953334	GGAAGTTGGGCCCCGGACATTGCAGAGGCTGTCGGGGTGTCCTCTTGCCG
Testis	*BAK1*	cg14666892	GCTGATTGGAGCCGGGTGCCGCTGGCACCTCTATGATCACTGGAGTCTCG
Testis	*MC1R*	cg14696348	GTGGCTGTTGGTGCAGGGCCTGTGGTGCCTTCCGCAGCGGAAATGGCGCG
Testis	*MC1R*	cg16790239	CATGTGGCCGCCCTCAGTGGGAGGGGCTCTGAGAACGACTTTTTAAAACG
Testis	*FAM57B*	cg16152813	GGGCTGGGCACGGAGTCTCTATGATGATGCCATGTGCGGTGTCTGTGCCG
Testis	*PTK6*	cg18248891	CGCCCATGGCGCTGGGGCCCAAGGCCACAGGTCCCTCCCAGGCAGCCCCT
Testis	*GPR162*	cg19286986	GGAGGGCGGGCGAGCTGGAGCCGGCAGGCAGCGGGAGCCCGAGAGAGCCG
Testis	*IKBKE*	cg22577136	CGCTCTATGTGAGAGCACCGCTGCCAACAAGCCCACACCCCTGCACCCGG
Testis	*GNG13*	cg24889366	TCATTGTCCCTCCGCTGTCACCTTTTCAAGGTAGGTCCGATGAACAGGCG

Table 3
Hypomethylated TSM loci.

Tissue	Gene	Probe ID	SourceSeq
Adrenal gland	*ELA1*	cg27114026	AAATTTTCCCTAAGTCCAGGCCAGCACCCTGTCCCAGGGCAGGTGGGACG
Brain	*STMN4*	cg02130905	ATTTAAAGGACCTAAAGATCCTGGAAATCATTCATTATACCCCCAGCTCG
Brain	*NLGN2*	cg03169180	CGCTAAAAGCCCTGCCTGTTGGCCAATCAAAGCCTAGCCTTAGTGACCAG
Brain	*BLK*	cg03860768	ACCTCCATGCTGACTCTACAAGGTAATTTGCCCTGCCGTGTGGACAAACG
Brain	*RIT2*	cg04711324	TTTAGTACGAGGTAAGAACCATCAGCGTCGGGCTGGCTGCTGGTCCTCCG
Brain	*40148*	cg04761824	CCCAAAGAGGCAGTCCTCAATAATGCCATCTTTGTTGCAGCAGAACATCG
Brain	*FLJ37538*	cg08626653	CGCAAGTAGGCCCTGGGCATAACTCTGCCTGTAGGTGTGTCCAGTTCTGT
Brain	*MYT1*	cg10071275	TGGAGCCCCAAGGGTTCATGGGTAGCGTATTTACAAAGGAGCCTCCTCCG
Brain	*MYT1*	cg16772207	CATTAGCAGCGGTGGCACGGGCTGGCGGAGGAGGCTCCTTTGTAAATACG
Brain	*MGC27121*	cg20189782	TTTCTTCAGATCAGCATCATTCACCATGGCAACCAGCAGGCATCTGTACG
Brain	*ANK3*	cg22150335	CATGTCATGGAAACATGCCCATGCCTATATAAAGTGAAGCACACTTTCCG
Brain	*AKAP6*	cg24812523	CTACATATTTTAATTCCTATATGACTCTTACAGGCCTTTGTCTTAACCCG
Kidney	*B3GALT7*	cg19201019	TGTTGGATCCAAGTTCCGGTTAGGCACCCAAGCAAGCTATTAGAACTACG
Liver	*LOC55908*	cg00881370	CGAGGAGTTCAAGCTGCATCTTCCAGCCTGCGTGACAGAGAACCATCACC
Liver	*LOC55908*	cg05718253	CGTCCAAGGCCTGAGGCCAGACCTCCCCGGCCATCGGCAACTGTTACTCA
Liver	*INHBC*	cg03399971	CGCCCAACACTGAACCGCCCTGTGTCCAGAGCTGCTTTGAGGACTGCACT
Liver	*DAK*	cg03483654	AAGGCGTGATTGTGCCAGTCGACTGCGAGTTCCTTCCGCAGCTTGTATCG
Liver	*SLC10A1*	cg05633152	CGCCCCACAGACCTGGCACTGAGCGTCATCCTGGTGTTCATGTTGTTCTT
Liver	*CCL16*	cg05766474	CGTGAAGAAATGGGCGAATGTGTGTCAGCTACCTTACATGCCCTATCTTA
Liver	*SERPINA10*	cg05788638	AGTCTGCAGTGGTAGCCCAGTAATTCCTGGGTGCTCCTGGACATATATCG
Liver	*THPO*	cg09736922	CGCCTGCCTGGGCCACTTCTGCCCAATCAGAGAAGGGAGCCACCAGACAC
Liver	*ITIH1*	cg10356463	CGCAGTTCTACACAGAGGGACATGGTCTGGAGCCCCATCAGTAGTTTAAC
Liver	*CA5A*	cg11667117	CAAGTGTTATTGCTGGTTTGCCATGCACAGGAACGCTGAGAACACCATCG
Liver	*CA5A*	cg12343082	CGCCAGTCCACAGTGGTCCTGATCAAAGTGAGAACAGACAGCAGGGAACA
Liver	*MASP2*	cg12888113	CGGCGCTGGACCCTGACTGCACCCCCGGCTACCGCCTGCGCCTCTACTT
Liver	*AGXT2*	cg16297030	GACTCTAATCTGGAGACATTTGCTGAGACCCTTGTGCCTGGTCACTTCCG
Liver	*AGXT*	cg16358738	TGAGTGGGTTCCTGGTCTGGAACACGTACTGGATGCCTTCCTTGATCTCG
Liver	*PGLYRP2*	cg17915429	CGCCTTCTGCAGAGCCAAGAGGTTTGGTCCCAGGACTCTGCCCCCTGACT
Liver	*HPR*	cg20672044	CGTAGCTGTGAGCATAGGATGGGGCATACAGCAGGCACTTAACAAATACT
Liver	*ITIH3*	cg26099316	CGCTCCTTATATGAGCAAGCCTGGTGTTTTCCAAGCAGGGTCAGTGACCT
Liver	*APOC2*	cg27436184	GCGTGGGTGGAGTCAGCAGGTCCCCATGATGGCCCTCACTGAGAGCTTCG
Muscle	*CASQ1*	cg00327483	TCCATGAGTGCTACAGACAGGATGGGGCCCAGAGCTGTGCCGGGTCTGCG
Muscle	*TNNC2*	cg08201421	GGGCCCTTGCAGAGAAATTTAAGCCTCCAAGCAGGTGGCAGGCCTTGACG
Muscle	*ZNF537*	cg03555203	TAGCAGCAGCAGCAGCTGTGGCAGCGGGAGCTTCGACTGGCACCAGAGCG
Muscle	*CHRND*	cg11695684	CGGCTGATCCGGCACCTGTTTCAAGAGAAGGGCTACAACAAGGAGCTCCG
Muscle	*MYOZ3*	cg13214422	CGGAAGCTACCAGCAGCTGACCCTCAACATTTCCAGGTGACTTTGGTGTG
Muscle	*STAC3*	cg14747072	CATGAACAGAAACTGTCCCTTCCTGAATTCAGCCATTATTCACCTGTTCG
Muscle	*STAC3*	cg25189085	CGCCTAAAACCCAAAAGACTCACAGACAAGGAGAGAAATGAAGAAGCTGA
Muscle	*CLCN1*	cg26756862	ACCAGTAGTAGGCTTCCAGCTCCATGTCACTGGTCCCTCTATAAATATCG
Ovary	*NR5A1*	cg00691625	TGACTCTGCAGGCCTCTCGCCTTCTTTGTTGGTGTTTCTCTTCATTTACG
Ovary	*NR5A1*	cg16666160	CGCACCCACAGTCGCCACCGTCCCACCTGGGCTGCCGGAGCCTCCCCCTG
Ovary	*BPESC1*	cg03552688	CGCAATTAAAAAGGCATGAAGTGCCAGACAGCAAGGTTCAGTTCTAGAAT
Ovary	*FLJ25102*	cg06785822	TTCTGTCCAAAGAGGTCGGCCAATGGGGGCCATTCTGAGTTCAGAAACCG
Ovary	*FASLG*	cg10161121	TTCCGCCCACAATTTTCTGATAACAGCCTTCAAGGCCTCAGTTGCTGTCG
Ovary	*SSTR3*	cg14297029	GTGACCTCCCGGTCGGCTGCAGGGGCAGGGGCGTTAGTCTCAGAATCTCG
Ovary	*GMEB2*	cg24674220	CGTGGTCCTGACCCTAAAGGGCAAAGGGAAGAAAACTGACCTACAGGATA
Pancreas & islet	*RBPSUHL*	cg16757724	GGGGTGTGCAGGGTTCCAGCGACAGCAGCACTGGACTCGTCCAGAGGGCG
Spleen	*C1orf54*	cg15120247	CTTTTATGTTTCCCATGTTCATTCAATTCAGAAACCCTTAGCAACATACG
Testis	*C3orf24*	cg05291178	CGCTCTCGTCCCATGTTGGTTCTGCCGAATATTTAGGCTGACTCCTGACC
Testis	*ANKRD7*	cg16192029	TACGGCCGTTATGGCTGTTAAGGTCGTTATGGTCCGGTCCTAGGGGCTCG
Testis	*SLC25A2*	cg19215261	CGGCGTCTAGAGTTCCCGGCCATAATTGCAAGAATTTATCGAAAAGCTTT
Testis	*HIST1H4G*	cg19801560	TGATAAACAAGTCAGAACTATCTCTAAACAAAACGATTACTCGCTTTCCG

Table 4
Characteristics of TSM loci. Positions of TSM loci in the human genome.

Organs	Tissue specific CpG sites			
	Intragenic		Intergenic	Total
	Exon	Intron		
Adrenal gland	2	1	0	3
Brain	7	9	0	16
Kidney	0	1	0	1
Liver	13	11	1	25
Muscle	4	4	0	8
Ovary	1	5	1	7
Pancreas	2	0	0	2
Pancreas & Langerhans cell	3	1	0	4
Spleen	0	1	0	1
Stomach	1	0	0	1
Testis	11	6	1	18
Total	44	39	3	86

Table 5
TSM loci (CGI and non-CGI).

Organs	Tissue specific methylation sites						
	Hypermethylation			Hypomethylation			Total
	CGI	Non-CGI	Total	CGI	Non-CGI	Total	
Adrenal gland	2	0	2	0	1	1	3
Brain	3	2	5	3	8	11	16
Kidney	0	0	0	0	1	1	1
Liver	7	0	7	2	16	18	25
Muscle	0	0	0	1	7	8	8
Ovary	0	0	0	3	4	7	7
Pancreas	2	0	2	0	0	0	2
Pancreas & Langerhans cell	3	0	3	1	0	1	4
Spleen	0	0	0	0	1	1	1
Stomach	1	0	1	0	0	0	1
Testis	7	7	14	4	0	4	18
Total	25	9	34	14	38	52	86

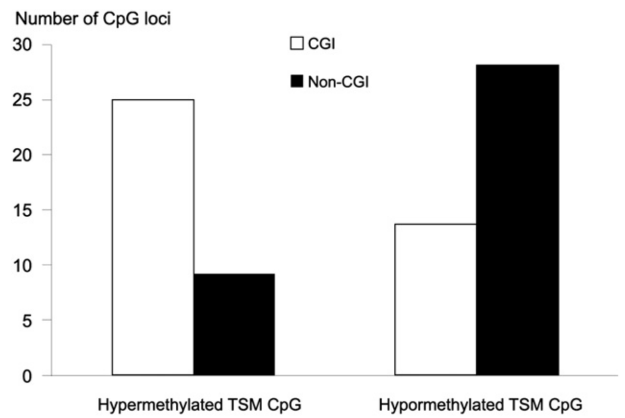

Fig. 2. TSM loci according to CGI. The Y-axis represents the number of CpG loci. The white bar shows the CGI and the black bar shows the non-CGI.

3.3. Positions of TSM loci according to CGI and TSS

The locations of TSM loci were evaluated, and we found that the majority of TSM loci are intragenic, but their locations within exons/introns were not clearly differentiable (Table 4). We also analyzed TSM loci considered to be hypermethylated and hypomethylated, and found that more hypermethylated TSM loci were located in CGI regions than in non-CGI regions, whereas more hypomethylated TSM loci were located in non-CGI regions than in CGI regions (Table 5 and Fig. 2).

The majority of TSM loci (both hyper- and hypomethylated) were found in gene bodies (83 of 86 CpG loci). Interestingly, the majority of TSM loci are located immediately after the TSS. The presence of both hypermethylated and hypomethylated TSM loci sharply declines 300 bp downstream (3′) from the TSS, and then gradually declines up to 1000 bp away from the TSS (Fig. 3).

3.4. The association between methylation levels and expression values of TSM genes

We compared the mRNA levels of TSM genes from CpG methylation modified organs with other organs. The mRNA levels of 19 out of 31 hypermethylated TSM genes were significantly low (Fig. 4A). On the contrary, the expression values of 41 of 46 hypomethylated TSM genes were significantly high (Fig. 4B). Therefore, the methylation of TSM genes may play a role in down-regulating gene transcription.

3.5. TSM gene function

TSM genes' functions were investigated using the DAVID bioinformatics program. A total of 75 genes (29 hypermethylated genes and 46 hypomethylated genes) from 78 TSM genes were available in the program. Most hypermethylated gene functions are associated with membranes, receptors, and signal transduction, while most hypomethylated genes encode signal peptides, extracellular space proteins, and metabolic process proteins (Fig. 5). Interestingly, some hypomethylated TSM genes encode known tissue-specific proteins (Table 6).

3.6. Validation test at Cg03096975 of EML2

Sequencing analysis of Cg03096975 of *EML2* was performed. From two autopsy cases only two brains have methylated sequence, the other 18 samples (fifteen organs; 2 kidneys, 2 lungs, 2 livers and each of the spleen, pancreas, heart, stomach, skin, gall bladder, small intestine, bone marrow, muscle, aorta and nerve) are totally unmethylated. The TSM graph, sequence of primers and example of DNA sequencing are illustrated in Fig. 6.

4. Discussion

We evaluated methylation in an array of 22 organs and found 86 TSM loci that were hypermethylated (34) or hypomethylated (52) exclusively in one organ. Interestingly, the liver, testis, and brain possess many TSM loci while the kidney, spleen, and stomach possess only 1 locus each. This suggests that TSM loci are commonly found in multifunctional organs such as the liver or in organs with unique physiological functions such as the brain and testis.

TSMs are primarily located directly 3′ from the TSS. This differs from the locations of other methylation promoters, such as the CpG methylation of tumor suppressor genes, which is located 5′ to the TSS (Jones and Takai, 2001; Eckhardt et al., 2006). Several studies by ChIP-Seq reported that RNA polymerase II (Pol II) occupied a 200-bp-wide peak centered on 50 bp downstream of the TSS (Zeitlinger et al., 2007; Sultan et al., 2008; Gilchrist et al., 2010; Fenouil et al., 2012; Le Martelot et al., 2012; Quinodoz et al., 2014). This characteristic has been accepted as one of the major checkpoints in gene transcription (Levine, 2011; Smith and Shilatifard, 2013). Moreover, promoter methylation of tumor suppressor gene, the formation of methylation-initiated heterochromatin may prevent the formation of an initiation complex. Consequently, the binding of RNA polymerase II to a gene promoter is inhibited (Jones, 2012). The mechanism by which the hypermethylated TSM reduces mRNA levels should be investigated further. Nevertheless, due to its location 3′ to the TSS, we hypothesize that methylation of TSM loci promotes heterochromatin formation, which blocks the transcription process of RNA polymerase.

Previously, we reported that *SHP1P2* is heavily methylated in epithelial tissue but exhibits reduced methylation in psoriatic skin (Ruchusatsawat et al., 2006). Many silenced hypermethylated TSM genes are membrane proteins and receptors. These proteins, if expressed,

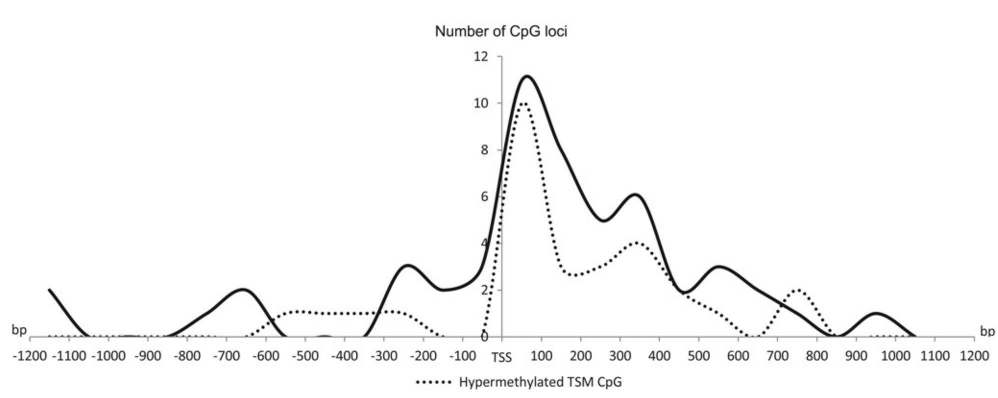

Fig. 3. Distance from each TSM locus to the transcription start site (TSS). The Y-axis represents the number of CpG loci. The X-axis represents the distance to the TSS (base pairs: bp). The dotted line represents hypermethylated TSM loci and the black line represents hypomethylated TSM loci.

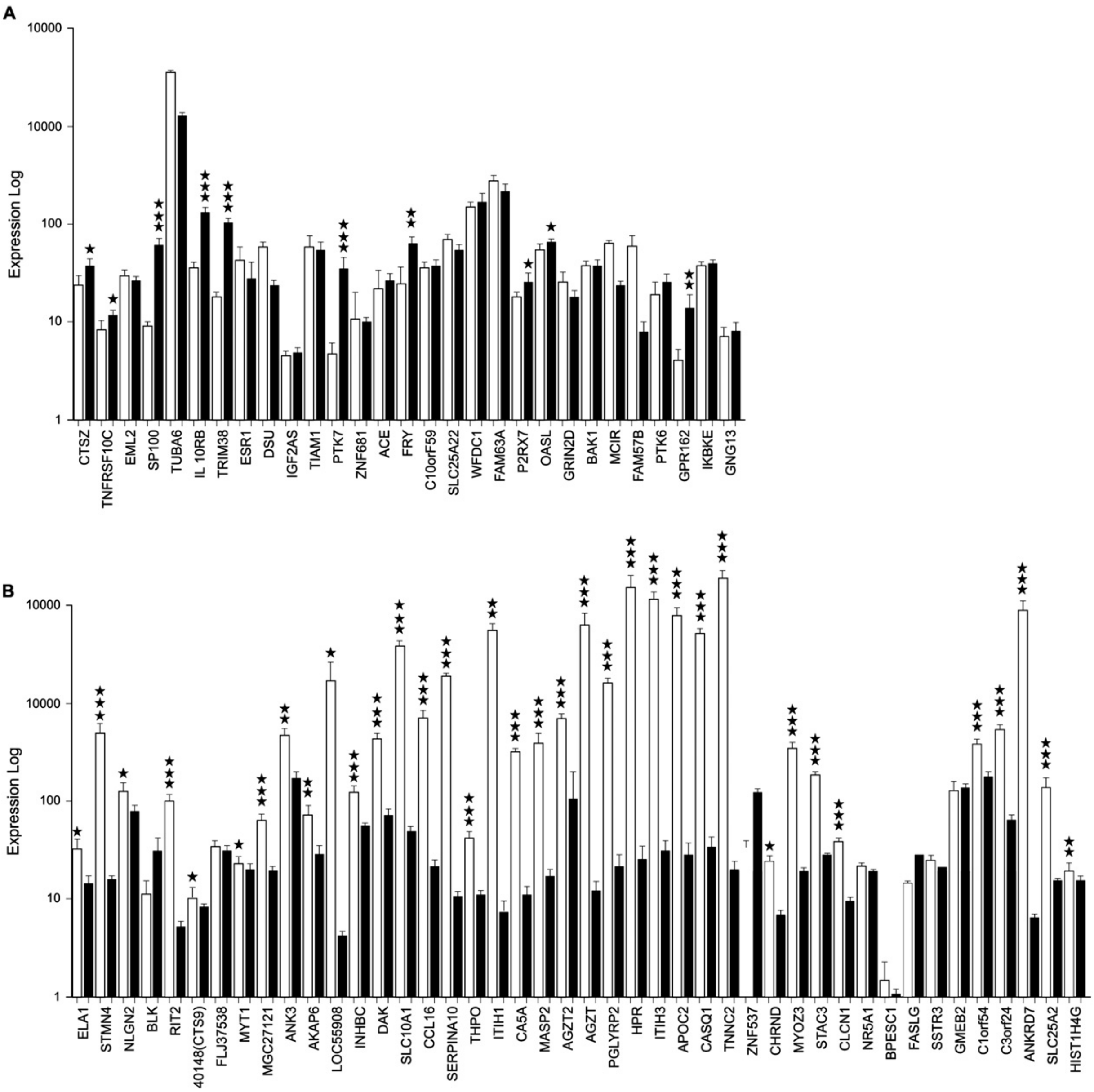

Fig. 4. Expression values of TSM genes. The Y-axis represents the log of the expression value and the X-axis represents each TSM gene. The white bar indicates the expression value of each gene in a specific tissue, and the black bar indicates the expression values of that gene from a collective average of the other tissues. The number of stars indicates the p-value of a comparison of the two bars. One star indicates a p-value lower than 0.5, two stars indicate a p-value lower than 0.1, and three stars indicate p-value lower than 0.01. (A) Histogram of hypermethylated TSM genes. (B) Histogram of hypomethylated TSM genes.

would be harmful to the particular organ in which they reside. Therefore, the organ suppresses the expression of these genes through CpG methylation. In contrast, hypomethylated TSM genes primarily encode signal peptides and tissue-specific proteins. Therefore, demethylation of these CpG dinucleotides may be a key process of organ development. Specificity in methylated or demethylated TSM loci is crucial to the maintenance of normal organ function and the prevention of unexpected organ damage. Therefore, the locations of TSM loci may be useful for future research in

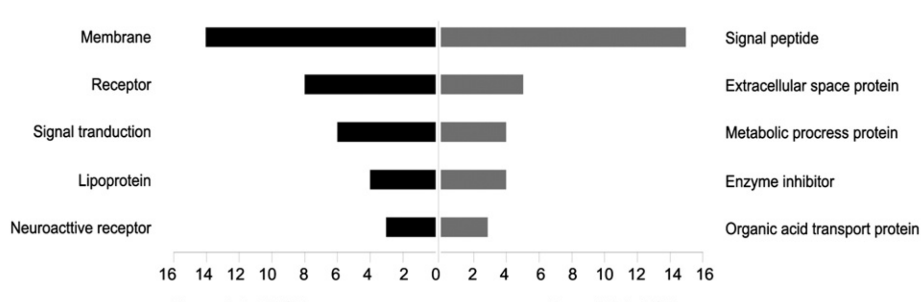

Fig. 5. Gene function analysis from DAVID bioinformatics. The number below the histogram represents the number of genes.

Table 6
Gene function influences from specific TSM.

Organ	Gene	Probe ID	Function
Brain	NLGN2	cg03169180	Neuronal cell surface proteins.
Brain	FLJ37538	cg08626653	Neuronal tyrosine-phosphorylated phosphoinositide-3-kinase adaptor.
Brain	MYT1	cg10071275	Member of a family of neural specific.
Brain	MYT1	cg16772207	Member of a family of neural specific.
Liver	SLC10A1	cg05633152	Glycoproteins that participate in the enterohepatic circulation of bile acids.
Liver	SERPINA10	cg05788638	Serpin family, predominantly expressed in the liver and secreted in plasma.
Liver	CA5A	cg11667117	Localized in the mitochondria and expressed primarily in the liver.
Liver	CA5A	cg12343082	Localized in the mitochondria and expressed primarily in the liver.
Liver	AGXT	cg16358738	Protein is localized mostly in the peroxisomes, expressed only in liver.
Liver	HPR	cg20672044	Haptoglobin-related protein.
Muscle	CASQ1	cg00327483	Skeletal muscle specific member of the calsequestrin protein family.
Muscle	TNNC2	cg08201421	Troponin (Tn), protein complex in the regulation of striated muscle contraction.
Muscle	CHRND	cg11695684	Cholinergic receptor, nicotinic, delta (muscle).
Muscle	MYOZ3	cg13214422	Specifically expressed in the skeletal muscle, and belongs to the myozenin family.
Muscle	CLCN1	cg26756862	Regulates the electric excitability of the skeletal muscle membrane.
Ovary	NR5A1	cg00691625	Transcriptional activator involved in sex determination.
Ovary	NR5A1	cg16666160	Transcriptional activator involved in sex determination.
Testis	ANKRD7	cg16192029	Ankyrin repeat domain 7, testis specific.

tissue and stem cell engineering. Similar to *SHP1P2* hypomethylation in psoriatic skin (Ruchusatsawat et al., 2006), the methylation of TSM loci may be altered by disease involvement.

5. Conclusions

We reported the sequences of 86 TSM loci from 11 human organs. Most TSM loci locate immediately after TSS and regulate gene expression. These sequences are essential in the further exploration of the role of TSM on cellular differentiation, organ development and function. Moreover, these sequences can be used to develop PCR tests for the tissue sources of DNA. These PCR tests may be useful for the diagnosis of several human diseases.

Supplementary data to this article can be found online at http://dx.doi.org/10.1016/j.gene.2014.09.060.

Authors' contributions

TM performed the bioinformatics analysis and statistical analysis, and drafted the manuscript. NK participated in the design of the study, performed bioinformatics analyses, and drafted the manuscript. JS and PT participated in the bioinformatics study. AM conceived the study, participated in its design and coordination, and helped to draft the manuscript. All authors read and approved the final manuscript.

Competing interests

The authors received part funding from the Four Seasons Hotel Bangkok's 4th Cancer Care charity fun run. This does not alter the authors' adherence to all the Gene policies on sharing data and materials.

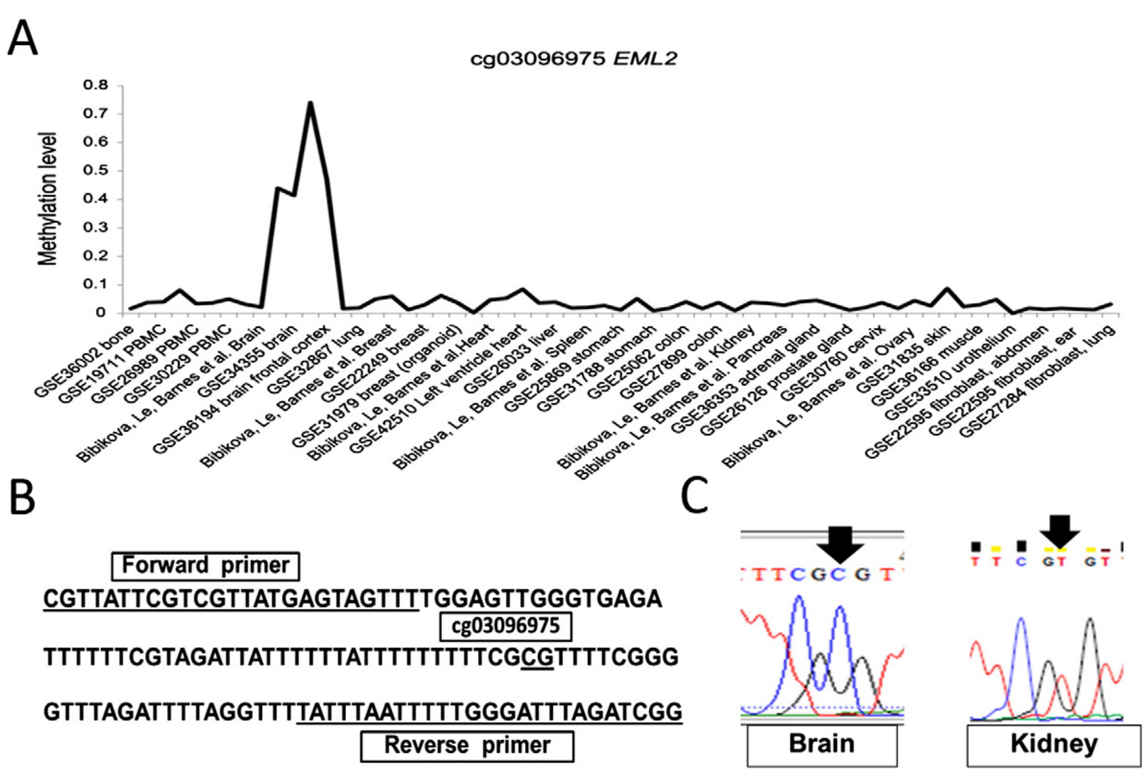

Fig. 6. Validation test at Cg03096975 of *EML2*. (A) TSM graph at cg03096975 of *EML2* demonstrates that these loci are hypermethylated specific to the brain. (B) Sequence of primers. (C) Example of sequence at Cg03096975.

Acknowledgments

This project has been funded in whole or in part with Research Chair Grant 2011 from the National Science and Technology Development Agency (NSTDA), Thailand and the Four Seasons Hotel Bangkok's 4th Cancer Care charity fun run in coordination with the Thai Red Cross Society and Chulalongkorn University. NK is supported by RSA 5580013. We gratefully thank Professor Kevin L Gunderson for his kindness in providing raw data from his previous publications.

References

Aporntewan, C., A.M., 2011. Connection up- and down-regulation expression analysis of microarrays (CU-DREAM): a physiogenomic discovery tool. Asian Biomed. 5, 257–262.

Aporntewan, C., Phokaew, C., Piriyapongsa, J., Ngamphiw, C., Ittiwut, C., Tongsima, S., Mutirangura, A., 2011. Hypomethylation of intragenic LINE-1 represses transcription in cancer cells through AGO2. PLoS One 6, e17934.

Bibikova, M., Le, J., Barnes, B., Saedinia-Melnyk, S., Zhou, L., Shen, R., Gunderson, K.L., 2009. Genome-wide DNA methylation profiling using Infinium® assay. Epigenomics 1, 177–200.

Bocklandt, S., Lin, W., Sehl, M.E., Sanchez, F.J., Sinsheimer, J.S., Horvath, S., Vilain, E., 2011. Epigenetic predictor of age. PLoS One 6, e14821.

Byun, H.M., Siegmund, K.D., Pan, F., Weisenberger, D.J., Kanel, G., Laird, P.W., Yang, A.S., 2009. Epigenetic profiling of somatic tissues from human autopsy specimens identifies tissue- and individual-specific DNA methylation patterns. Hum. Mol. Genet. 18, 4808–4817.

Campan, M., Moffitt, M., Houshdaran, S., Shen, H., Widschwendter, M., Daxenbichler, G., Long, T., Marth, C., Laird-Offringa, I.A., Press, M.F., Dubeau, L., Siegmund, K.D., Wu, A.H., Groshen, S., Chandavarkar, U., Roman, L.D., Berchuck, A., Pearce, C.L., Laird, P. W., 2011. Genome-scale screen for DNA methylation-based detection markers for ovarian cancer. PLoS One 6, e28141.

Cedar, H., Bergman, Y., 2012. Programming of DNA methylation patterns. Annu. Rev. Biochem. 81, 97–117.

Chalitchagorn, K., Shuangshoti, S., Hourpai, N., Kongruttanachok, N., Tangkijvanich, P., Thong-ngam, D., Voravud, N., Sriuranpong, V., Mutirangura, A., 2004. Distinctive pattern of LINE-1 methylation level in normal tissues and the association with carcinogenesis. Oncogene 23, 8841–8846.

Dedeurwaerder, S., Desmedt, C., Calonne, E., Singhal, S.K., Haibe-Kains, B., Defrance, M., Michiels, S., Volkmar, M., Deplus, R., Luciani, J., Lallemand, F., Larsimont, D., Toussaint, J., Haussy, S., Rothe, F., Rouas, G., Metzger, O., Majjaj, S., Saini, K., Putmans, P., Hames, G., van Baren, N., Coulie, P.G., Piccart, M., Sotiriou, C., Fuks, F., 2011. DNA methylation profiling reveals a predominant immune component in breast cancers. EMBO Mol. Med. 3, 726–741.

Eckhardt, F., Lewin, J., Cortese, R., Rakyan, V.K., Attwood, J., Burger, M., Burton, J., Cox, T.V., Davies, R., Down, T.A., Haefliger, C., Horton, R., Howe, K., Jackson, D.K., Kunde, J., Koenig, C., Liddle, J., Niblett, D., Otto, T., Pettett, R., Seemann, S., Thompson, C., West, T., Rogers, J., Olek, A., Berlin, K., Beck, S., 2006. DNA methylation profiling of human chromosomes 6, 20 and 22. Nat. Genet. 38, 1378–1385.

Etcheverry, A., Aubry, M., de Tayrac, M., Vauleon, E., Boniface, R., Guenot, F., Saikali, S., Hamlat, A., Riffaud, L., Menei, P., Quillien, V., Mosser, J., 2010. DNA methylation in glioblastoma: impact on gene expression and clinical outcome. BMC Genomics 11, 701.

Fackler, M.J., Umbricht, C.B., Williams, D., Argani, P., Cruz, L.A., Merino, V.F., Teo, W.W., Zhang, Z., Huang, P., Visvananthan, K., Marks, J., Ethier, S., Gray, J.W., Wolff, A.C., Cope, L.M., Sukumar, S., 2011. Genome-wide methylation analysis identifies genes specific to breast cancer hormone receptor status and risk of recurrence. Cancer Res. 71, 6195–6207.

Fenouil, R., Cauchy, P., Koch, F., Descostes, N., Cabeza, J.Z., Innocenti, C., Ferrier, P., Spicuglia, S., Gut, M., Gut, I., Andrau, J.C., 2012. CpG islands and GC content dictate nucleosome depletion in a transcription-independent manner at mammalian promoters. Genome Res. 22, 2399–2408.

Fonseca, A.L., Kugelberg, J., Starker, L.F., Scholl, U., Choi, M., Hellman, P., Akerstrom, G., Westin, G., Lifton, R.P., Bjorklund, P., Carling, T., 2012. Comprehensive DNA methylation analysis of benign and malignant adrenocortical tumors. Genes Chromosomes Cancer 51, 949–960.

Frumkin, D., Wasserstrom, A., Budowle, B., Davidson, A., 2011. DNA methylation-based forensic tissue identification. Forensic Sci. Int. Genet. 5, 517–524.

Gibbs, J.R., van der Brug, M.P., Hernandez, D.G., Traynor, B.J., Nalls, M.A., Lai, S.L., Arepalli, S., Dillman, A., Rafferty, I.P., Troncoso, J., Johnson, R., Zielke, H.R., Ferrucci, L., Longo, D.L., Cookson, M.R., Singleton, A.B., 2010. Abundant quantitative trait loci exist for DNA methylation and gene expression in human brain. PLoS Genet. 6, e1000952.

Gilchrist, D.A., Dos Santos, G., Fargo, D.C., Xie, B., Gao, Y., Li, L., Adelman, K., 2010. Pausing of RNA polymerase II disrupts DNA-specified nucleosome organization to enable precise gene regulation. Cell 143, 540–551.

Guenin, S., Mouallif, M., Deplus, R., Lampe, X., Krusy, N., Calonne, E., Delbecque, K., Kridelka, F., Fuks, F., Ennaji, M.M., Delvenne, P., 2012. Aberrant promoter methylation and expression of UTF1 during cervical carcinogenesis. PLoS One 7, e42704.

Haas, J., Frese, K.S., Park, Y.J., Keller, A., Vogel, B., Lindroth, A.M., Weichenhan, D., Franke, J., Fischer, S., Bauer, A., Marquart, S., Sedaghat-Hamedani, F., Kayvanpour, E., Kohler, D., Wolf, N.M., Hassel, S., Nietsch, R., Wieland, T., Ehlermann, P., Schultz, J.H., Dosch, A., Mereles, D., Hardt, S., Backs, J., Hoheisel, J.D., Plass, C., Katus, H.A., Meder, B., 2013. Alterations in cardiac DNA methylation in human dilated cardiomyopathy. EMBO Mol. Med. 5, 413–429.

Hasler, R., Feng, Z., Backdahl, L., Spehlmann, M.E., Franke, A., Teschendorff, A., Rakyan, V.K., Down, T.A., Wilson, G.A., Feber, A., Beck, S., Schreiber, S., Rosenstiel, P., 2012. A functional methylome map of ulcerative colitis. Genome Res. 22, 2130–2137.

Hernandez, D.G., Nalls, M.A., Gibbs, J.R., Arepalli, S., van der Brug, M., Chong, S., Moore, M., Longo, D.L., Cookson, M.R., Traynor, B.J., Singleton, A.B., 2011. Distinct DNA methylation changes highly correlated with chronological age in the human brain. Hum. Mol. Genet. 20, 1164–1172.

Hernandez, D.G., Nalls, M.A., Moore, M., Chong, S., Dillman, A., Trabzuni, D., Gibbs, J.R., Ryten, M., Arepalli, S., Weale, M.E., Zonderman, A.B., Troncoso, J., O'Brien, R., Walker, R., Smith, C., Bandinelli, S., Traynor, B.J., Hardy, J., Singleton, A.B., Cookson, M.R., 2012. Integration of GWAS SNPs and tissue specific expression profiling reveal discrete eQTLs for human traits in blood and brain. Neurobiol. Dis. 47, 20–28.

Hill, V.K., Ricketts, C., Bieche, I., Vacher, S., Gentle, D., Lewis, C., Maher, E.R., Latif, F., 2011. Genome-wide DNA methylation profiling of CpG islands in breast cancer identifies novel genes associated with tumorigenicity. Cancer Res. 71, 2988–2999.

Hinoue, T., Weisenberger, D.J., Lange, C.P., Shen, H., Byun, H.M., Van Den Berg, D., Malik, S., Pan, F., Noushmehr, H., van Dijk, C.M., Tollenaar, R.A., Laird, P.W., 2012. Genome-scale analysis of aberrant DNA methylation in colorectal cancer. Genome Res. 22, 271–282.

Horvath, S., Zhang, Y., Langfelder, P., Kahn, R.S., Boks, M.P., van Eijk, K., van den Berg, L.H., Ophoff, R.A., 2012. Aging effects on DNA methylation modules in human brain and blood tissue. Genome Biol. 13, R97.

How Kit, A., Nielsen, H.M., Tost, J., 2012. DNA methylation based biomarkers: practical considerations and applications. Biochimie 94, 2314–2337.

Jacobsen, S.C., Brons, C., Bork-Jensen, J., Ribel-Madsen, R., Yang, B., Lara, E., Hall, E., Calvanese, V., Nilsson, E., Jorgensen, S.W., Mandrup, S., Ling, C., Fernandez, A.F., Fraga, M.F., Poulsen, P., Vaag, A., 2012. Effects of short-term high-fat overfeeding on genome-wide DNA methylation in the skeletal muscle of healthy young men. Diabetologia 55, 3341–3349.

Jin, S.G., Kadam, S., Pfeifer, G.P., 2010. Examination of the specificity of DNA methylation profiling techniques towards 5-methylcytosine and 5-hydroxymethylcytosine. Nucleic Acids Res. 38, e125.

Jones, P.A., 2012. Functions of DNA methylation: islands, start sites, gene bodies and beyond. Nat. Rev. Genet. 13, 484–492.

Jones, P.A., Takai, D., 2001. The role of DNA methylation in mammalian epigenetics. Science 293, 1068–1070.

Kibriya, M.G., Raza, M., Jasmine, F., Roy, S., Paul-Brutus, R., Rahaman, R., Dodsworth, C., Rakibuz-Zaman, M., Kamal, M., Ahsan, H., 2011. A genome-wide DNA methylation study in colorectal carcinoma. BMC Med. Genomics 4, 50.

Kim, Y.H., Lee, H.C., Kim, S.Y., Yeom, Y.I., Ryu, K.J., Min, B.H., Kim, D.H., Son, H.J., Rhee, P.L., Kim, J.J., Rhee, J.C., Kim, H.C., Chun, H.K., Grady, W.M., Kim, Y.S., 2011. Epigenomic analysis of aberrantly methylated genes in colorectal cancer identifies genes commonly affected by epigenetic alterations. Ann. Surg. Oncol. 18, 2338–2347.

Kitkumthorn, N., Mutirangura, A., 2011. Long interspersed nuclear element-1 hypomethylation in cancer: biology and clinical applications. Clin. Epigenetics 2, 315–330.

Ko, M., Huang, Y., Jankowska, A.M., Pape, U.J., Tahiliani, M., Bandukwala, H.S., An, J., Lamperti, E.D., Koh, K.P., Ganetzky, R., Liu, X.S., Aravind, L., Agarwal, S., Maciejewski, J.P., Rao, A., 2010. Impaired hydroxylation of 5-methylcytosine in myeloid cancers with mutant TET2. Nature 468, 839–843.

Kobayashi, Y., Absher, D.M., Gulzar, Z.G., Young, S.R., McKenney, J.K., Peehl, D.M., Brooks, J.D., Myers, R.M., Sherlock, G., 2011. DNA methylation profiling reveals novel biomarkers and important roles for DNA methyltransferases in prostate cancer. Genome Res. 21, 1017–1027.

Koch, C.M., Suschek, C.V., Lin, Q., Bork, S., Goergens, M., Joussen, S., Pallua, N., Ho, A.D., Zenke, M., Wagner, W., 2011. Specific age-associated DNA methylation changes in human dermal fibroblasts. PLoS One 6, e16679.

Kresse, S.H., Rydbeck, H., Skarn, M., Namlos, H.M., Barragan-Polania, A.H., Cleton-Jansen, A.M., Serra, M., Liestol, K., Hogendoorn, P.C., Hovig, E., Myklebost, O., Meza-Zepeda, L.A., 2012. Integrative analysis reveals relationships of genetic and epigenetic alterations in osteosarcoma. PLoS One 7, e48262.

Kwon, O.H., Park, J.L., Kim, M., Kim, J.H., Lee, H.C., Kim, H.J., Noh, S.M., Song, K.S., Yoo, H.S., Paik, S.G., Kim, S.Y., Kim, Y.S., 2011. Aberrant up-regulation of LAMB3 and LAMC2 by promoter demethylation in gastric cancer. Biochem. Biophys. Res. Commun. 406, 539–545.

Langevin, S.M., Koestler, D.C., Christensen, B.C., Butler, R.A., Wiencke, J.K., Nelson, H.H., Houseman, E.A., Marsit, C.J., Kelsey, K.T., 2012. Peripheral blood DNA methylation profiles are indicative of head and neck squamous cell carcinoma: an epigenome-wide association study. Epigenetics 7, 291–299.

Lauss, M., Aine, M., Sjodahl, G., Veerla, S., Patschan, O., Gudjonsson, S., Chebil, G., Lovgren, K., Ferno, M., Mansson, W., Liedberg, F., Ringner, M., Lindgren, D., Hoglund, M., 2012. DNA methylation analyses of urothelial carcinoma reveal distinct epigenetic subtypes and an association between gene copy number and methylation status. Epigenetics 7, 858–867.

Le Martelot, G., Canella, D., Symul, L., Migliavacca, E., Gilardi, F., Liechti, R., Martin, O., Harshman, K., Delorenzi, M., Desvergne, B., Herr, W., Deplancke, B., Schibler, U., Rougemont, J., Guex, N., Hernandez, N., Naef, F., Cycli, X.C., 2012. Genome-wide RNA polymerase II profiles and RNA accumulation reveal kinetics of transcription and associated epigenetic changes during diurnal cycles. PLoS Biol. 10, e1001442.

Levine, M., 2011. Paused RNA polymerase II as a developmental checkpoint. Cell 145, 502–511.

Lin, J.C., Wang, W.Y., Chen, K.Y., Wei, Y.H., Liang, W.M., Jan, J.S., Jiang, R.S., 2004. Quantification of plasma Epstein–Barr virus DNA in patients with advanced nasopharyngeal carcinoma. N. Engl. J. Med. 350, 2461–2470.

Matsusaka, K., Kaneda, A., Nagae, G., Ushiku, T., Kikuchi, Y., Hino, R., Uozaki, H., Seto, Y., Takada, K., Aburatani, H., Fukayama, M., 2011. Classification of Epstein–Barr virus-positive gastric cancers by definition of DNA methylation epigenotypes. Cancer Res. 71, 7187–7197.

Maunakea, A.K., Nagarajan, R.P., Bilenky, M., Ballinger, T.J., D'Souza, C., Fouse, S.D., Johnson, B.E., Hong, C., Nielsen, C., Zhao, Y., Turecki, G., Delaney, A., Varhol, R., Thiessen, N., Shchors, K., Heine, V.M., Rowitch, D.H., Xing, X., Fiore, C., Schillebeeckx, M., Jones, S.J., Haussler, D., Marra, M.A., Hirst, M., Wang, T., Costello, J.F., 2010. Conserved role of intragenic DNA methylation in regulating alternative promoters. Nature 466, 253–257.

Mutirangura, A., Pornthanakasem, W., Theamboonlers, A., Sriuranpong, V., Lertsanguansinchi, P., Yenrudi, S., Voravud, N., Supiyaphun, P., Poovorawan, Y., 1998. Epstein–Barr viral DNA in serum of patients with nasopharyngeal carcinoma. Clin. Cancer Res. 4, 665–669.

Navab, R., Strumpf, D., Bandarchi, B., Zhu, C.Q., Pintilie, M., Ramnarine, V.R., Ibrahimov, E., Radulovich, N., Leung, L., Barczyk, M., Panchal, D., To, C., Yun, J.J., Der, S., Shepherd, F.A., Jurisica, I., Tsao, M.S., 2011. Prognostic gene-expression signature of carcinoma-associated fibroblasts in non-small cell lung cancer. Proc. Natl. Acad. Sci. U. S. A. 108, 7160–7165.

Ohgane, J., Yagi, S., Shiota, K., 2008. Epigenetics: the DNA methylation profile of tissue-dependent and differentially methylated regions in cells. Placenta 29 (Suppl. A), S29–S35.

Pai, A.A., Bell, J.T., Marioni, J.C., Pritchard, J.K., Gilad, Y., 2011. A genome-wide study of DNA methylation patterns and gene expression levels in multiple human and chimpanzee tissues. PLoS Genet. 7, e1001316.

Phutikanit, N., Suwimonteerabutr, J., Harrison, D., D'Occhio, M., Carroll, B., Techakumphu, M., 2010. Different DNA methylation patterns detected by the Amplified Methylation Polymorphism Polymerase Chain Reaction (AMP PCR) technique among various cell types of bulls. Acta Vet. Scand. 52, 18.

Quinodoz, M., Gobet, C., Naef, F., Gustafson, K.B., 2014. Characteristic bimodal profiles of RNA polymerase II at thousands of active mammalian promoters. Genome Biol. 15, R85.

Rakyan, V.K., Down, T.A., Maslau, S., Andrew, T., Yang, T.P., Beyan, H., Whittaker, P., McCann, O.T., Finer, S., Valdes, A.M., Leslie, R.D., Deloukas, P., Spector, T.D., 2010. Human aging-associated DNA hypermethylation occurs preferentially at bivalent chromatin domains. Genome Res. 20, 434–439.

Roberson, E.D., Liu, Y., Ryan, C., Joyce, C.E., Duan, S., Cao, L., Martin, A., Liao, W., Menter, A., Bowcock, A.M., 2012. A subset of methylated CpG sites differentiate psoriatic from normal skin. J. Invest. Dermatol. 132, 583–592.

Ruchusatsawat, K., Wongpiyabovorn, J., Shuangshoti, S., Hirankarn, N., Mutirangura, A., 2006. SHP-1 promoter 2 methylation in normal epithelial tissues and demethylation in psoriasis. J. Mol. Med. (Berl.) 84, 175–182.

Sanders, Y.Y., Ambalavanan, N., Halloran, B., Zhang, X., Liu, H., Crossman, D.K., Bray, M., Zhang, K., Thannickal, V.J., Hagood, J.S., 2012. Altered DNA methylation profile in idiopathic pulmonary fibrosis. Am. J. Respir. Crit. Care Med. 186, 525–535.

Selamat, S.A., Chung, B.S., Girard, L., Zhang, W., Zhang, Y., Campan, M., Siegmund, K.D., Koss, M.N., Hagen, J.A., Lam, W.L., Lam, S., Gazdar, A.F., Laird-Offringa, I.A., 2012. Genome-scale analysis of DNA methylation in lung adenocarcinoma and integration with mRNA expression. Genome Res. 22, 1197–1211.

Shen, J., Wang, S., Zhang, Y.J., Kappil, M., Wu, H.C., Kibriya, M.G., Wang, Q., Jasmine, F., Ahsan, H., Lee, P.H., Yu, M.W., Chen, C.J., Santella, R.M., 2012. Genome-wide DNA methylation profiles in hepatocellular carcinoma. Hepatology 55, 1799–1808.

Shiota, K., Kogo, Y., Ohgane, J., Imamura, T., Urano, A., Nishino, K., Tanaka, S., Hattori, N., 2002. Epigenetic marks by DNA methylation specific to stem, germ and somatic cells in mice. Genes Cells 7, 961–969.

Smith, E., Shilatifard, A., 2013. Transcriptional elongation checkpoint control in development and disease. Genes Dev. 27, 1079–1088.

Sulewska, A., Niklinska, W., Kozlowski, M., Minarowski, L., Naumnik, W., Niklinski, J., Dabrowska, K., Chyczewski, L., 2007. Detection of DNA methylation in eucaryotic cells. Folia Histochem. Cytobiol. 45, 315–324.

Sultan, M., Schulz, M.H., Richard, H., Magen, A., Klingenhoff, A., Scherf, M., Seifert, M., Borodina, T., Soldatov, A., Parkhomchuk, D., Schmidt, D., O'Keeffe, S., Haas, S., Vingron, M., Lehrach, H., Yaspo, M.L., 2008. A global view of gene activity and alternative splicing by deep sequencing of the human transcriptome. Science 321, 956–960.

Sun, Z., Chai, H.S., Wu, Y., White, W.M., Donkena, K.V., Klein, C.J., Garovic, V.D., Therneau, T.M., Kocher, J.P., 2011. Batch effect correction for genome-wide methylation data with Illumina Infinium platform. BMC Med. Genomics 4, 84.

Teschendorff, A.E., Menon, U., Gentry-Maharaj, A., Ramus, S.J., Weisenberger, D.J., Shen, H., Campan, M., Noushmehr, H., Bell, C.G., Maxwell, A.P., Savage, D.A., Mueller-Holzner, E., Marth, C., Kocjan, G., Gayther, S.A., Jones, A., Beck, S., Wagner, W., Laird, P.W., Jacobs, I.J., Widschwendter, M., 2010. Age-dependent DNA methylation of genes that are suppressed in stem cells is a hallmark of cancer. Genome Res. 20, 440–446.

Teschendorff, A.E., Jones, A., Fiegl, H., Sargent, A., Zhuang, J.J., Kitchener, H.C., Widschwendter, M., 2012. Epigenetic variability in cells of normal cytology is associated with the risk of future morphological transformation. Genome Med. 4, 24.

Vinayanuwattikun, C., Sriuranpong, V., Tanasanvimon, S., Chantranuwat, P., Mutirangura, A., 2011. Epithelial-specific methylation marker: a potential plasma biomarker in advanced non-small cell lung cancer. J. Thorac. Oncol. 6, 1818–1825.

Vinayanuwattikun, C., Winayanuwattikun, P., Chantranuwat, P., Mutirangura, A., Sriuranpong, V., 2013. The impact of non-tumor-derived circulating nucleic acids implicates the prognosis of non-small cell lung cancer. J. Cancer Res. Clin. Oncol. 139, 67–76.

Volkmar, M., Dedeurwaerder, S., Cunha, D.A., Ndlovu, M.N., Defrance, M., Deplus, R., Calonne, E., Volkmar, U., Igoillo-Esteve, M., Naamane, N., Del Guerra, S., Masini, M., Bugliani, M., Marchetti, P., Cnop, M., Eizirik, D.L., Fuks, F., 2012. DNA methylation profiling identifies epigenetic dysregulation in pancreatic islets from type 2 diabetic patients. EMBO J. 31, 1405–1426.

Wang, D., Yan, L., Hu, Q., Sucheston, L.E., Higgins, M.J., Ambrosone, C.B., Johnson, C.S., Smiraglia, D.J., Liu, S., 2012. IMA: an R package for high-throughput analysis of Illumina's 450 K Infinium methylation data. Bioinformatics 28, 729–730.

Weisenberger, D.J., 2014. Characterizing DNA methylation alterations from The Cancer Genome Atlas. J. Clin. Invest. 124, 17–23.

Wu, X., Northcott, P.A., Dubuc, A., Dupuy, A.J., Shih, D.J., Witt, H., Croul, S., Bouffet, E., Fults, D.W., Eberhart, C.G., Garzia, L., Van Meter, T., Zagzag, D., Jabado, N., Schwartzentruber, J., Majewski, J., Scheetz, T.E., Pfister, S.M., Korshunov, A., Li, X.N., Scherer, S.W., Cho, Y.J., Akagi, K., MacDonald, T.J., Koster, J., McCabe, M.G., Sarver, A.L., Collins, V.P., Weiss, W.A., Largaespada, D.A., Collier, L.S., Taylor, M.D., 2012. Clonal selection drives genetic divergence of metastatic medulloblastoma. Nature 482, 529–533.

Yagi, S., Hirabayashi, K., Sato, S., Li, W., Takahashi, Y., Hirakawa, T., Wu, G., Hattori, N., Hattori, N., Ohgane, J., Tanaka, S., Liu, X.S., Shiota, K., 2008. DNA methylation profile of tissue-dependent and differentially methylated regions (T-DMRs) in mouse promoter regions demonstrating tissue-specific gene expression. Genome Res. 18, 1969–1978.

Zeitlinger, J., Stark, A., Kellis, M., Hong, J.W., Nechaev, S., Adelman, K., Levine, M., Young, R.A., 2007. RNA polymerase stalling at developmental control genes in the *Drosophila melanogaster* embryo. Nat. Genet. 39, 1512–1516.

Zhu, Y., Davis, S., Stephens, R., Meltzer, P.S., Chen, Y., 2008. GEOmetadb: powerful alternative search engine for the Gene Expression Omnibus. Bioinformatics 24, 2798–2800.

Zhuang, J., Jones, A., Lee, S.H., Ng, E., Fiegl, H., Zikan, M., Cibula, D., Sargent, A., Salvesen, H.B., Jacobs, I.J., Kitchener, H.C., Teschendorff, A.E., Widschwendter, M., 2012. The dynamics and prognostic potential of DNA methylation changes at stem cell gene loci in women's cancer. PLoS Genet. 8, e1002517.

Zouridis, H., Deng, N., Ivanova, T., Zhu, Y., Wong, B., Huang, D., Wu, Y.H., Wu, Y., Tan, I.B., Liem, N., Gopalakrishnan, V., Luo, Q., Wu, J., Lee, M., Yong, W.P., Goh, L.K., Teh, B.T., Rozen, S., Tan, P., 2012. Methylation subtypes and large-scale epigenetic alterations in gastric cancer. Sci. Transl. Med. 4, 156ra140.